Coordination Chemistry Reviews 482 (2023) 215071

Contents lists available at ScienceDirect

Coordination Chemistry Reviews

journal homepage: www.elsevier.com/locate/ccr

Review

Elucidating the speciation of extracted lanthanides by diglycolamides

Allison A. Peroutka, Shane S. Galley, Jenifer C. Shafer *

Department of Chemistry, Colorado School of Mines, Golden, CO 80401, USA

ARTICLE INFO

Article history:
Received 8 October 2022
Accepted 5 February 2023
Available online 21 February 2023

Keywords:
Diglycolamides
Lanthanide separations
Spectroscopy
Small-angle scattering

ABSTRACT

Many studies over the past few decades have been devoted to addressing the application of diglycolamides (DGAs) for hydrometallurgical-based, *f*-element separations. Work to date has shown the molecular structure of a DGA derivative can have a significant impact on *intra*-lanthanide partitioning patterns. More recent studies have pushed towards probing the structure function relationship of the lanthanide-DGA complex to enable the design of more efficient lanthanide separation systems. Spectroscopic techniques, such as UV–Visible, Fourier Transformed Infrared Spectroscopy (FT-IR), Nuclear Magnetic Resonance (NMR), and Extended X-ray Absorption Fine Structure (EXAFS), provide information regarding the inner-sphere coordination of a given lanthanide-DGA complex. Scattering techniques, such as Dynamic Light Scattering (DLS), Small-Angle X-ray Scattering (SAXS), and Small-Angle Neutron Scattering (SANS), address nanoscale structures including aggregate sizes and morphology. This review assesses the current state-of-knowledge regarding lanthanide-DGA hydrometallurgical (i.e., solvent extraction systems) interrogated using spectroscopic and scattering techniques to characterize the extracted Ln^{3+} DGA species. Of particular interest to this review is the impact of varied diluents, inclusion and variation of phase modifiers, and DGA derivatization on system characteristics. While there has been extensive literature on the application of DGAs for *f*-element separations, the literature lacks a collective assessment of the speciation of Ln^{3+} in the organic phase. This review provides new insights into the field of DGA separations, explicitly with an application to intra-lanthanide separations. Specifically, this review illustrates the importance of both the co-extraction anion (Cl^-, NO_3^-, or ClO_4^-) as it pertains to both the aggregate size and Ln^{3+} distribution coefficient. It is evident the ability of the anion to disrupt the hydrogen bonding network limits both aggregate size and distribution coefficients according to the Hoffmeister series. This suggests the importance of the large, softer anions with a low charge-to-surface area ratio on encouraging hydrogen bond interactions. In addition, the co-extracted cation (H^+ vs Na^+) is important for mitigating transfer of Ln^{3+} from the aqueous to the organic phase through extensive hydrogen bonding networks. These networks are responsible for forming supramolecular aggregates where a change in morphology is observed with increasing concentrations of H^+ and/or Ln^{3+} in the organic phase.

Abbreviations: CAC, critical aggregate concentration; D, distribution coefficient; DGA, diglycolamide; DHOA, dihexyl octanamide; DiPrDODGA, diisopropyl dioctyl diglycolamide; DLS, dynamic light scattering; DMDODGA, dimethyl dioctyl diglycolamide; DMDOHEMA, dimethyl dioctyl hexylethoxymalonamide; DMDPhDGA, dimethyl diphenyl diglycolamide; DPrDODGA, dipropyl dioctyl diglycolamide; ESI-MS, electrospray ionization mass spectrometry; EXAFS, extended X-ray absorbance fine structure; Formal n-1, 1,1,2,2,8,8,9,9-octafluor-4,6-dioxanonane; FS-13, phenyltrifluoromethyl sulfone; FT-IR, Fourier transform - infrared spectroscopy; FWHM, full width at half maximum; GIFT, Generalized Indirect Fourier Transformation; LAS, limited aggregate size; LLE, Liquid-liquid extraction; Ln, lanthanide; LOC, limited organic concentration; MD, molecular dynamic; NMR, nuclear magnetic resonance; SANS, small angle neutron scattering; SAXS, small angle X-ray scattering; SWAXS, small and wide angle X-ray scattering; T2EHDGA, tetra (2-ethylhexyl) diglycolamide; TBDGA, tetrabutyl diglycolamide; TDdDGA, tetradodecyl diglycolamide; TDDGA, tetradecyl diglycolamide; TEDGA, tetraethyl diglycolamide; THDGA, tetrahexyl diglycolamide; TMAN, Tetramethyl ammonium nitrate; TMDGA, tetramethyl diglycolamide; TODGA, tetraoctyl diglycolamide; TPDGA, tetrapentyl diglycolamide; TPF, third phase formation; TRLFS, time resolved laser-induced fluoresence spectroscopy; TiBDGA, tetra (isobutyl) diglycolamide; VDW, Van der Waals.

* Corresponding author.
E-mail address: jshafer@mines.edu (J.C. Shafer).

https://doi.org/10.1016/j.ccr.2023.215071
0010-8545/

Contents

1. Introduction

1.1. Lanthanide-DGA overview

The fifteen lanthanide (Ln) elements of the 4*f* period and the two elements—Sc and Y—of Group III in the periodic table are collectively referred to as the rare earth elements. These have a variety of applications due to their unique magnetic and electronic properties, some of which include digital technology, clean energy, catalytic converters, lasers, and permanent magnets [1–3]. The multitude of applications for Ln elements has created a worldwide shortage where industrial production is insufficient relative to current demand [1]. Currently, the vast majority of Lns are obtained through mining geological formations followed by hydrometallurgical (i.e., solvent extraction) processing [1,4]. Key operations in hydrometallurgy involve dissolution of the ore into aqueous medium, followed by recovery and separation of trivalent Ln ions (Ln^{3+}) through solvent extraction [5]. Production of purified Ln^{3+} salts are limited by each country's environmental policies [6]. In hydrometallurgy, there are significant environmental, health, and safety concerns associated with large amount of chemical release, particularly with volatile organic compounds and pollution [7,8]. Therefore, it is imperative that responsible waste management occurs and overall waste production is limited [6]. Improving the efficiency of hydrometallurgical lanthanide processing is one pathway to limiting the environmental impact of lanthanide production.

The most challenging step in hydrometallurgical processing involves the partitioning of the lanthanides, which have similar physiochemical properties [3,8–10]. Effective intra-lanthanide separations utilize extractants that take advantage of the lanthanide contraction across the 4*f* period, where a difference in 0.01 Å is observed in the ionic radii of adjacent lanthanides [3,11]. Ideal extractants facilitate fast metal transfer between the two phases and have high chemical stability under operating conditions [5,12]. Extractant classes (i.e., acidic, solvating, and basic) determine the general extraction mechanism [13]. All extractant molecules are surface active agents, since they combine good solubility in select organic diluents with a polar head, responsible for complexation of Ln [3,14,15]. Many extractants are amphiphilic, allowing both hydrophilic and oleophilic environments to co-exist within solution by assembling into nano-scale structures that stabilize each domain [16]. Polar functionalities incorporated on an extractant (e.g., etheric, amidic, carboxylic, or phosphoryl) tune coordination and subsequent separation of target metal ions from aqueous solutions [17].

Intra-lanthanide separations have been extensively studied with phosphoric acids, as they achieve a linear trend in log D_{Ln} across the lanthanides, with an average adjacent lanthanide separation factor of 2.5 [18]. Extraction of Ln is measured by the distribution coefficient (D) – the ratio of Ln equilibrium concentration in the organic phase to the Ln equilibrium concentration in the aqueous phase. A linear trend in distribution coefficients across the Ln

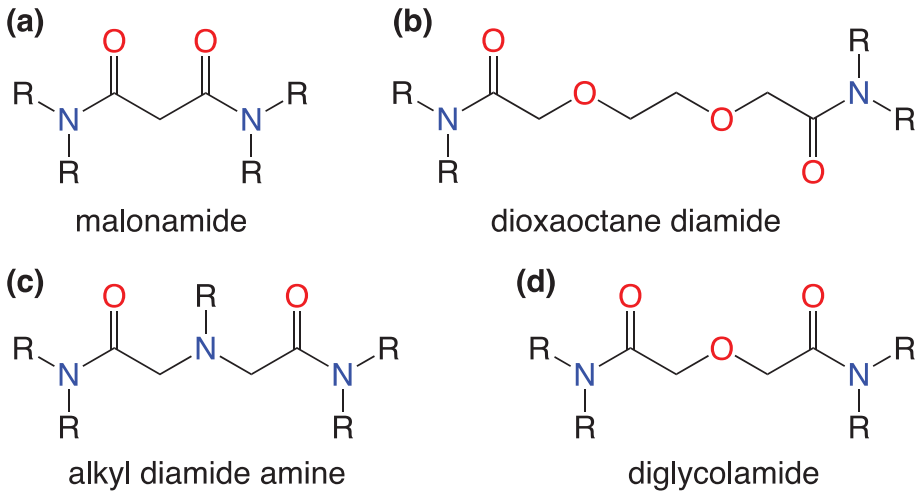

Fig. 1. Center framework structures for solvating extractants (a) malonamide, (b) dioxaoctane diamide, (c) alkyl diamide amine, and (d) diglycolamide are represented, where R represents an alkyl chain.

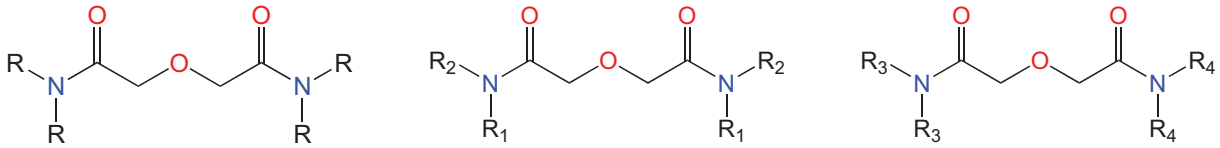

TMDGA	R = methyl	TODGA	R = octyl	DMDODGA	R_1 = methyl, R_2 = octyl
TEDGA	R = ethyl	TDDGA	R = decyl	asym. DMDODGA	R_3 = methyl, R_4 = octyl
TBDGA	R = butyl	TDdDGA	R = dodecyl	DMDPhDGA	R_1 = methyl, R_2 = phenyl
TPDGA	R = pentyl	TiBDGA	R = isobutyl	DiPrDODGA	R_1 = isopropyl, R_2 = octyl
THDGA	R = hexyl	T2EHDGA	R = 2-ethylhexyl	DPrDODGA	R_1 = propyl, R_2 = octyl

Fig. 2. DGA derivatives discussed herein.

series indicates separation efficacy between lanthanides is similar for the series [19–22].

Recent advances in *f*-element separations have focused on CHON based extractants for mitigating the abundance of secondary waste generated [8,23,24]. These investigations have implemented efficient extractants, (tetraoctyl diglycolamide) TODGA or (tetra(2-ethylhexyl) diglycolamide) T2EHDGA, specifically for Ln^{3+} as well as the actinides (An) [25]. Most importantly, the light lanthanides (La-Nd) can be separated from the middle lanthanides (Sm-Gd) with (tetradecyl diglycolamide) TDDGA/*n*-dodecane in just 15 stages [10]. The ability to only have 15 stages to obtain optimal purity for Ln is desirable, as there are typically hundreds of stages required as a result of similar Ln chemistry. These extractants are various alkyl derivatives of diglycolamides (DGAs) and are attractive for hydrometallurgy as both processes operate under similar conditions and they don't require acid-base neutralization during extraction [26,27]. The principal advantage of amides over organophosphorus compounds is their complete incinerability, as well as the benign nature and easy removal of degradation products [28,29]. DGAs abide by the CHON principle with a high affinity for Ln^{3+} and unique selectivity across the Ln series, which may be exploited for separations [30–35]. Other diamide extractants that follow the CHON principle include malonamides, alkyl diamide amines, and dioxaoctane diamides, with their center framework depicted in Fig. 1 [25,32,36,37]. Of these various extractants, DGAs are of particular interest as they play an important role in chelating to Ln^{3+} from HNO_3, have a simple synthesis, milder stripping conditions, higher extraction efficiency and increased partitioning across Ln^{3+} than malonamides [17,32,38–43]. Additionally, DGAs are size selective for metals with ionic radii ranging from 83 to 119 pm (which describes the size of *f*-element cations) making DGAs a suitable extractant for Ln separations [31].

Across the Ln period, log D_{Ln} obtained with linear DGAs steadily increases, until a plateau is formed, deviating from the expected trend if the driving force was the iconic Ln contraction [44]. Probing the origin of this behavior has been the goal of several research efforts, where multiple working hypotheses have formed. Such hypotheses for this unique trend include co-extracted water molecules, co-extracted anions, hydration enthalpy of Ln^{3+}, and the ability for the complexes with heavier Ln^{3+} to reorganize into distinct geometries [6,11,24,28]. As a result of the above-mentioned hypotheses, the extraction efficiency of DGAs is thought to be related to both electrostatic effects and steric hindrances around the binding site [28,41,45]. Chemical and extraction properties of DGAs are strongly dependent on the structure of substituents on the amidic nitrogen atoms and the diluent type [13,26,46–48]. DGAs with shorter alkyl chains, are water soluble and cannot be used for extraction, but those with longer alkyl chains readily dissolve in non-polar diluents (e.g., *n*-alkanes and kerosene) and exhibit poor solubility in water ($\leq$0.04 mM) [23,48–50]. The variety of DGA derivatives and their respective R-groups discussed throughout this paper are shown in Fig. 2.

1.2. Lanthanide-DGA organic phase complexities

Understanding the speciation of the organic phase is particularly difficult with DGAs due to the ability for DGAs to self-aggregate in non-polar diluents (e.g., *n*-dodecane). DGAs have aggregate numbers exceeding that for dimers, corresponding to supramolecular aggregates [51–54]. Formation of supramolecular aggregates depends on the nature of the ligand, number of polar moieties present, basicity of polar moieties, aliphatic chain length, branching of aliphatic chain length, in addition to solvent properties [52,55]. Upon their extraction, polar molecules interact with the polar heads of extractants, acting as nucleates for supramolecular aggregate formation [14,56]. Supramolecular aggregates refer to the ability of DGA extractant molecules to arrange in a typically globular manner around a polar, hydrophilic core surrounded by an oleophilic corona of the non-polar tails of extractants oriented away from the core, stabilizing the aggregate [15,57]. In these systems, the weak van der Waals (VDW) forces beyond the inner coordination sphere of Ln ions control the solution microstructure [16,58]. Diluents with low dielectric constants, cause strong electrostatic forces to drive the outer-sphere coordination of nitrates and chlorides to the extracted Ln^{3+} complex [59]. These varying interactions that are strongly favored in aliphatic hydrocarbon oils with large Bjerrum length – the separation (in Å) between two elementary charges for which the electrostatic energy is comparable to k_BT – can result in several different aggregate shapes, spheres and cylinders are common structural motifs [15,50,60,61]. Specifically in industrial solvent extraction cases, the oil phase systems are described as tubular domains, arising from inter-globular interactions consistent with reverse micellar-like aggregates or bicontinuous microemulsions, thus explaining the high conductivity that is observed in the organic phase [62,63]. Understanding the physiochemical properties and modeling the distribution of various chemical species in the system, requires an understanding of aggregate size, aggregation number, and free extractant concentration [64].

1.3. Mitigating third phase formation and phase modifiers

An unwanted property of interest in these DGA systems is third phase formation (TPF) typically caused by high loading of acid or Ln in the organic phase, resulting in splitting of the organic phase into extractant rich and diluent rich phases [49,50]. This phenomenon occurs through liquid–liquid demixing from aggregates in the organic phase [51]. Consideration of TPF is particularly relevant as the impacts of TPF on industrial processes are always deleterious. For example, commercial scale mixer-settlers and centrifugal contactors are designed for two liquid phases—not three—and the increased viscosity of a third phase adversely affects flow rate [4]. Prevention of TPF involves reducing the dispersive forces inside the polar core of aggregates. Under high loading of either acid or metal, TPF is prevented by introducing phase modifiers into the organic phase [52,53]. Modifiers have been defined by the IUPAC as, "A substance added to a solvent to improve its properties e.g., by increasing the solubility of an extractant, changing interfacial parameters or reducing adsorption losses." [54] Adding phase modifiers increases the complexity of the organic phase by inducing a change in speciation at the molecular and supramolecular scales as their concentration is large relative to that of the extractant [44,46,55–57]. Phase modifiers are commonly selected to be slightly more polar than the diluent, to increase the overall polarity of the organic phase and enhance solubility of aggregates [44]. Increasing the polarity of the organic phase increases the strength of the VDW interactions pushing the LOC to higher concentrations of loading [58,59]. Phase modifiers have been hypothesized to disrupt the polymer chains in the organic phase, hereby preventing TPF [52].

The role of phase modifiers has previously been reported by Whittaker *et al.*, where they hypothesized that phase modifiers solubilize DGA aggregates through outer-sphere interactions [65]. There have been several studies that support this hypothesis, by identifying Ln to be extracted by DGAs as a $[Ln(DGA)_3]X_3$ ($X = Cl^-$, NO_3^-) complex [66]. As anions are located on the outer-sphere, hydrogen bonding interactions are especially relevant to DGA systems [11]. Phase modifiers, such as 1-alcohols, can interact with these Ln-DGA complexes, as their –OH functional group provides hydrogen bond donor capabilities to the hydrogen bond acceptor DGA carbonyl group, and their long alkyl chains allow them to be soluble in organic diluents (e.g., dodecane and kerosene). The addition of phase modifiers breaks up the dimeric and tetrameric aggregates through interaction with co-extracted anions, limiting the interaction between outer-sphere $(DGA)\cdot(HNO_3)$ adducts and the extracted Ln-DGA complex. While phase modifiers are generally understood to inhibit TPF due to their ability to limit interactions between the outer sphere adducts and Ln-DGA complexes, the impact of phase modifiers on *trans*-lanthanide partitioning patterns is poorly understood. Since studies have shown the coordination distance of outer sphere nitrates can be correlated with *trans*-lanthanide partitioning trends [11], understanding how phase modifiers impact outer sphere coordination could be central in understanding the effect phase modifiers might have on *trans*-lanthanide partitioning patterns.

1.4. Current State-of-Knowledge and summarization

Previous literature has explored the use of DGAs for two purposes: Sr^{2+} extraction, as a replacement for 18-crown-6 ether from used nuclear fuel, and separation of Ln^{3+} from An^{3+} with applications to reprocessing high level radioactive waste [67]. Leoncini *et al.* focused on the synthesis of organophosphorus, diamide, and *N*-heterocycle extractants and determining which extractants yield the best distribution ratios for separation of An and Ln [68]. A previous review focused on DGA systems that selectively separated An^{3+} from Ln^{3+}, with particular emphasis on solvent extraction [25]. Werner *et al.* evaluated the design, synthesis, and distribution ratios of supramolecular extractants for An/Ln separations where the most effective extractants completely surround the targeted Ln or An cation [69]. Another review further probed the coordination chemistry of diglycolamides attached to different scaffolds such as calix arenes, pillar arenes, C/N center tripod, benzene center tripod and azacyclane for understanding the selective separation of An and Ln for high level waste reprocessing [70]. The effects and roles of phase modifiers on the properties of TODGA-based process flowsheets for minor actinide (i.e., Am, Np, *Cm*) recovery operations were summarized by Whittaker *et al.* [65]. Applications of several DGAs to the selective extraction of Np, Pu, Am, and Cm from high level radioactive waste–have been accomplished with various ionic liquids as diluents to prevent TPF [71]. A review by Mohapatra *et al.* discussed the extraction of An by DGAs on tripodal ligands and calix arenes in ionic liquids [72].

Throughout the past decade, DGAs have been applied to hydrometallurgical processes and intra-lanthanide separations [6,11]. There are limited studies that focus on probing the structure of the organic phase in DGA *f*-element systems. In addition, it is unknown to what degree some of the diluent molecules are embedded into the aggregate shell, and the morphology of the solvated complex on the chemical nature of the extractant and diluent is unclear [59,73,74]. Whereas there is extensive literature on the synthesis of DGAs and distribution ratios for Ln/An separations, the literature lacks a collective assessment of the speciation of Ln^{3+}

in the organic phase. This review provides new insights into the field of DGA separations, specifically with an application to intra-lanthanide separations. This review focuses on providing an understanding of the lanthanide extracted complex through probing the effects of phase modifiers, diluents, and DGA aliphatic chain length on extraction and aggregation. The effects of ionic liquids as solvents on the structures of extracted DGA complexes is not discussed herein: there are already-two reviews that focus on understanding the DGA systems in ionic liquid media [71,72]. Therefore, the focus of this review is on extraction into alkane and polar diluents. Additional work from the Mohapatra group on attaching DGA molecules to various scaffolds [69,72] is not discussed as the focus herein is on DGA derivatives with various R-groups on the amide moieties. Toward this end, a collective assessment of techniques will be used, solvent extraction, dynamic light scattering (DLS), small-angle scattering, including X-ray (SAXS, small-angle X-ray scattering) and neutron (SANS, small-angle neutron scattering) studies, and various spectroscopy techniques (e.g., optical, vibrational, X-ray, NMR, etc.). A substantial part of this review is focused on understanding the aggregation behavior and mesoscale character in various DGA systems to provide a more holistic view in characterization of organic phase structure.

2. Molecular structure

An attractive technique for Ln^{3+} separations is solvent extraction due to the ease in scalability and flexibility of the process [3]. Solvent extraction involves the targeted transfer of a desired metal into the organic phase from the aqueous phase using an organic-soluble amphiphilic extractant [3]. Specifically for solvating extractants like DGAs, the extraction strength corresponding to Ln^{3+}, is dependent on the ability of the organic phase to solvate the cation in addition to co-extracted anions [59]. Taking a ratio of distribution coefficients corresponding to two Ln^{3+} calculates the separation factor for those select Ln^{3+} of a particular system. For intra-lanthanide separations, it is ideal to have a separation factor of at least two, for efficient industrial applications [3].

Additionally, distribution studies are used to determine two important parameters, separation factors across the Ln^{3+} for optimizing systems for performing intra-lanthanide separations and the average number of extractants involved in an extracted Ln^{3+} complex. Distribution studies are supported by Karl Fischer titrations and potentiometric titrations, which measure the concentration of H_2O and H^+ in the organic phase, respectively. [44] Further investigation of the molecular structure in the organic phase relies on a variety of spectroscopic techniques. FT-IR is useful for evaluating relative strengths of interactions involving DGAs after acid extraction and after metal extraction, based on frequency shifts observed in the C=O, C—O—C, and O—N—O vibrational stretches. In contrast to FT-IR, which focuses on understanding changes to the motifs on DGAs following extraction, UV–Visible spectroscopy can be used to detect changes regarding the inner coordination sphere of select Ln^{3+} through observing changes in the hypersensitive and non-hypersensitive absorbance bands. Hypersensitive bands are extremely sensitive to changes on the inner-coordination sphere of specific Ln^{3+} (Pr^{3+}, Nd^{3+}, Sm^{3+}, Ho^{3+}, Er^{3+}) where an increase in absorbance is correlated with increasing the number of coordinating ligands [75]. Non-hypersensitive bands are additional absorbance bands that are less sensitive than the hypersensitive bands, and provide information regarding the symmetry around Ln^{3+} [29,75]. Fluorescence Spectroscopy is a useful technique for Eu^{3+} containing samples to determine the number (if any) of H_2O molecules are coordinating to Eu^{3+} [50]. Information pertaining to the coordination of Ln^{3+} is provided via EXAFS, which is advantageous because it provides element-specific metrical information about the inner coordination spheres of Ln^{3+} ions in solution phases and solid-state salts.

2.1. Interactions of HNO_3 and $NaNO_3$ with DGAs

Several solvent extraction studies have analyzed the behavior of TODGA in aliphatic diluents, as commonly used in industry [6,11,30,32]. Understanding Ln interactions in these systems, first requires knowledge of the interactions present regarding DGAs, acid, and diluent in absence of Ln. The 0.1 M TODGA/*n*-octane system extracts 7.1 mM H_2O, with the number of extracted H_2O molecules per TODGA molecule rapidly increasing after the initial concentration of HNO_3 exceeds 1 M [49]. Increasing the concentration of HNO_3 in the aqueous phase increases extraction of HNO_3. The number of extracted HNO_3 molecules per TODGA molecule increases with a power dependence of 1.7 on the equilibrium concentration of HNO_3 in the aqueous phase, suggesting the presence of 1:1 and 1:2 DGA:HNO_3 adducts [49,76]. The hypothesis for HNO_3 and H_2O interactions for both the 1:1 and 1:2 DGA:HNO_3 adducts is shown in Fig. 3, as described by Campbell *et al.* and Lefrancois *et al.* [77,78] Interactions between HNO_3, H_2O, and DGAs are critical as they enable the formation of supramolecular aggregates through both protonation and hydrogen bonding interactions.

The quantities of H_2O and HNO_3 that are extracted by T2EHDGA/*n*-dodecane will exploit differences compared to TODGA/*n*-dodecane system. In a 0.1 M T2EHDGA/*n*-dodecane system, the extraction of H_2O increases with increasing T2EHDGA concentration at a constant rate of 0.15 M H_2O per 1 M T2EHDGA [78]. Compared to TODGA, T2EHDGA extracts 10-fold the number of H_2O molecules per 1 M DGA. The addition of HNO_3 to the system results in a drastic increase in the extraction of H_2O after the concentration of HNO_3 is increased to 1 M, with a constant ratio of 3.6 HNO_3 molecules per H_2O molecule [78]. This increase in loading the organic phase results from the presence of both the 1:1 (DGA)·(HNO_3) and the 1:2 (DGA)·(HNO_3)$_2$ adducts [29]. High concentrations of HNO_3 are extracted by DGAs as a result of DGAs

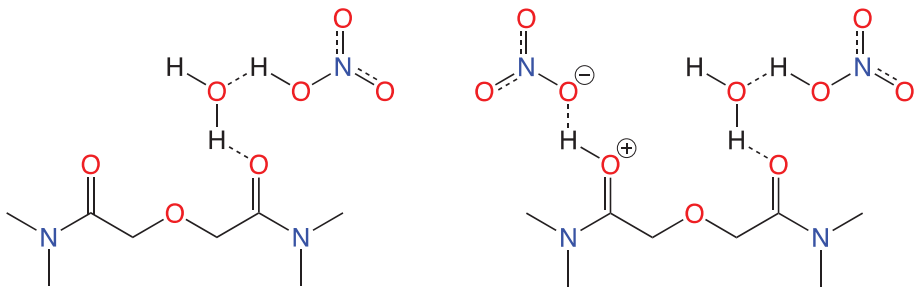

Fig. 3. Interactions of H_2O and HNO_3 with polar component of DGAs, (left) 1:1 (DGA)·(HNO_3) adduct via hydronium nitrate ion pair and (right) 1:2 (DGA)·(HNO_3)$_2$ adduct with an additional HNO_3 directly interacting with C=O [77,78].

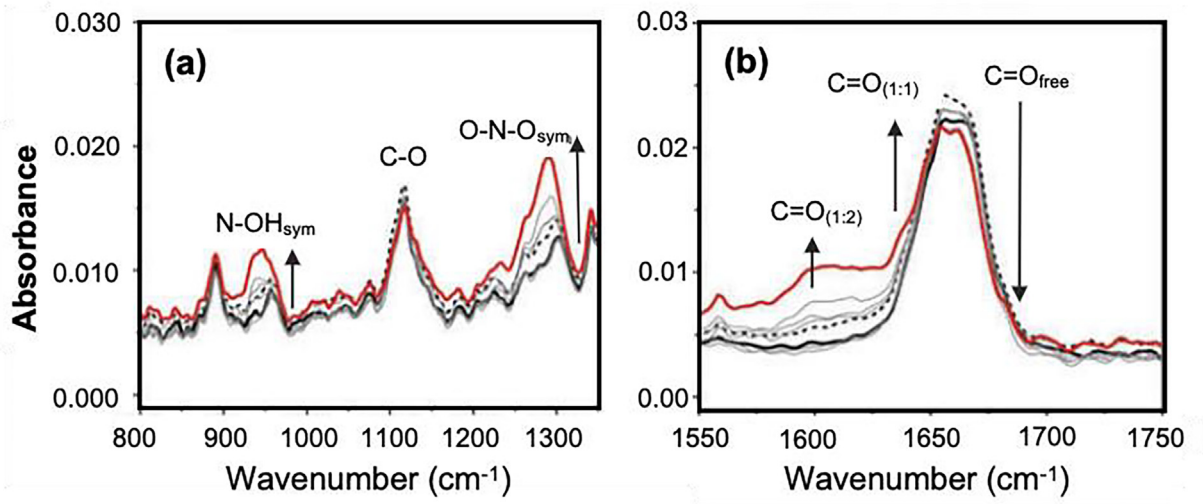

Fig. 4. FT-IR of the organic phase following extraction of 0.1 M to 3 M HNO_3 by T2EHDGA/*n*-dodecane, where (a) is the frequency associated with the NO_3^- and C—O—C stretches and (b) corresponds to the C=O window. Black line indicates solvent before contact with aqueous phase, gray lines indicate increasing HNO_3 concentration, and red line indicates 3 M HNO_3. Figure obtained from Campbell *et al.* [78].

ability to act as a hydrogen bond acceptor, which enables interaction with both H_2O and HNO_3 molecules via hydrogen bonding.

Evidence of both the 1:1 and 1:2 DGA:HNO_3 adducts is supported by FT-IR, as shown in Fig. 4. Of particular interest is the DGA C=O stretch at approximately 1600 cm^{-1}, (as seen in Fig. 4b) where a redshift from the free C=O band in the dry-solvent corresponds to a weaker C=O bond and therefore protonation from HNO_3 [58]. Assigning the shift in carbonyl frequency to HNO_3 presence was validated by no observed change in the C=O stretch following contact with H_2O. For T2EHDGA/*n*-dodecane contacted with 1.25 M HNO_3, there are two different C=O stretches present, with the stretch at 1660 cm^{-1} associated with the 1:1 (DGA)·(HNO_3) adduct and 1604/1610 cm^{-1} is associated with the 1:2 (DGA)·$(HNO_3)_2$ adduct [78]. Increasing the concentration of HNO_3 to 3 M increases the intensity of the vibrational stretch associated with the 1:2 (DGA)·$(HNO_3)_2$ adduct while decreasing the intensity of the stretch associated with the 1:1 (DGA)·(HNO_3) adduct. Under these higher concentrations of HNO_3 there is an in-growth of a O—N—O symmetric stretch at 1292 cm^{-1} and a N-OH symmetric stretch at 945 cm^{-1}, as seen in Fig. 4a [78]. With increasing HNO_3 concentration, the red-shifted C=O stretch and the presence of both O—N—O and N-OH stretches indicate that the 1:2 (DGA)·$(HNO_3)_2$ adduct involves direct protonation of T2EHDGA by HNO_3. The slight redshift observed for the C=O stretch and lack thereof a O—N—O symmetric stretch under low concentrations of HNO_3, results in the 1:1 (DGA)·(HNO_3) adduct having a hydronium nitrate ion-pair interact with T2EHDGA [17,78]. These results support the 1:1 and 1:2 adducts hypothesized for DGAs based on previously determined adducts for malonamide systems, as shown in Fig. 3 [77].

Table 1
Trend in the various (DGA)·(HNO_3) adduct formation in different diluents according to their dielectric constants [81].

Diluent	# DGA Molecules	# HNO_3 Molecules	Dielectric Constant
1-octanol	2–3	1	10.30
Dichloroethane	2–3	1	10.45
Chloroform	2	1	4.9
Toluene	1	1	2.24
Dodecane	1	1–2	2.016

Further investigations to understand interactions between T2EHDGA/*n*-dodecane and extracted HNO_3 utilized ^{13}C NMR. The sp^2 hybridized C=O resonance remained unchanged before and after H_2O contact, resulting in weak hydrogen bonding interactions between H_2O and T2EHDGA, too weak of an interaction to result in a detectable chemical shift [78]. This is consistent with the FT-IR data which exhibited no frequency changes following H_2O contact. Following contact with 1.5 M HNO_3, the chemical shift associated with the sp^2-hybridized C atom of the C=O groups shifts increasingly downfield with increasing HNO_3 extraction, resulting from 1:1 and 1:2 (DGA)·(HNO_3) adducts [78]. After contact with 3 M HNO_3, major peak broadening indicates significant change in organic T2EHDGA speciation, most likely due to the formation of a 1:2 (DGA)·$(HNO_3)_2$ adduct [78]. This increase in (DGA)·$(HNO_3)_2$ decreases the quantity of the (DGA)·(HNO_3) adduct, which is consistent with observations regarding the C=O stretch in FT-IR [78]. The presence of both 1:1 and 1:2 (DGA)·(HNO_3) adducts was supported through solvent extraction. Specifically for 0.1 M T2EHDGA/*n*-dodecane in contact with 3 M HNO_3, 0.12 M HNO_3 was extracted. The concentration of HNO_3 at 0.12 M is greater than the initial extractant concentration of 0.1 M T2EHDGA, indicating the presence of a higher order (DGA)·(HNO_3) adduct. Under these conditions, the 1:1 (DGA)·(HNO_3) adduct is observed, in addition to the 1:2 (DGA)·$(HNO_3)_2$ adduct, as hypothesized in Fig. 3, and supported via FT-IR and ^{13}C NMR [17,33].

In *n*-dodecane and aliphatic diluents solvent extraction and spectroscopic investigations of both linear and branched DGAs report a mixture of 1:1 and 1:2 (DGA)·(HNO_3) adducts. Through modeling the equilibria of HNO_3 extracted by TODGA, Bell *et al.* demonstrate that there are more (DGA)·(HNO_3) adducts in the organic phase than previously described via solvent extraction and spectroscopy [79]. A model with the best fit for experimental solvent extraction data was achieved when 1:1, 2:1, 1:2, 1:3, and 1:4 (DGA)·(HNO_3) adducts were used. The importance of forming these adducts creates extensive hydrogen bonding networks facilitating an increase in polar solutes. For these extended networks to take place, this requires an aqueous phase concentration of HNO_3 greater than 0.7 M, which is important particularly for Ln studies. Understanding interactions between DGAs and polar solutes in various industrially relevant solvents, like alkanes, provides a basis on which to optimize solvent conditions.

To provide a better understanding of differences in (DGA)·(HNO_3) adduct formation, various DGAs were considered. DGA derivatives implemented in this study involved the straight chain tetrabutyl diglycolamide (TBDGA), tetrahexyl diglycolamide (THDGA), and TODGA, in addition to the branched T2EHDGA. A slope analysis for log D(HNO_3) vs log [DGA] yields the average number of extracted HNO_3 molecules per DGA. This slope analysis was performed varying concentrations of DGA/kerosene with 30 vol% 1-octanol in contact with 3 M HNO_3. For each of the DGAs, one HNO_3 molecule was extracted per molecule of DGA [28,80]. This study suggests the formation of a 1:1 (DGA)·(HNO_3) adduct, which deviates from the previously discussed experiments where evidence of higher order adducts were found. The decrease in 1:2 (DGA)·(HNO_3) adduct formation results from the presence of 1-octanol which acts as a hydrogen bond donor, where 1-octanol and DGA interact with each other via hydrogen bonding. This increases the interaction between the solvent and DGA, thereby reducing the interaction of HNO_3 and DGA. These results suggest that if the solvent is made of molecules that act as hydrogen bond donors, there will be a decrease in HNO_3 associated with a DGA adduct.

The importance of the solvent on adduct formation was further observed via solvent extraction methods by Sasaki *et al.*, as shown in Table 1 [81]. Several diluents (1-octanol, dichloroethane, chloroform, toluene, and dodecane) were explored for 0.1 M TODGA in contact with 3 M HNO_3, to identify the various (DGA)·(HNO_3) adducts present. The trend in these select diluents for number of DGA molecules per HNO_3 molecule is as follows: 1-octanol ~ dichl oroethane > chloroform > toluene > dodecane. Interestingly, this trend closely resembles the trend in dielectric constants which is, dichloroethane > 1-octanol > chloroform > toluene > dodecane. These results suggest a change in mechanism between diluents with high dielectric constants (1-octanol and dichloroethane) forming adducts with a lower number of HNO_3 molecules per DGA than the diluents with a low (chloroform, toluene, dodecane) dielectric constant. Ionic liquids are not listed in Table 1 as there are specific review articles that focus on *f*-elements in DGA systems with ionic liquid media [71,72]. The focus of this review is on the solvent effects of alkanes in addition to polar diluents, and how they impact the organic phase structure.

This unique behavior where the trend in number of DGA molecules per HNO_3 molecule follows the trend in dielectric constants for each diluent, resembles protein interactions with H_2O molecules [82]. The ability for H_2O molecules to form a hydration shell around proteins impacts the protein structure. Similarly, the structure of the diluent molecules solvating DGAs influences conformers and organic phase structure. Therefore, as there is an increase in the dielectric constant, there will be a higher degree of solvation occurring from the diluent, without the need for (H_2O)·(HNO_3) adducts to solvate DGAs, thereby reducing the number of HNO_3 molecules associated with DGAs. However, interactions between DGAs and diluent remain unclear when there is a lack of H^+ in the system.

The preference for H^+ in DGA systems indicates the driving force for DGA extraction operates on an anion swing basis, where extraction is favored under a high concentration of H^+ [33,78]. When the concentration of H^+ is limited, as found in neutral media systems ($NaNO_3$ or $LiNO_3$), different interactions are expected between nitrate and DGA. In contrast to observations in acidic media, for T2EHDGA/*n*-dodecane contacted with 3 M $NaNO_3$ (neutral media), no changes were observed in the measured FT-IR spectrum from 1100 cm^{-1} to 1700 cm^{-1} when compared to the FT-IR spectrum for T2EHDGA/*n*-dodecane [29]. This study suggests the importance of H^+ in DGA systems and that the adducts observed in systems containing HNO_3 involve the H^+ and not solely the NO_3^- anion. These spectroscopic investigations indicate that in alkane diluents, H^+ is important for forming the 1:1 and 1:2 (DGA)·(HNO_3) adducts, where without H^+ these adducts do not form. In neutral media systems, there is a different organic phase structure, where any NO_3^- anions that are extracted are not associated with DGAs or form very weak interactions. In the malonamide literature, specific attention to DMDOHEMA and DMDBTDMA shows that Li^+ has very low, almost negligible, extraction, whereas H^+ is readily extracted [83]. The hydration enthalpies of Li^+ and Na^+ are relatively high in comparison to the hydronium cation. Therefore, the organic phase structure greatly depends on the solvent and the concentration of H^+ in the system.

2.2. Speciation of Ln-DGA complexes in alkanes

2.2.1. Slope analysis speciation analysis for DGA systems

Distribution coefficients are fundamental to separations chemistry and understanding organic phase coordination chemistry. The distribution coefficient describes the equilibrium concentrations of a specific species in two phases. However, the distribution ratio is commonly reported as the ratio of total metal concentration in the organic phase to the total metal concentration in the aqueous phase. While slope analysis methods derived from distribution ratios are a common approach to assessing molecular speciation, the high concentrations of water and nitric acid in DGA-containing organic phases can complicate these interpretations.

A relationship between the number of DGA molecules associated with either HNO_3 or Ln can be derived from the chemical equilibrium equation for a DGA solvent extraction system. These equations are expressed in terms of activity; however, it is commonly assumed that the organic phases are ideal, where the activity coefficient is 1. This decreases the complexity of the following equations, where instead of activity of a species, concentration is used.

The relationships obtained following pre-equilibration with HNO_3 are described below with Eqn. 1–4 [79,84].

$$mH^+ + mNO_3^- + \overline{n(DGA)} \overset{K_H}{\leftrightarrow} \overline{n(DGA) \cdot m(HNO_3)} \quad (1)$$

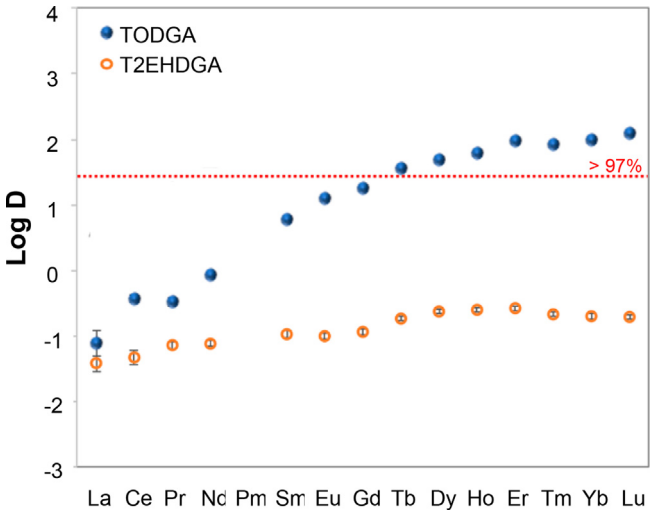

Fig. 5. Log of distribution ratios across the lanthanide series for TODGA (filled blue circles) and T2EHDGA (open orange circles). Organic phase: 0.1 M DGA / Isopar L + 30 vol% Exxal 13. Aqueous phase: 0.5 mM Ln in 3 M HCl. Figure obtained from Stamberga *et al.* [24] The dashed red line represents 97 % extraction.

$$K_H = \frac{\left[\overline{n(DGA)\cdot m(HNO_3)}\right]}{\left[\gamma_{H^+}H^+\right]^m\left[\gamma_{NO_3^-}NO_3^-\right]^m\left[\overline{DGA}\right]_{free}^n} \quad (2)$$

$$m\log\left[\gamma_{H^+}\overline{H^+}\right] - 2m\log\left[\gamma_{H^+}H^+\right] = n\log\left[\overline{DGA}\right]_{free} + \log K_H \quad (3)$$

$$\left[\overline{DGA}\right]_{free} = \left[\overline{DGA}\right]_{initial} - \left[\overline{H^+}\right] \quad (4)$$

Following extraction of Ln, the equilibrium relationship is defined by Eqn. 5–7 [2].

$$Ln^{3+} + 3NO_3^- + \overline{m(DGA)} \overset{K_{ex}}{\leftrightarrow} \overline{Ln(DGA)_m(NO_3)_3} \quad (5)$$

$$K_{ex} = \frac{\left[\overline{Ln(DGA)_m(NO_3)_3}\right]}{\left[\gamma_{Ln^{3+}}Ln^{3+}\right]\left[\gamma_{NO_3^-}NO_3^-\right]^3\left[\overline{DGA}\right]_{free}^m} \quad (6)$$

$$\log D = m\log\left[\overline{DGA}\right]_{free} + 3\log\left[\gamma_{NO_3^-}NO_3^-\right] + \log K_{ex} \quad (7)$$

The activity coefficients for free nitrates in the aqueous phase are calculated according to the extended SIT theory or other suitable methods, as given in Eqn. (8). [2]

$$\log\gamma_{NO_3^-} = -z_i^2 D_H + \sum_j \varepsilon_{H^+}(i,j,I_m) + \varepsilon_{NO_3^-}(i,j,I_m)\log(I_m)m_j \quad (8)$$

Here z (charge), γ (activity coefficient), D_H (limiting law slope), ε (aqueous species interaction coefficient), I (ionic strength), and m (molality).

The relationship between the number of DGA molecules per acid (pre-equilibrium) or per Ln (extraction) is then determined through a linear regression analysis of Eqn. (3) and Eqn. (7), respectively. At a constant acid concentration, the number of DGA molecules per Ln-DGA complex is determined from the slope, whereas the y-intercept represents a combination of the equilibrium constant and anion concentration. While these species are customarily described as functions of concentration, accurate assessment of molecular speciation can require the invocation of species activity and, consequentially, activity coefficients. This is particularly relevant for DGA systems, since DGA systems deviate significantly from ideality because of the large quantities of H_2O and HNO_3 in the organic phase.

The large quantities of H_2O and HNO_3 impact interpretation of slope analysis methods for DGA systems in two ways. The first is accurate assessment of molecular speciation through slope analysis methods most likely requires the use of activity coefficients to describe the activity of a given species. The second is the presence of significant H_2O and HNO_3 provides an opportunity for the formation of many DGA adducts with H_2O and HNO_3. The variety of H_2O and (DGA)·(HNO_3) adduct species means the amount of $[DGA]_{free}$ available for complexation is far below the actual amount. This deviation from ideal systems means models that only include the concentration of DGA would be accurate. As this requires additional modeling of the data, most of the papers use

Table 2
Coordination information of molecules involved in the extracted Ln-DGA complex, obtained via solvent extraction.

Acid System	Ln	DGA	Diluent	no. DGA	no. NO_3^-	PM vol%	Modifier	no. DGA	no. NO_3^-	Ref.
HNO_3	La-Pr	TBDGA	Dodecane			30	1-octanol	2		[80]
	Nd-Lu	TBDGA	Dodecane			30	1-octanol	3		[80]
	La-Pr	THDGA	Dodecane			30	1-octanol	2		[80]
	Nd-Gd	THDGA	Dodecane			30	1-octanol	3		[80]
	Tb-Lu	THDGA	Dodecane			30	1-octanol	4		[80]
	La	TODGA	Dodecane	2.95						[73]
	Ce	TODGA	Dodecane		2.7					[43]
	Eu	TODGA	Dodecane	3.7						[2]
	Eu	TODGA	Dodecane		3.5					[81]
	Lu	TODGA	Dodecane	2.79						[73]
	La-Pr	TODGA	Dodecane			30	1-octanol	2		[80]
	Nd-Gd	TODGA	Dodecane			30	1-octanol	3		[80]
	Tb-Lu	TODGA	Dodecane			30	1-octanol	4		[80]
	Nd	TODGA	1-octanol					2		[102]
	Eu	TODGA	1-alcohol					2.8		[2]
	Eu	TODGA	1-alcohol					2.48	2	[81]
	Eu	TODGA	2-alcohol					2.8		[2]
	Eu	TODGA	2-ketone					2.9		[2]
	Eu	TODGA	Dichloroethane					2.2	2	[81]
	Eu	TODGA	Chloroform					2.6	3.50	[81]
	La-Lu	T2EHDGA	Dodecane	2		30	1-octanol	2		[80]
	La-Pr	DMDODGA	Kerosene			40	1-octanol	3	1	[23]
	Nd-Lu	DMDODGA	Kerosene			40	1-octanol	3	1	[23]
HCl	Nd	TBDGA	Kerosene			30	1-octanol	2		[100]
	Yb	TODGA	Dodecane			10	1-octanol	3		[26]
	La-Lu	TiBDGA	Dodecane			25	1-octanol	2		[28]
	La-Lu	T2EHDGA	Dodecane			25	1-octanol	2		[28]
	Yb	DPrDODGA	Octane			10	1-octanol	2.7		[26]
	Yb	DiPrDODGA	Octane			10	1-octanol	3		[26]
	La-Nd	DiBDDdDGA	Dodecane			25	1-octanol	2		[29]
	Dy	DiBDDdDGA	Dodecane			25	1-octanol	3		[29]
Citric	La-Lu	TODGA	Dodecane	2						[76]
Lactic	La-Lu	TODGA	Dodecane	2						[76]
Malonic	La-Lu	TODGA	Dodecane	2						[76]
Tartaric	La-Lu	TODGA	Dodecane	2						[76]
HNO_3, Malonic	La-Lu	TODGA	Dodecane	3.50						[76]
$NaNO_3$	Eu	TODGA	Dichloroethane	2.11						[81]
	Eu	TODGA	Chloroform	2.39						[81]

the equations with concentration alone, which is important to consider for the results presented herein.

2.2.2. DGA systems with HNO_3

Interactions between DGAs and diluents are crucial for forming supramolecular aggregates [85]. Non-polar alkane diluents have low dielectric constants, where extracted water and acid interact with the polar component of TODGA molecules via hydrogen bonding [49]. In alkane diluents, the distribution coefficient is independent of diluent alkyl chain length, as evident in studies conducted with 0.1 M TODGA in either *n*-dodecane or *n*-octane resulting in similar distribution coefficients [2,49]. The independence of D_{Ln} on alkane diluent has motivated the use of industrial alkane solvents, such as Exxal and Isopar derivatives. Distribution ratios across the Ln series have been measured with such industrial solvents and exhibit the characteristic trend as shown in Fig. 5, which explicitly shows the differences in both extraction and separation ability of TODGA in comparison to T2EHDGA. Specifically, with TODGA, there is an approximately linear increase in log D_{Ln} across the Ln series, which approaches a plateau around Tb. This trend is not observed when T2EHDGA is used, where log D_{Ln} only slightly increases throughout the Ln series with log D_{Ln} values below zero, suggesting minimal extraction. The stark differences observed in trends across the Ln series with TODGA in comparison to T2EHDGA is correlated with linear vs branched alkyl chains and the impact it has on coordination to Ln.

Increasing the concentrations of HNO_3 encourages extraction of Ln^{3+} salts into the organic phase containing TODGA/*n*-dodecane, resulting in both Ln^{3+} and protonated solvates [51,52]. To form either solvate, H_2O acts as a driving force behind local aggregation [86]. These solvates are more polar than the extractant alone, with extracted Ln^{3+}, H^+, and H_2O migrating inside the polar aggregate core [44]. Merging of these solvates into larger aggregates results from extracted H_2O and HNO_3, which increase with increasing initial HNO_3 in the aqueous phase [44,51,57,87]. Favorable extraction for Ln^{3+} under high H^+ concentrations contradicts optimal extraction conditions for solvating extractants. Typically, as observed in other solvating extraction systems (e.g., TBP) increasing the H^+ concentration increases Ln^{3+} extraction, until a point where there is competition between H^+ and Ln^{3+} for TBP [88–90]. The enhancement of distribution values for Ln^{3+} in the presence of H^+ suggests a synergistic effect for DGA systems, even under high acid concentrations [2].

Under acidic conditions, the average number of co-extracted nitrate molecules per Ln in a TODGA complex was determined via a linear regression of a log D_{Ln} vs log [HNO_3], for systems containing either Ce or Eu, as shown in Table 2. Increasing the concentration of HNO_3 above 1 M, resulted in the co-extraction of 2.7 nitrate molecules per Ce [41]. However, this deviates from the expected value of 3 nitrate molecules as indicated in Eqn. (5), to obtain charge neutrality in the organic phase. DGAs are solvating extractants, which are charge neutral meaning that any extracted solutes from the aqueous phase also need to be charge neutral. As Ln^{3+} are extracted as the trivalent cation, this requires 3 nitrate molecules to charge balance the extracted complex. The value of 2.7 nitrates that Metwally *et al.* obtained illustrates the importance for incorporating the activity of each species into Eqn. (7).

This follows trends without Ln present where systems containing greater than 0.7 M HNO_3 were found to form (DGA)·(HNO_3) adducts responsible for increased H_2O and HNO_3 interactions with DGAs. It is therefore suggested that with Ln present, similar behavior occurs with a critical HNO_3 concentration around 0.7 M. Progressing through the Ln series to Eu, results in an increase to 3–4 nitrate molecules associated with each Eu. [81] From these results, a 1:3 Ce:NO_3^- complex forms, whereas some combination of 1:3 and 1:4 Eu:NO_3^- complexes form. Since the extracted species requires charge neutrality, perhaps inclusion of activity coefficients or speciation corrections to the mass balance may be needed to bring the Eu:NO_3^- complexes in alignment with the anticipated 1:3 speciation. The increase in number of nitrate molecules that Sasaki *et al.* reported could be from an inaccurate definition of the concentration of nitrates in the organic phase. If an assumption was made that the H^+ concentration is equal to the NO_3^- concentration, this may not have accounted for the possibility that HNO_3 could be both associated and dissociated in the organic phase. The ability for some HNO_3 molecules to not dissociate would explain the higher number of nitrate molecules reported by Sasaki *et al.* In support of this, Chavan *et al.* showed a hyper-stoichiometric nitrate dependence on Ln extraction can be explained by the extraction of a $[Ln(DGA)_x](NO_3)_3(HNO_3)_y$ complex, where y is the number of nitrates that are extracted as HNO_3 molecules [91]. Coincidentally hyper-stoichiometric complexation of Eu^{3+} was noted with physisorbed TODGA on solid support materials [92].

As high acid concentrations are typically involved in extraction systems, evaluating the number of H^+ incorporated per complex was determined for extraction of Ln^{3+} by TODGA. The distribution of Ln^{3+} from a mixture of HNO_3 and $NaNO_3$ was studied while varying the concentration of HNO_3 and keeping the concentration of nitrate at 3 M. In the Ce system, log D_{Ln} vs log [HNO_3] resulted in an average of 1.1 molecules of HNO_3 associated with the extracted Ce TODGA complex [41]. However, the Eu complex has an average of 2 HNO_3 molecules [81]. In both the Ce and Eu studies, the extracted complexes involve 1–2 HNO_3 molecules in addition to 3–4 nitrate anions. As the Eu system on average contains 1 additional NO_3^- molecule more than the Ce system, and Eu also contains 1 additional H^+ ion, it is likely that both the Ce and Eu systems contain 3 NO_3^- molecules, with Ce containing 0-1 HNO_3 and Eu containing 1-2 HNO_3 molecules.

As protons are important for forming the 1:1 and 1:2 (DGA)·(HNO_3) adducts, H^+ favors Ln^{3+} extraction, creating a synergistic effect. The presence of this effect is important because it explains why H^+ are necessary in this process, where H^+ works with DGAs to extract Ln^{3+} rather than in a competing fashion. Comparison of the role of H^+ interactions across the Ln series reveals a change in the total number of nitrates per Ln. However, there is a constant number of free NO_3^- molecules involved in each Ln complex with an increase in the number of HNO_3 molecules. Having a greater number of HNO_3 molecules per complex would enable larger hydrogen bonding networks with the later Ln, and a higher degree of extraction if the hydrogen bonding networks are responsible for or involved in extraction.

Solvent extraction has been widely used to probe coordination chemistry of metal-extractant interactions in the organic phase. Through varying the concentration of TODGA and analyzing the relationship between log D_{Ln} vs log [TODGA], the slope from the linear regression fit is equivalent to the number of TODGA molecules participating in the extracted Ln^{3+} complex. The assumption that the slope corresponds to the metal-to-ligand ratio is only valid if the extraction mechanism is the same at low and high metal loading [93]. Additionally, if there is deviation from linearity, the slope method also becomes invalid due to the existence of multiple extracted complexes and aggregation phenomena [94]. Interpretation of the slope can also be skewed from other competing equilibria in either the organic or aqueous phase [49]. Applying the slope analysis to the DGA systems presents difficult interpretation due to the polydispersity of aggregates in the organic phase. Nonetheless, it is still important to consider the multitude of studies and their results [49].

The formation of aggregates in the organic phase can be minimized by either working in low HNO_3 concentrations or at low

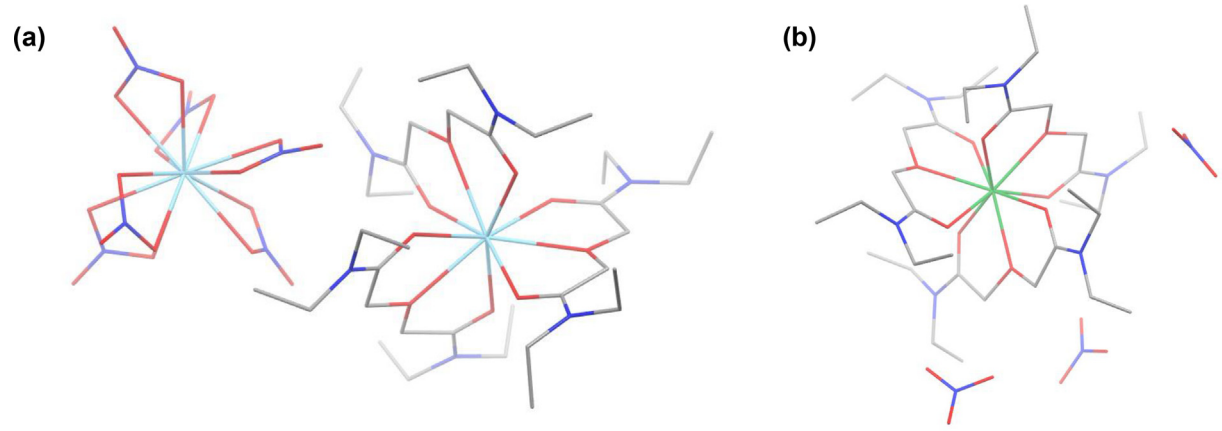

Fig. 6. Two crystal structures occur across the lanthanide series with TEDGA, (a) $[Ln(TEDGA)_3][Ln(NO_3)_6]$ for La-Gd and (b) $[Ln(TEDGA)_3](NO_3)_3$ for Tb-Lu [95,96]. The colors represent different atoms, with La (teal), Tb (green), O (red), N (blue), C (gray), and H are omitted for clarity.

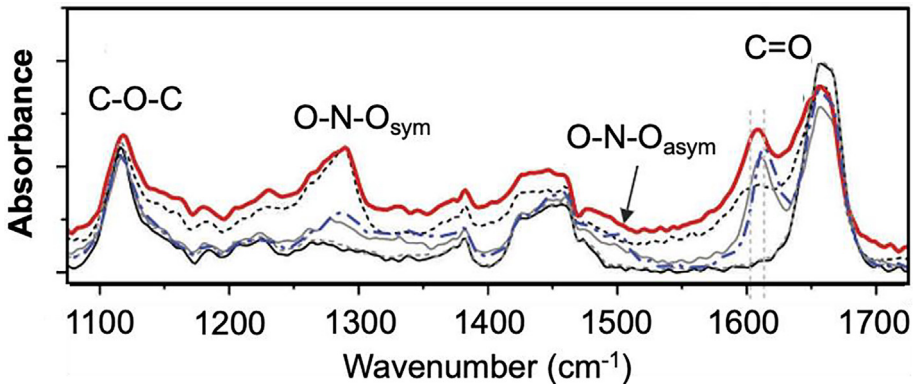

Fig. 7. FT-IR spectra of the organic phase from T2EHDGA/*n*-dodecane in contact with, (black) solvent, (red) 2 mM Eu/3 M HNO_3, (gray) 30 mM Eu/1 M HNO_3, (blue) 15 mM Eu/3 M $NaNO_3$, (black-dash) 3 M HNO_3, (gray-dash) 3 M $NaNO_3$. Figure obtained from Campbell *et al.* [29].

TODGA concentrations [11,30]. In a system of 0.1 M TODGA/*n*-dodecane in contact with 1 M HNO_3 and either La^{3+} or Lu^{3+} yielded a slope of log D_{Ln} vs log [TODGA] corresponding to 2.95 and 2.79, respectively. This indicates the presence of a 1:3 Ln:TODGA complex [73]. The extracted Ln-TODGA complex, therefore, involves 1 Ln^{3+}, 3 TODGA, 3 NO_3^-, and 1–2 HNO_3. As these results were obtained via solvent extraction methods, the values obtained for the number of participating molecules in the complex, merely describes the average number of molecules and does not account for whether they coordinate within the inner- or outer-spheres. Lanthanide coordination complexes typically occur in 8–9 coordinate geometries with O atoms, therefore, the Ln^{3+} cannot accommodate all these molecules in the inner-coordination sphere, suggesting the importance of outer-sphere effects. If three TODGA molecules coordinate via 9 O atoms to the Ln^{3+} in the organic phase, then any co-extracted anions would be involved in outer-sphere coordination. Under systems with dilute HNO_3 (less than 2 M), the number of TODGA molecules involved in the Ln complex across the Ln series remains relatively constant, with the main change in composition occurring in the number of HNO_3 molecules involved in the complex. As HNO_3 does not coordinate with the Ln, these molecules are likely found in the outer-coordination sphere participating in the hydrogen bonding network. Understanding the hydrogen bonding network within the organic phase for these DGA systems provides the foundation for these extended structures and supramolecular aggregates.

This coordination complex stoichiometry is supported by solid-state X-ray crystallographic studies with the shorter, water-soluble DGA derivative TEDGA (tetraethyl diglycolamide) across the 4*f* period. Kawaski *et al.* crystallized La^{3+} to Gd^{3+} where two distinct Ln^{3+} environments form, one with a 1:3 $[Ln(TEDGA)_3]^{3+}$ complex and the second forms a 1:6 $[Ln(NO_3)_6]^{3-}$ complex, as shown in Fig. 6a. [95] In contrast to this, Okumura *et al.* crystallized Tb^{3+} to Lu^{3+} and found the homoleptic 1:3 $[Ln(TEDGA)_3]^{3+}$ with three nitrate molecules in the outer-coordination sphere, as shown in Fig. 6b [96]. It is interesting to note that the light Ln can form a 12-coordinate geometry complex, with six nitrate anions coordinating bidentate. Most importantly, is the change in structure across the Ln series, which could also be relevant for the organic phase Ln-DGA complexes. Organic phase structures are expected to deviate from the crystal structures for several reasons. First, DGAs used as extractants have longer alkyl chains increasing the complexity and movement of the oleophilic tails. Second, the organic phase is a solution where the interactions are dynamic, unlike the static structure of a solid-state crystal structure. Therefore, probing the structure of the organic phase is desirable.

Interactions between Eu and longer, solvent-soluble TODGA has been characterized by EXAFS in both solution and solid-state. This same structural motif—namely the tris-TODGA homoleptic cationic complex—was found for Ce in the organic solution phase of 1 M TODGA in *n*-dodecane obtained by extraction of 0.1 M $[Ce(NO_3)_3]$ from 5 M HNO_3 [60]. Solid-state EXAFS reported for a Nd TODGA

system with either chloride or nitrate as the counter anion are also in agreement, showing that homoleptic $[Nd(TODGA)_3]^{3+}$ complexes are prevalent [59]. These independent EXAFS structures without either water or nitrate molecules in the inner-coordination sphere support both crystal structures with TEDGA either $[Ln(TEDGA)_3]^{3+}$ or $[Ln(TEDGA)_3](NO_3)_3$ about the complexation of the Ln^{3+}, as shown in Fig. 6, in which three DGA molecules coordinate to Ln^{3+}. Additional characterization via Time Resolved Laser-induced Fluorescence Spectroscopy (TRLFS) determined no H_2O molecules were in the inner-coordination sphere of Eu^{3+} in the extracted Eu-TODGA complex, in support of the 1:3 homoleptic $[Ln(DGA)_3]^{3+}$ complex where the Ln^{3+} is coordinatively-saturated by DGAs [50].

These homoleptic 1:3 Ln:DGA complexes are supported by FT-IR spectra from a Eu^{3+}/T2EHDGA/HNO_3 system, as shown in Fig. 7. Following contact with 3 M HNO_3 there is a slight red shift of the C=O band at 1608 cm^{-1} indicating coordination of Eu^{3+} to T2EHDGA. Campbell *et al.* suggested that the appearance of both symmetric and asymmetric O—N—O stretches indicate metal-nitrate interactions, since there was a 206 cm^{-1} shift between the symmetric and asymmetric O—N—O stretches [29]. Comparison of the symmetric and asymmetric stretch of O—N—O provides information regarding whether the nitrate is coordinating monodentate (<115 cm^{-1} difference) or bidentate (>186 cm^{-1} difference) [29]. Campbell *et al.* suggested this is evidence of bidentate nitrate coordination to Eu^{3+}. In contrast to the conclusions by Campbell *et al.*, through analyzing the FT-IR spectra no change is observed for the O—N—O symmetric stretch in 3 M HNO_3 versus the stretch for $Eu(NO_3)_3$ in 3 M HNO_3. Therefore, the lack of shift in the frequency of the O—N—O symmetric stretch with addition of Eu^{3+} likely has zero coordinating nitrate molecules. Instead, the nitrate molecules remain interacting with T2EHDGA molecules that are not participating in a Ln-DGA complex. These results suggest complexation of Eu^{3+} by T2EHDGA, with nitrate anions participating in outer-sphere coordination, consistent with the homoleptic $[Ln(DGA)_3](NO_3)_3$ structure observed in X-ray diffraction and EXAFS. However, this structure does not align with the results predicted by solvent extraction which suggests a 1:2 Ln: T2EHDGA complex, therefore indicating the inner-coordination sphere is saturated with H_2O molecules, as FT-IR indicated there are no bound NO_3^- to Eu. Understanding the Ln-T2EHDGA complex presents challenges, as solvent extraction predicted 1:2 Ln: T2EHDGA coordination complexes, but EXAFS was unable to validate if a 1:2 or 1:3 coordination complex exists, as modeling $[Eu(T2EHDGA)_3]^{3+}$ yielded the same results as $[Eu(T2EHDGA)_2(H_2O)_3]^{3+}$ [24]. To determine if this hypothesis is correct, it would be advantageous to conduct TRLFS studies for evaluating if there are in fact H_2O molecules in the inner-coordination sphere of Ln, specifically with Eu or Tb.

Results from the crystallization studies suggest a change in coordination across the Ln series. Evaluating the differences in FT-IR spectra across the light Ln (La-Nd) indicates a potential structural change in the extracted Ln-DGA complex across the series. A system containing TODGA/*n*-octane was contacted with 1 M HNO_3 and Ln^{3+} [97]. Of particular interest was the observed change in C=O vibrational stretch, where upon contact with La^{3+} the stretch red-shifted from 1653 cm^{-1} to 1612 cm^{-1}, Ce^{3+} to 1606 cm^{-1}, Pr^{3+} to 1607 cm^{-1}, and Nd^{3+} to 1613 cm^{-1}. [97] The initial red-shift for La^{3+} and Ce^{3+}, followed by decreasing red-shifts for Pr^{3+} and Nd^{3+} suggests a change in extracted Ln-complex, specifically regarding Ln-TODGA interactions. The authors did not analyze changes in either the O—N—O symmetric and/or asymmetric stretches making it difficult to draw conclusions regarding coordination of nitrate to the Ln^{3+}. Similarly, changes across the light Ln (La-Nd) were analyzed with particular attention to the C=O vibrational stretch for TODGA/petroleum ether in 5 M HNO_3. Complexation of 0.01 M

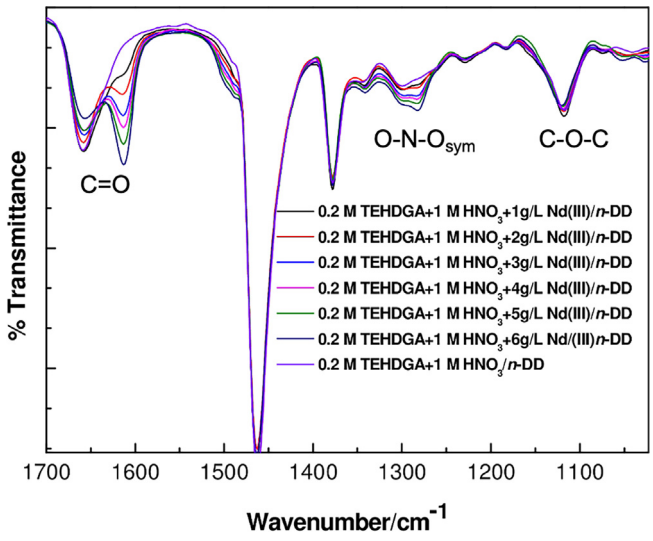

Fig. 8. FT-IR spectrum of the organic phase from T2EHDGA/*n*-dodecane contacted with HNO_3 and Nd^{3+}. Figure obtained from Swami *et al.* [17].

Ln, results in smaller red shifts for the C=O band as the Ln^{3+} ionic radii decrease [98]. While FT-IR results provide information where there is a change in the C=O shift and likely the bond length between Ln-$O_{carbonyl}$ across the Ln series, it does not provide evidence of a different structural complex altogether. These results from FT-IR are consistent with the EXAFS results which determined that the average Ln-TODGA structure is the $[Ln(TODGA)_3]^{3+}$ complex for Ce, Nd, and Eu, with slight changes being observed with respect to the Ln-O bond lengths but not the structure.

However, solvent extraction suggests a change in complexation, following evaluation of the average number of DGA molecules per Ln. Combining these results from the TODGA/*n*-dodecane system, it has been suggested that 3 to 4 TODGA molecules are involved in the extraction of Ln^{3+} [2,57]. While the varying number of TODGA molecules per Ln complex appears to change from 3 to 4, it is important to remember that across the Ln series there are more HNO_3 molecules present in the extracted complex. Therefore, the inner coordination sphere could remain the same with the additional HNO_3 molecules participating in a $(DGA)\cdot(HNO_3)$ adduct that engages in hydrogen bonding interactions to participate in the extracted Ln complex. Thus far, there is a lack of evidence that suggests significant structural changes towards the inner-coordination sphere of Ln complexes in these DGA systems across the Ln series.

To further probe the coordination of Ln^{3+} in these DGA systems, a variety of DGAs in *n*-dodecane were analyzed via solvent extraction. A linear regression analysis of log D_{Eu} vs log [DGA] for 0.1 M DGA/*n*-dodecane in contact with 3 M HNO_3 resulted in a distribution trend following the hypothesis that shorter alkyl DGAs have higher distribution coefficients. The established trend is: tetrapentyl diglycolamide (TPDGA) > THDGA > TODGA > TDdDGA > T2EHDGA [99]. Further proving there is a relationship between the structure of the amidic alkyl chain and the extraction of Ln^{3+}. Shorter alkyl DGAs more efficiently extract Ln^{3+} by means of forming a specific extracted complex that has increased selectivity for Ln^{3+} [51,67]. An average of 4 DGAs per Ln in the extracted complex were reported for shorter DGAs (TPDGA and THDGA), whereas a slight decrease to 3–4 DGA per Ln is observed in the longer DGAs, TODGA and TDdDGA. Sengupta *et al.* attributed the decrease in extraction efficiency associated with increasing the alkyl chain lengths to increasing oleophilicity [99]. These results align with previous data with TODGA for the heavy Ln which also form 1:4 complexes, and have higher distribution values than the lighter

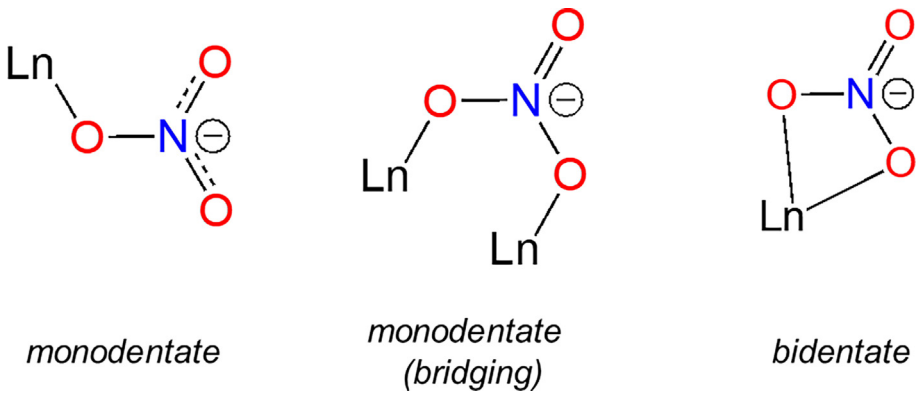

Fig. 9. Various possible interactions between nitrate anion and Ln^{3+}.

Ln. It appears that the 1:4 complex as predicted to involve a $[Ln(DGA)_3]^{3+}$ with outer-sphere nitrates and $(DGA)\cdot(HNO_3)$ adducts, has greater selectivity for Ln than the case with less DGAs involved in the extracted complex. From this hypothesis, fewer DGAs would be involved in the complex with a reduction in hydrogen bonding interactions.

However, the β-branched T2EHDGA derivative performs significantly worse than the linear alkyl DGA derivatives [80]. Increasing the alkyl chain lengths and the addition of branching reduces the binding strength of Ln^{3+} from steric interactions, resulting in an increase in VDW dispersion forces and a decrease in extraction efficiency [24,30,99]. Particularly for T2EHDGA, the reduced distribution coefficients are the product of the organic phase being dominated by monomers and dimers [80].

In the case of T2EHDGA, solvent extraction studies suggest the formation of a 1:2 Ln:DGA complex. To probe changes in the DGA coordination in the organic phase, a system containing 0.2 M T2EHDGA/*n*-dodecane in contact with 1–6 g/L $Nd(NO_3)_3$ in 1 M HNO_3 system was studied, where the FT-IR spectra are displayed in Fig. 8. Swami *et al.* observed an in growth of a C═O stretch at 1610 cm^{-1}, which increases in intensity with increasing Nd^{3+}, where the intensity of the 1663 cm^{-1} band decreases [17]. An ingrowth of another C═O band is red-shifted and associated with coordination of Nd-O via the C═O motifs, where the C═O bond is weakened as a result. As more Nd^{3+} is added to the system there is an increase in the Nd-T2EHDGA complex with a decrease in the $(DGA)\cdot(HNO_3)$ adduct. The addition of Nd^{3+} increases the intensities for the O—N—O symmetric stretch at 1298 cm^{-1} and ingrowth of a redshifted band at 1280 cm^{-1} is observed. Increasing Nd^{3+} increases the O—N—O asymmetric band, observed as a shoulder at 1500 cm^{-1}. [17] Based on this relationship between the O—N—O symmetric and asymmetric stretch, the Nd-T2EHDGA system having a difference in wavenumbers of ~ 198 cm^{-1}, and the progressive redshift upon increasing Nd^{3+}, it is likely that nitrate anions coordinate bidentate to Nd^{3+}. These various Nd-NO_3^- interactions are shown in Fig. 9.

Although nitrate coordinating bidentate to Ln^{3+} appears likely, as suggested by FT-IR evidence and that bidentate coordination typically exhibits lower required energy, this might not be the case in these DGA/*n*-alkane systems. Specifically for acidic media, when H^+ is available for hydrogen bonding networks, monodentate nitrate coordination to Ln^{3+} could happen. [58] This is the result of lower energy of the monodentate nitrate Ln^{3+} interaction and with monodentate coordination, more oxygen atoms are available for hydrogen bonding thereby increasing the hydrogen bonding network. To make the conclusion regarding the coordination of nitrate in this system, additional studies are needed that support these results.

This is particularly important because the two FT-IR studies with T2EHDGA, Nd [17] and Eu [29] provide evidence of different structures. The main difference between these structures is the location of NO_3^-, which has evidence for inner-sphere coordination for Nd, but this is not the case with Eu. In the Eu-T2EHDGA system, NO_3^- anions are likely located in the outer-coordination sphere as predicted for TODGA. The limited number of spectroscopic investigations with these systems makes it difficult to draw conclusions as to what the extracted Ln structure is. With this understanding of various Ln-NO_3 interactions and changes in the organic phase observed via FT-IR, comparisons can be made to the crystal structures for Ln-TEDGA complexes. The Ln-TEDGA crystal structures are consistent with the FT-IR spectra observed for both Nd^{3+} and Eu^{3+} with T2EHDGA. Evidence for Nd-NO_3^- coordination could either arise from a mixed coordination of NO_3^- and T2EHDGA coordinating to Nd^{3+}, or it could result from multiple unique Nd^{3+} centers existing in each complex. Conclusive critiques regarding a specific Ln-DGA structure require additional studies that probe the organic phase across the Ln for the particular DGA of interest. As the Ln series is traversed, for the middle Ln (Eu), the crystal structure of $[Ln(TEDGA)_3](NO_3)_3$ is consistent with FT-IR data, where no coordinating nitrates are observed [96]. This hypothesis for change in molecular structure across the Ln series is supported by TRLFS which had no evidence of coordinating H_2O molecules for Eu^{3+} and Tb^{3+} [100]. The spectroscopic investigations conducted thus far indicate there is a change in the interactions between Ln^{3+}/DGA/HNO_3 across the Ln series. The change in interactions for Ln^{3+}/DGA/HNO_3 species across the Ln series impact the observed distribution coefficients.

2.2.3. Acidic effects and the Hoffmeister series

In addition to understanding speciation of Ln-DGA molecules from HNO_3, it is equally important to assess how the extracted species change in different acids, as it is common for hydrometallurgical process to use either HNO_3 or HCl [101]. The distribution coefficients of Ln^{3+} in various strong acids were determined for TODGA/*n*-dodecane following contact with 0.01 M to 6 M HCl, HNO_3, and $HClO_4$. Gujar *et al.* demonstrated the ability of 0.01 M $HClO_4$ to result in distribution values exceeding that for the HNO_3 and HCl systems by 10,000-fold, [102] resulting in more efficient extraction of both H_2O and Ln^{3+} [85,103]. These results have led to the development in the following extractability trend, $HClO_4$ > HNO_3 > HCl. This has been attributed to the polarizability of the anion and the stronger hydration or greater dehydration penalty on transfer to organic phase depending on the anion [54,59,85].

Although HCl is not effective in extracting Ln^{3+}, inorganic chloride salts – $(FeCl_4)^{1-}$ or $(BiCl_4)^{1-}$ – impose a unique synergistic

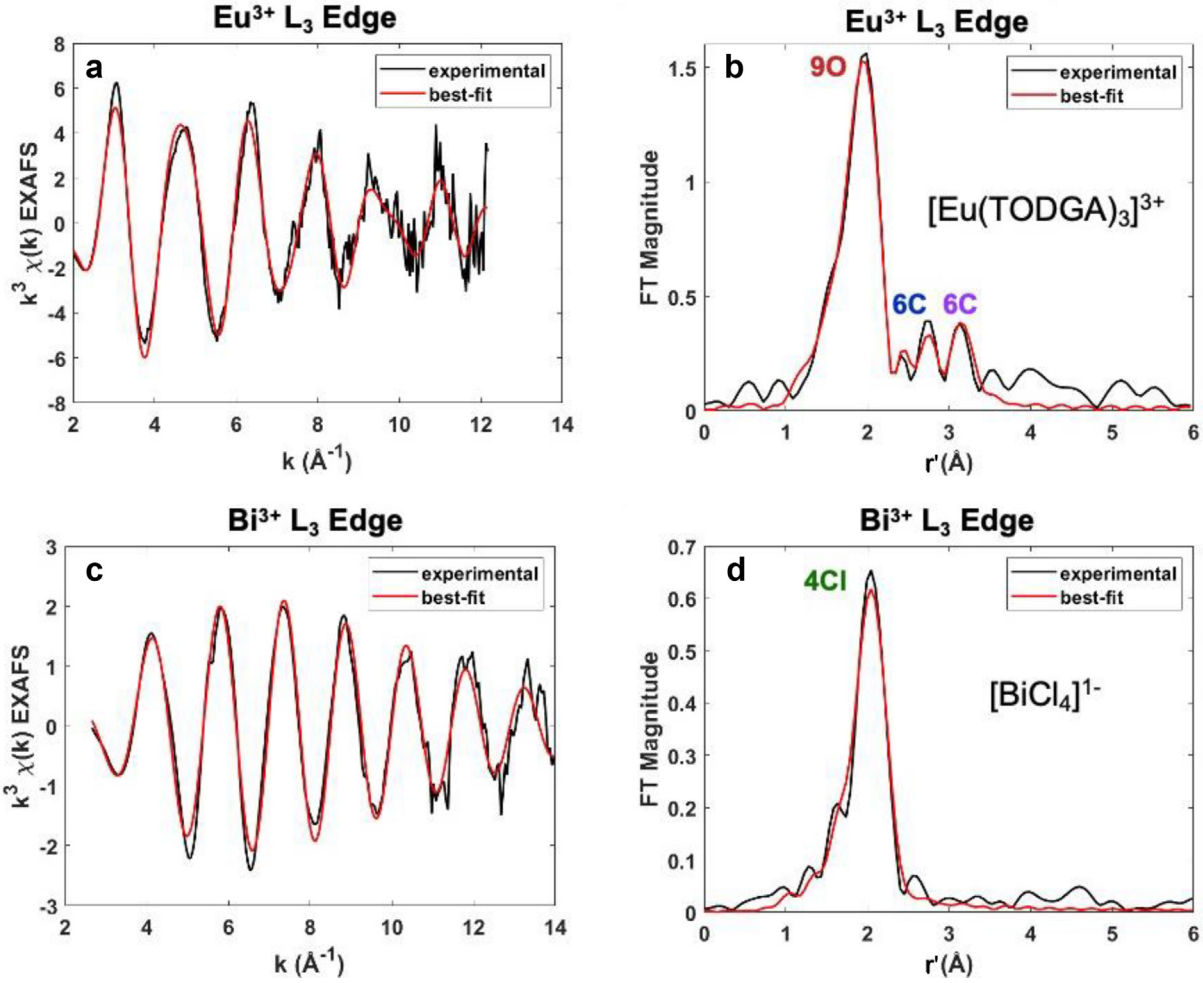

Fig. 10. Eu and Bi L_3-edge EXAFS for the system TODGA/methanol – Eu^{3+}/ $(BiCl_4)^{1-}$. (a) Experimental Eu EXAFS and fit using a 3 shell (O, C, C) model, (c) Experimental Bi EXAFS and fit using a 1 shell (Cl) model for Bi^{3+}, and Fourier transform data for (b) Eu^{3+}, and (d) Bi^{3+}. The colors of the atoms in the corresponding structure (Fig. 11) correspond to the colors on the labeled peaks [66].

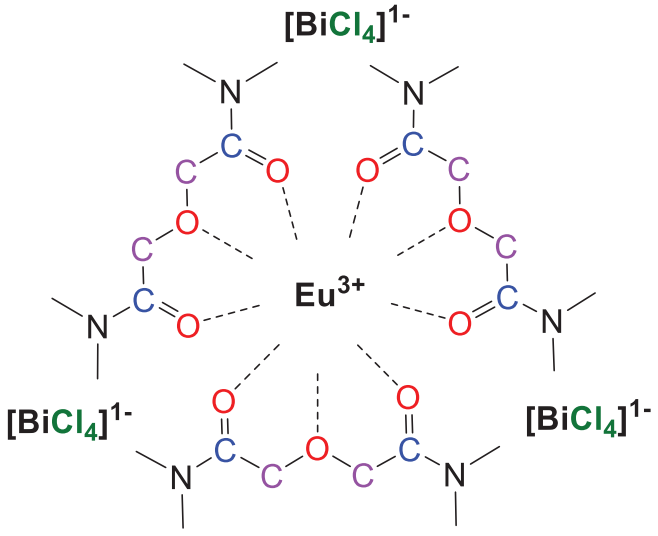

Fig. 11. Eu^{3+} coordination structure, $[Eu(TODGA)_3]$ $[(BiCl_4)_3]$ hypothesized from EXAFS organic phase data.

trend on Ln^{3+} extraction [104]. These *d*-block inorganic anions prevent disruption in the hydrogen bonding network, encouraging more acid transfer. Efficient extraction of trivalent cations follows the Hoffmeister series where $Cl^- < NO_3^- < FeCl_4^- \sim BiCl_4^- < ClO_4^-$ [105]. This suggests the large, softer anions (e.g., ClO_4^-) having a lower charge-to-surface ratio, bind to solutes. This contrasts the behavior of small, harder anions (e.g., Cl^-) with a higher charge-to-surface ratio that repel solutes. The large, softer anions are thereby able to be positioned in cavities between DGAs and diluents interacting with the extracted Ln-DGA complex without disrupting the water network. These results with various acids further support the fact that encouraging hydrogen bonding networks are vital for extraction of Ln, and the results previously obtained with the linear DGAs where the inner-coordination sphere is saturated with DGAs $[Ln(DGA)_3]^{3+}$ with co-extracted solutes participating in the outer-sphere.

Exploration of changes in coordination in the presence of various salts was accomplished with EXAFS. Similar to the HNO_3 system, the molecular structure was determined via EXAFS for a Eu^{3+} TODGA solid-state complex from methanol resulting in 9 ± 1 oxygen atoms with an average distance of 2.40 Å from the Eu^{3+} cation [66]. Thus, resulting in a $[Eu(TODGA)_3]^{3+}$ complex coordinating through 9 oxygen atoms with no features identified beyond carbon atoms, despite the presence of the bismuth tetrachloride anion [66]. The results from the Eu^{3+}/TODGA/$(BiCl_4)^{1-}$ study are shown in Figs. 10 and 11, where both the Eu^{3+} and Bi^{3+} were modeled via their L_3-edge EXAFS. For Bi^{3+}, the absence of

interacting atoms beyond the first-coordination sphere is evident in the Fourier transform data. As previous results with Ln-TODGA systems have suggested location of solute molecules to be in the outer-sphere, the complexes $[Eu(TODGA)_3]^{3+}$ and $[BiCl_4]^{1-}$ could be interacting through outer-sphere effects at longer distances than those detectable via EXAFS, as depicted in Fig. 11.

Interestingly, this same $[Eu(TODGA)_3]^{3+}$ structure was found in HCl media, suggesting the differences arising in solvent extraction distribution coefficients are impacted by the hardness of Cl^- and its ability to breakdown the extended H_2O hydrogen bonding network. The effectiveness of HNO_3 versus HCl on Ln^{3+} distribution values was demonstrated by Narita *et al.* with dimethyl diphenyl diglycolamide (DMDPhDGA) [32]. The DMDPhDGA-HNO_3 system is significantly more effective at both extracting (approx. 10,000 times more for Lu^{3+} extraction) and partitioning the lanthanides than the corresponding DMDPhDGA-HCl system. This hypothesis that the molecule's charge density is important in either encouraging or disrupting the hydrogen bonding network was further explored across the Ln.

DFT calculations were performed on 1:3 $[Ln(DGA)_3]^{3+}$ complexes that were validated through comparison of Ln-O bond lengths to Ln-TEDGA crystal structures and Ln-TODGA EXAFS [6,33,106–110]. Multiple studies reported a decrease in Ln-O bond length for heavier Ln, consistent with the Ln contraction where heavier Ln have a greater charge density [6,11,47,59,73,106,110]. Stronger electrostatic interactions between Ln ions and DGA oxygen donors are the result of greater overlap of donor–acceptor orbitals strengthening the Ln-DGA interaction for heavier Ln [6,111]. Incorporating outer-sphere anions (NO_3^- or Cl^-) into the calculation has proven to be invaluable for predicting the trend in D_{Ln} by DGA molecules [73]. This trend can be predicted through using either of two methods, 1) calculating free energy of extraction after implementing a dispersion model for a large molecular system (DFT-D3) in a $[Ln(TMDGA)_3](NO_3)_3$ complex [73] or 2) measuring the bond distance from Ln to outer-sphere anions (either Ln-Cl or Ln-ONO_2) in a $[Ln(TEDGA)_3]X_3$ (X = Cl^- or NO_3^-) complex [11]. Methylating the backbone of TODGA (Me_2-TODGA), allowed Wilden *et al.* to study the effects of additional steric interactions with outer-sphere nitrates [106]. In a [Ln(*cis*-Me_2-TODGA)$_3$]$(NO_3)_3$ complex, the HOMO is composed of only p-orbitals on oxygen atoms of outer-sphere nitrate molecules [106]. This suggests that the arrangement of nitrate molecules and interactions in the outer-sphere drive stability of Ln-DGA complexes. DFT calculations for $[Ln(TEDGA)_3](NO_3)_3$ and $[Ln(TEDGA)_3]Cl_3$ complexes, found the repulsion between either chloride or nitrate molecules and TODGA increases across the 4*f* period pushing the anions further away from Ln^{3+} [59]. This results from a higher charge density for the Ln-DGA complex for harder, heavy Ln^{3+} with smaller ionic radii, where solutes are repelled. In this case, there is a larger distance between heavy Ln^{3+} and co-extracted outer-sphere anions where the polar surfaces of either Cl^- or NO_3^- are more exposed allowing interactions with outer-sphere H_2O molecules [11,59]. Brigham *et al.* evaluated the energies of the hydrogen bonding interactions with $[Ln(TEDGA)_3](NO_3)_3$ and $[Ln(TEDGA)_3]Cl_3$ complexes [59]. The authors found small energies of hydrogen bonding interactions, indicating that TODGA and *n*-dodecane molecules can slightly stabilize Cl^- and NO_3^- anions, forming ion-pairing in non-polar solvents [59]. These DFT calculations have shown that outer-sphere interactions not only stabilize the extracted $[Ln(DGA)_3]^{3+}$ complex, but are the driving force for the unique Ln selectivity.

Further investigations into the extraction mechanism for DGAs following the Hoffmeister series compared the impact of HNO_3 to organic acids (e.g., citric, lactic, malonic, and tartaric). In the aqueous phase, 3 M organic acids were contacted with 0.2 M TODGA/*n*-dodecane resulting in regression analysis of log D_{Ln} vs log [TODGA] of approximately-two, suggesting 1:2 Ln:DGA coordination complexes [76]. The trend across the Ln^{3+} was similar to that observed with HNO_3 but with significantly lower distribution coefficients. This decrease in distribution coefficients results from ion-pair extraction where Ln^{3+} were stabilized in the aqueous phase by ion-pairing/complexation with carboxylate groups on the organic acids [27,76]. Of all the organic acids tested, malonic acid has the most promise as it has higher distribution coefficients and has a relatively linear trend from La to Tb. Thus, another system was studied involving 0.2 M TODGA/*n*-dodecane in contact with 1 M malonic acid and 0.05 M HNO_3, where adding even the smallest quantity of HNO_3 increases the average number of TODGA per Ln^{3+} above three, suggesting coordination complexes with 1:3 and higher (e.g., 1:4) stoichiometries [76]. From analyzing the extractability with organic acids and comparing that to the extractability with strong acids, it is evident that the extraction mechanism for Ln^{3+} by DGAs follows the Hoffmeister series where organic acids < Cl^- < NO_3^- < $FeCl_4^-$ ~ $BiCl_4^-$ < ClO_4^-. These results suggest that the extraction mechanism is dependent upon the anion's charge-to-surface ratio or "softness" in encouraging interactions with Ln-DGA complex by situating in extractant cavities and maintaining the H_2O hydrogen bonding network.

Although there is no evidence for the co-extracted solutes (nitrate, chloride, and perchlorate anions) participating within the inner-sphere of Ln, their role in outer-sphere effects via hydrogen bonding interactions plays a significant role. The changes in hydration energy across the Hoffmeister series suggests that the ability for an anion to either promote or inhibit hydrogen bonding interactions, directly effects the distribution ratio of Ln. Therefore, interactions occurring in the outer-sphere of the Ln complex are driving the extraction of Ln by DGAs.

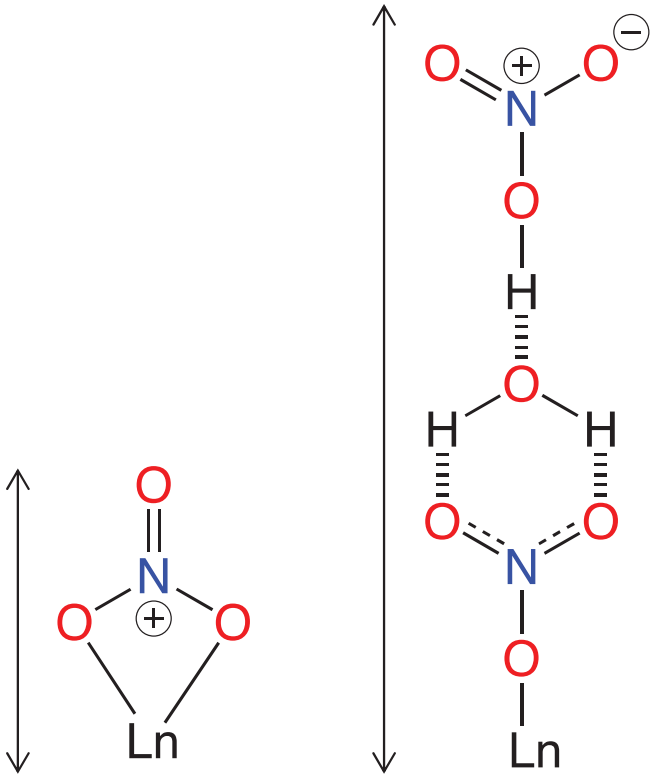

Fig. 12. NO_3^- coordination modes and outer-sphere effects for (left) neutral media and (right) acidic media. The figures are sourced from materials in Ellis *et al.* [146].

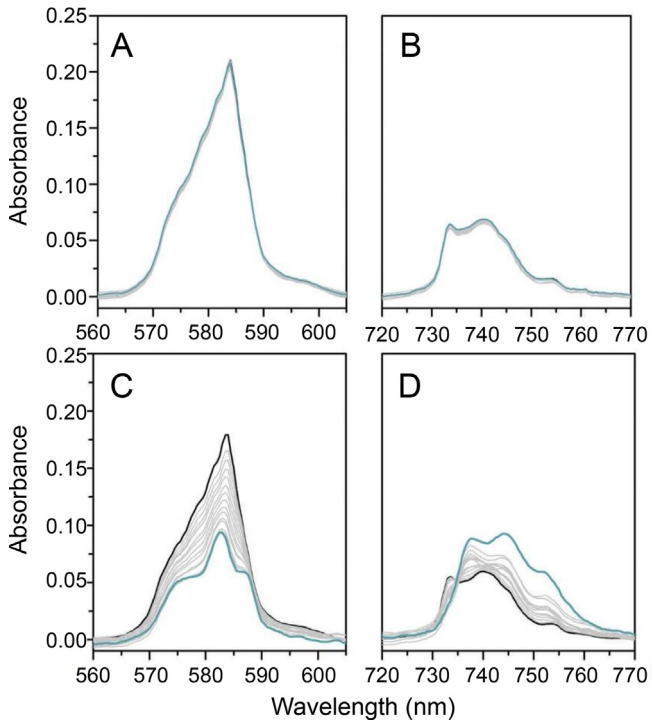

Fig. 13. UV–Visible spectrophotometric titrations for 0.1 M T2EHDGA/*n*-dodecane in contact with 15 mM $Nd(NO_3)_3$ in 3 M $NaNO_3$ and equilibrated with either H_2O (A, B) or 3 M HNO_3 (C, D). Figure obtained from Campbell *et al.* [29].

2.2.4. Importance of H^+ in speciation

In addition to determining the importance of the counter-anion in extraction and the molecular structure, the role of the counter-cation, H^+, was determined through comparison of acidic (HNO_3) to neutral ($NaNO_3$) media. An increase in the distribution coefficients of Ln^{3+} in a T2EHDGA/*n*-dodecane system were observed for HNO_3 when compared to $NaNO_3$ [78]. This suggests HNO_3 participates and/or facilitates the formation of the extracted Ln^{3+} T2EHDGA complex. The importance of HNO_3 in the system was further supported by measuring the distribution ratios of Eu^{3+} in the presence of either 2.5 M HNO_3 or 2 M $NaNO_3$ in contact with 0.1 M T2EHDGA/*n*-dodecane, where a drop by more than two orders of magnitude was observed when switching the counter cation from H^+ in HNO_3 to Na^+ in $NaNO_3$ [29]. The selectivity of T2EHDGA for HNO_3 instead of $NaNO_3$ indicates that the solvating extractant is selective towards the nitrate source in the system and that HNO_3 is vital for pre-organization of the supramolecular extractant structure (presumably through hydrogen-bonding associations that are not possible with Na^+) involved in Eu^{3+} extraction [29,44,83,85]. As previously discussed, the extraction mechanism appears to change after the concentration of HNO_3 exceeds 1 M, as evident by the hyper-stoichiometric nitrate dependence for the extraction of Eu^{3+} [29]. Increasing the system's acidity results in more hydrogen bonding in the core since DGAs, HNO_3 (both associated and dissociated), and H_2O are all hydrogen bond promoting molecules, either as a donor or acceptor [91].

To provide insight regarding if different nitrate sources effect the Ln^{3+} coordination environment, a 0.1 M T2EHDGA/*n*-dodecane system in HNO_3 was compared with $NaNO_3$, following addition of Eu^{3+}, as shown in Fig. 7. Under neutral conditions (3 M $NaNO_3$) a red-shift was observed in the C=O stretch at 1614 cm^{-1} but was blue-shifted in comparison to the 3 M HNO_3 system. This indicates a weaker C=O bond and therefore a stronger Eu-O bond in acidic (HNO_3) media. In $NaNO_3$, the O—N—O symmetric stretch was absent following $NaNO_3$ contact, but appeared following Eu^{3+} contact, indicating either nitrate coordination to Eu^{3+} or some degree of HNO_3 interaction (as acidic Eu^{3+} sources have some concentration of H^+). The availability of H^+ in the Eu^{3+} source makes it difficult to make conclusions regarding the location of NO_3^- molecules in this system. Based on previous data, it would be unlikely that a 1:3 Eu:T2EHDGA complex forms due to the steric hindrance of the β-branching of T2EHDGA with the remainder of the inner-sphere saturated with either H_2O or NO_3^- molecules.

The change in Eu^{3+} DGA speciation in $NaNO_3$ media was further determined via solvent extraction of TODGA/*n*-dodecane from 3 M $NaNO_3$. A regression analysis from log D_{Eu} vs log [TODGA] resulted in a decreased average number of TODGA molecules per Eu^{3+} of 3.17 in $NaNO_3$ as compared to 4.10 in HNO_3 [81]. A reduced number of DGA molecules per Ln^{3+} results from reducing the propensity for outer-sphere coordination in neutral media, starved of H^+. This further supports the hypothesis that the fourth DGA involved in the Ln-TODGA complex participates in the outer-coordination sphere through hydrogen interactions as a (DGA)·(HNO_3) adduct. Different interactions, specifically regarding outer-sphere coordination following the Ln-NO_3^- interaction are shown in Fig. 12. In the case of Na^+ environment, the hydrogen bonding interactions are restricted due to the system being H^+ starved. However, when H^+ is involved in the system, there can be an expansive hydrogen bonding network allowing interactions between the extracted Ln complex and additional molecules beyond the inner-sphere.

In support of the importance of H^+ in the extraction of Ln^{3+} from *n*-alkane diluents, the coordination sphere of Nd^{3+} was further studied via UV–Visible spectroscopy. For a system containing 0.1 M T2EHDGA/*n*-dodecane, there was no change in both the hypersensitive band and non-hypersensitive bands when varying the concentration of T2EHDGA from 0.09 M to 0.9 M, following contact with H_2O, as shown in Fig. 13. [29] This is consistent with other spectroscopic data, both FT-IR and NMR which also show no spectral changes under these conditions. Similar observations were noted when in contact with 3 M $NaNO_3$, although under acidic conditions (3 M HNO_3) there was a drastic change in Nd^{3+} electronic structure for both the hypersensitive Nd^{3+} band at 584 nm and the non-hypersensitive band at 735 nm. This resulted in two Nd^{3+} species, as indicated by the singular isosbestic point at 735 nm. Increasing the absorbance of the hypersensitive band results in increasing the number of coordinating ligands, accompa-

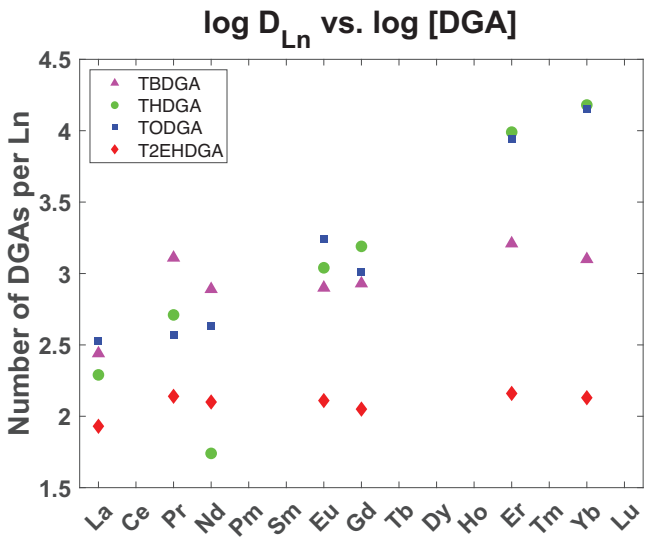

Fig. 14. Trends across the Ln series for various DGAs/kerosene with 30 vol% 1-octanol in contact with 3 M HNO_3 [80].

nied by a decrease in the metal-to-ligand bond distance. Regarding the system containing 3 M HNO_3, a decrease in the hypersensitive band and an increase in the non-hypersensitive band, indicates a loss of symmetry following Nd^{3+} extraction while decreasing the number of coordinated ligands.

Systems that can achieve a larger number of DGAs per Ln are typically more selective (have a higher distribution ratio) for Ln. It was previously discussed that the shorter linear DGAs (TBDGA, THDGA), which can achieve a 1:4 Ln:DGA ratio, form a pre-organized structure with DGAs through a hydrogen bonding network. When a system is H^+ starved, this hydrogen bonding network is restricted thus preventing the pre-organized structure selective for Ln^{3+}, therefore reducing the distribution ratio of Ln and the number of DGAs per Ln. Further proving that the extensive hydrogen bonding networks are vital for the structures that result in high distribution ratios of Ln.

2.3. Impact of phase modifiers on Ln-DGA speciation

Maintaining the chemical properties of aliphatic diluents while preventing TPF is desired for applying intra-lanthanide separations via DGAs to industry. A focus of recent investigations involves introducing phase modifiers into the DGA/*n*-alkane system to increase polarity of solvent [65]. As the solvent is a homogeneous fluid, extraction properties and viscosity of the solvent can be tuned by using aliphatic alcohols as phase modifiers [94]. Effective phase modifiers have high interfacial tension so they cannot escape to the aqueous phase. Three classes of phase modifiers, 1-alcohols, organophosphorus compounds (TBP), and amides (including DMDOHEMA and DHOA), are attractive for biphasic solvent extraction systems as they have high interfacial tension [4,44].

These different classes of phase modifiers enable different interactions with DGAs. Alcohol phase modifiers are hydrogen bond donors, enabling interactions with the hydrogen bond acceptors (DGAs). In contrast, TBP and amides are hydrogen bond acceptors, which will compete with DGAs for protons. Herein this review addresses systems involving 1-alcohols as phase modifiers, while TBP and the amides are important organic compounds in *f*-element chemistry [112], there are limited studies that explored their coordination chemistry across the Ln period. An understanding of the coordination chemistry with TBP and various amidic phase modifiers is of interest and an avenue for future investigations. Evaluation of systems utilizing multimodal techniques have resulted in identifying systems that enhance the separation efficiency without causing TPF, which is discussed in detail below [12,22,113]. Understanding the mechanisms behind solvent extraction is vital for developing the extracted Ln^{3+} complex, which is based on the ability for an extractant to chelate and form supramolecular aggregates [113]. This unique complexation observed in the presence of synergistic systems could be from the presence of mixed (extractant and phase modifier) aggregates rather than pure (extractant) aggregates [113]. The ability for synergistic extraction to occur depends on aggregate nucleation resulting from the extraction of Ln^{3+}, water, and acid [113].

Table 3
^{1}H NMR chemical shifts before and after loading with Eu^{3+}. δ and δ' represent the chemical shift of methylene in between the carbonyl C and ether O groups. [80].

Ligand	δ	δ'	$\Delta\delta$
TBDGA	4.32	4.75	0.43
THDGA	4.31	4.51	0.20
TODGA	4.34	4.69	0.35
T2EHDGA	4.35	4.36	0.01

2.3.1. HNO_3 systems

Insight into the driving force behind Ln^{3+} extraction with DGAs requires the comparison of DGA derivatives [80]. For 0.1 M DGA/kerosene with 30 vol% 1-octanol in contact with 3 M HNO_3, the trend in Ln^{3+} distribution coefficients is THDGA ~ TODGA > TBDGA ≫ T2EHDGA, which contradicts the previous hypothesis that increasing alkyl chain length causes a decrease in extractability [80]. For linear DGAs, La-Gd have a similar number of DGAs per Ln, where a more pronounced difference is observed for Er and Yb. Specifically, for T2EHDGA, increasing the concentration of 1-isodecanol resulted in a negative effect on extraction of Ln^{3+} [114]. Evaluation of a regression analysis of log D_{Ln} vs log [DGA], revealed a unique trend in speciation. Like the systems without phase modifiers, T2EHDGA forms 1:2 Ln:DGA complexes. A change in speciation is observed with the linear DGA derivatives in the presence of 1-alcohol, as shown in Fig. 14. TBDGA forms 1:2 Ln:DGA complexes for La-Pr, and 1:3 Ln:DGA complexes for Nd-Lu. Both THDGA and TODGA form 1:2 Ln:DGA complexes for La-Pr, 1:3 Ln:DGA complexes for Nd-Gd, and 1:4 Ln:DGA complexes for Tb-Lu. This suggests that for the linear DGAs, the presence of 1-octanol limits the number of DGAs per Ln, especially for La-Pr.

To provide an understanding regarding the trends in slope analysis between various DGAs, these systems were also evaluated via NMR spectroscopy, which detects the strength of interactions between Ln^{3+} and extractants based on the observed chemical shift. Understanding the relative interaction strength between Ln^{3+} and alkyl DGA derivatives can provide insight into driving forces behind extractability trends [80]. Specifically for 0.1 M DGA/kerosene in 30 vol% *n*-octanol with Eu^{3+} in 3 M HNO_3, the trend in extractability follows TBDGA > THDGA > TODGA > T2EHDGA. The same trend was observed for the ^{1}H NMR chemical shifts of the two methylene groups with sp^3-hybridized C atoms between the carbonyl carbon and the ether oxygen, as observed in Table 3 [80].

This suggests the order of extractability from various alkyl chain length DGAs containing phase modifiers is dependent on either its Ln-DGA bond distance or the bite-angle of $O_{carbonyl}$-Ln-O_{ether}. This variation in bite-angle results from rearrangement of DGA molecules on Ln^{3+} with smaller ionic radii, was determined to follow a similar trend observed for the distribution coefficients across Ln series with Ln-TEDGA complexes [96].

Particularly for TODGA, additional spectroscopy methods (UV–Visible and FT-IR) were implemented to further probe the coordination in the organic phase. Berthon *et al.* used a system containing 0.2 M TODGA/*n*-heptane in contact with 0.02 M Nd^{3+} in 3 M $LiNO_3$ and 0.01 M HNO_3, with limited HNO_3 and high $LiNO_3$. The authors did not observe a change in the hypersensitive bands and therefore the inner coordination sphere of Nd^{3+} upon addition of 5 vol% 1-octanol into the organic phase does not change [44]. The –OH group on 1-octanol enables participation in inner-sphere Ln^{3+} coordination, however the UV–Visible results suggest that 1-octanol solely participates in outer-sphere effects. Whittaker *et al.* demonstrated that phase modifiers are used to increase dispersion between DGAs and diluents, which is a result of outer-sphere effects [65]. Without changing inner-sphere coordination to Nd^{3+} there are significant changes in number of extractant molecules per Ln^{3+} with modifiers. [26,38,39,47,80] The absence of modifier effects on the spectra suggest that *the D values reflect influences other than metal–ligand coordination chemistry that are beyond the Ln-O bonds* [11]. FT-IR was then implemented, to elucidate changes in the DGA motifs, where a decrease in the free C=O stretch with an increase in the bound C=O stretch, at the same frequency was observed both with and without 5 vol% 1-octanol [44]. However, without knowledge of the FT-IR spectrum following acid contact, it is difficult to make conclusions regarding if this red-shift of the C=O stretch is a result of acid incorporation or Nd^{3+} and whether

NO_3^- is bound to Nd^{3+}. However, these results indicate that the addition of 1-octanol does not result in structural change to the Ln inner-sphere, with changes likely being experienced in the outer-sphere.

2.3.2. HCl systems

In systems with counter-anions other than NO_3^-, the anion is less likely to coordinate to Ln^{3+}, creating a potentially different molecular structure. Changing the acidic conditions from 3 M HNO_3 to 3 M HCl for 0.1 M TBDGA/kerosene with 30 vol% *n*-octanol reduces D_{Nd} from 200 to 15, respectively. In addition to lowering the distribution coefficient, the linear regression analysis of log D_{Nd} vs log [TBDGA] in the 3 M HCl system resulted in a 1:2 Nd:TBDGA complex [101]. Similarly, a decrease in the average number of TODGA molecules per Ln was observed in HCl media resulting in a 1:3 Yb:TODGA complex. [26] These results align with previous studies without phase modifiers, where the distribution coefficients for Ln^{3+} in HCl were lower than the distribution coefficients in HNO_3. Systems containing phase modifiers remain consistent with this trend, where the softer nitrate increases extraction of Ln^{3+} through promoting hydrogen bond formation and hydrogen bonded structured fluids, in contrast to the harder, charge dense chloride.

Probing coordination changes present in the HCl systems were accomplished with FT-IR, which resulted in a red-shift of the C=O band for both TODGA and T2EHDGA/*n*-octane with 10 vol% 1-octanol. [26] The addition of Yb^{3+} resulted in an additional red-shift of the C=O vibrational stretch, where TODGA had a larger red-shift than T2EHDGA suggesting stronger interactions between Yb-TODGA than Yb-T2EHDGA. Under these conditions, TODGA could form the 1:3 homoleptic $[Ln(DGA)_3]Cl_3$ complex. However, extraction results indicate that this complex is unlikely for T2EHDGA, which forms a 1:2 Ln:DGA complex, with the remainder of the inner-coordination sphere is likely saturated with H_2O molecules.

In contrast to the results obtained in HCl for TBDGA and TODGA, branched DGAs, T2EHDGA and (tetraisobutyl diglycolamide) TiBDGA, exhibited significantly lower distribution coefficients, resulted in a similar number of DGAs per Ln [28]. These branched systems involved DGA/*n*-dodecane with 25 vol% 1-octanol in contact with 2 M HCl. There was no change in the coordination number for T2EHDGA, which resulted in 1:2 Ln:DGA complexes across the Ln^{3+} series. Similarly, TiBDGA, also formed 1:2 Ln:DGA complexes, suggesting the lower coordination number of DGA per Ln could be a result of branching effects on the overall steric interactions of the complex. The role of β-branching in T2EHDGA was previously discussed as the hypothesis for this decrease in number of DGAs per Ln as well as distribution coefficient.

In the presence of phase modifiers, TODGA and T2EHDGA interact with Ln similarly to without phase modifiers when comparing differences observed between HNO_3 and HCl systems. This suggests a similar inner-sphere coordination complex of Ln, with the most drastic change occurring in the outer-sphere. Modifiers, in particular 1-octanol, participate in outer-sphere interactions, where solvation of polar solute molecules occurs, creating a solvation shell of 1-octanol molecules around the polar solutes preventing DGA adducts interacting with the Ln complex via hydrogen bonding interactions. This solvation shell breaks up the DGA aggregates therefore preventing third phase formation.

2.3.3. Asymmetrical DGAs

Whereas most of the literature focuses on symmetrical DGA derivatives, the bulkiness and steric hindrances that coincide with these derivatives have motivated some groups to pursue asymmetrical DGAs. These are DGAs with two types of alkyl chains attached to the amidic nitrogen atom [67]. For 0.024 M (dimethyl dioctyl diglycolamide) DMDODGA/kerosene with 40 vol% 1-octanol in contact with 3 M HNO_3 and Ln^{3+}, the distribution coefficient gradually increases, until Dy^{3+} where a larger increase in distribution coefficient between adjacent Ln^{3+} is observed [23,47]. This trend in Ln^{3+} distribution coefficients results from a weaker interaction between light Ln^{3+} and DGA, than the interaction between heavy Ln^{3+} and DGA [47]. Additionally, this trend is attributed to the hydration energy of each Ln^{3+} ion and the extent to which the extractant can dehydrate Ln^{3+} during extraction [23]. The stoichiometry of asymmetrical DGA Ln^{3+} complexes strongly depends on the nature of the diluents and the acids [23]. It is hypothesized that these results stem from salting out the nitrate under low acidity, however H^+ concentration is important for inhibiting Ln^{3+} extraction under higher HNO_3 concentrations [47].

In a system containing DMDODGA in kerosene and 40 vol% 1-octanol in contact with 3 M HNO_3, extraction forms the 1:1 (DGA)·(HNO_3) adduct [23]. Asymmetric DGAs all have similar trends in slopes of D_{Ln} vs log [DGA] across the Ln series, forming 1:2 Ln:DGA complexes for La-Nd and 1:3 Ln:DGA complexes for Nd-Lu, as depicted in Fig. 15. [23,47] These results suggest that around Nd, a structural change occurs providing two unique

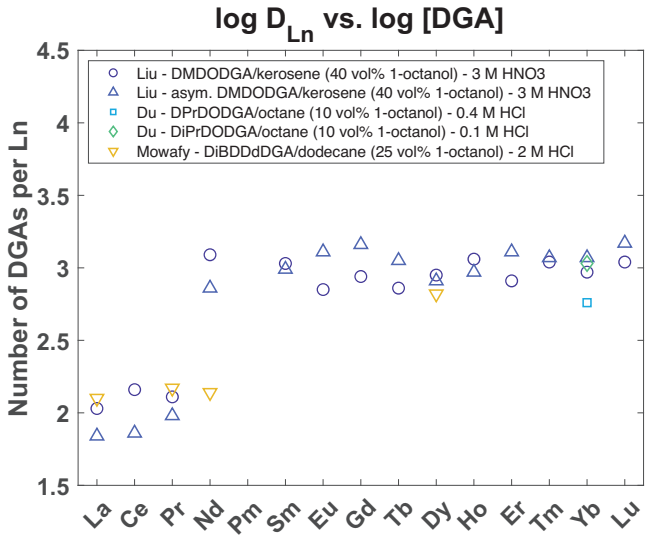

Fig. 15. Trends across the Ln series for various asymmetrical DGAs in both HNO_3 and HCl. [23,26,39].

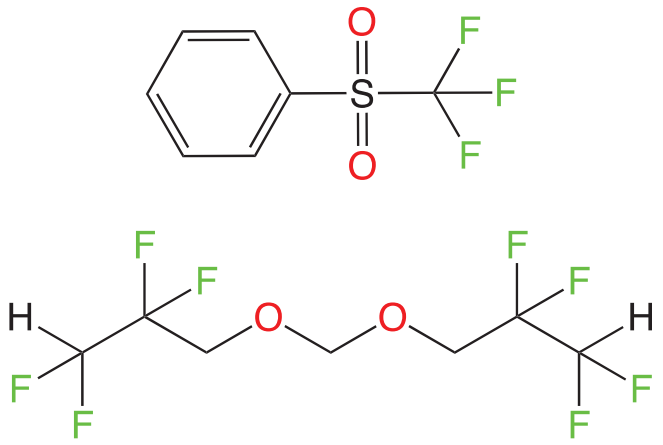

Fig. 16. Fluorinated diluents (top) phenyl trifluoromethyl sulfone (FS-13) and (bottom) 1,1,2,2,8,8,9,9-octafluor-4,6-dioxanonane (Formal n-1).

complexes across the Ln series. This is particularly important, as it suggests different structures are possible with the 1:2 and 1:3 Ln: DGA structures dominating the organic phase.

Although the number of DGAs per Ln is similar among the several systems analyzed, it is also important to gain a better understanding of their various interactions through FT-IR. In particular, two such systems used the DMDODGA with two unique isomers, where there are conjugation and induction effects that exist specifically in the amide group simultaneously, with strong nitrogen conjugation weakening the C=O bond [47]. Conjugation effects arise from interactions between orbitals in a σ-bond (C—H or C—C) with those in a π-bond (C=O or C=N) [115]. In contrast, inductive effects refer to dipole induced interactions due to the different electronegativities of the oxygen atom and nitrogen atoms in the amide [116]. These effects create the charge distributions of either $N^{\delta+}$-C=$O^{\delta-}$ or $N^{\delta-}$-C=$O^{\delta+}$. The weakening degree of two C=O bonds is different due to the difference in induction between groups, creating a clear split in the C=O stretch [47]. The authors claim that asymmetric DGAs have tridentate coordination through two C=O groups and one C—O—C group, [47] however this is a difficult conclusion to make from purely FT-IR data, as the C—O—C stretch is merely the response of the DGA backbone to the change in the C=O stretch. To make the claim that these asymmetric DGAs are in fact tridentate, additional studies are recommended, particularly EXAFS. It should be noted that EXAFS has yet to be done on these systems in the presence of a phase modifier, thereby making it difficult to hypothesize the actual solution structure. Further evaluation regarding the O—N—O symmetric and asymmetric stretches are required before making assumptions as to whether nitrates are located in the inner or outer-sphere.

The similar data shown in Fig. 15, for both the HNO_3 and HCl systems suggests that the counter-anions likely are located in the outer-sphere, as chlorides are unlikely to coordinate to Ln under these conditions. Asymmetrical DGAs have previously been studied predominantly in HCl media for applications to hydrometallurgy, with a focus on heavy Ln^{3+}. Both DiPrDODGA and DPrDODGA have similar distribution coefficients to TODGA, which Du *et al.* attribute the extraction trend with increasing alkyl chain length to its increase in oleophilicity and increase in steric crowding [26]. However, Du *et al.* overlooked the structure of the extractant impacting extraction of Ln^{3+}. Amongst these select DGAs, it was found that the extraction of lanthanides by both DiPrDODGA and DPrDODGA are independent of Ln^{3+} concentration, as is true for TODGA [26]. This suggests the absence of polynuclear Ln-DGA complexes. For each DGA a different concentration of HCl was used, and Du *et al.* did not clarify as to why the concentration of HCl was not kept constant [26]. The variability in HCl concentrations prevents conclusive comparisons between systems from being made.

Although EXAFS has not yet been completed in the presence of phase modifiers, solid state and solution EXAFS studies of the nitrate and chloride salts of Er^{3+} complexes with DMDPhDGA reveal differences in the coordination chemistry with the TODGA complexes of Ce^{3+}, Nd^{3+} and Eu^{3+} ions. Most notably, the Er^{3+} complexes are heteroleptic [32]. Only two DMDPhDGA molecules coordinate to Er^{3+} in tridendate fashion for both the solid salt and ethanol solution, with 3 coordinating H_2O molecules [32]. The inner shell Er^{3+} environment is completed by the coordination of three water molecules in the solid state and two water molecules in ethanol solution. [32,117] The structures of the heteroleptic complex cations $[Er(DMDPhDGA)_2(H_2O)_3]^{3+}$ and $[Er(DMDPhDGA)_2(H_2O)_2]^{3+}$, respectively, are independent of the identity of the anions, nitrate and chloride. Similar EXAFS structures have been reported for malonamides where heavier Ln^{3+} with increased charge density form a more structured second solvation shell, allowing the formation of larger clusters [16,58,60,61] It is evident the aggregation properties that are imperative to selective Ln^{3+} extraction are present. Systems with asymmetrical DGAs are also selective for the heavy Ln^{3+}, thus providing another synthesis route to potential extractants within this class of DGA extractants.

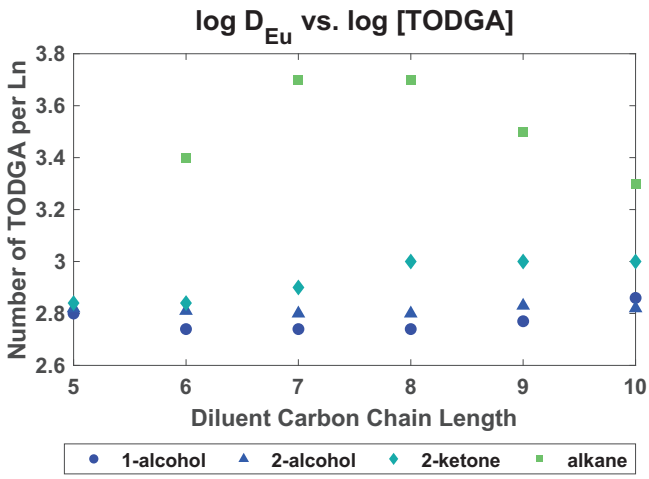

Fig. 17. Average extractant numbers from the slope of log D_{Eu} vs log [TODGA] for 0.02 M TODGA/diluent in contact with 4 M HNO_3 and tracer Eu^{3+}. The alkyl chain lengths on the diluents were varied from 5 to 10 for each class of diluents tested. [2].

2.4. Effects of polar diluents on Ln-DGA speciation

The number of carbons in the diluent (i.e., the alkyl chain length) and the diluent type (e.g., aliphatic or polar) influence the distribution coefficients [2]. TODGA in polar diluents (e.g., alcohols, ketones, chloroform, dichloroethane) extracts more HNO_3 with shorter alkyl chains than their longer alkyl chain counterparts [2]. In polar diluents, the distribution coefficient increases with the diluent chain length [2,46]. Particularly with perfluorinated diluents, such as FS-13 or Formal n-1 (structures are shown in Fig. 16), no plateau is observed in distribution ratios across the Ln series, deviating from the trend for both TODGA and T2EHDGA shown in Fig. 5. Increasing the polarity of the solvent with the perfluorinated diluents reduces the solubility of TODGA, thereby restricting the systems to dilute conditions. Polar diluents clearly demonstrate a different structure or organization of the organic phase than in TODGA systems with an aliphatic diluent.

Similarly, this trend in distribution coefficients was observed for TODGA in either dichloroethane or chloroform in contact with 5 M HNO_3. Although the distribution coefficients for light Ln, La-Nd in dichloroethane or chloroform, are less than that for the petroleum ether and *n*-alkane systems, they follow the trend across the Ln series previously observed with linear DGAs [98,100]. Decreasing HNO_3 below 2 M and DGA below 0.1 M, results in competitive distribution coefficients between select polar diluents and *n*-dodecane. In addition, the separation factors for nitrobenzene, dichloroethane, 1-octanol, and chloroform for TPDGA, TODGA, and TDdDGA are similar to the aliphatic diluent systems [30]. Understanding the coordination chemistry of Ln-DGA complexes in polar diluents can then be compared to aliphatic diluents, to elucidate changes between the extracted Ln-DGA complex and the outer-sphere interactions with the diluents.

2.4.1. Alcohols and ketones

In these DGA systems, 1-octanol is of particular interest as its long octyl chain enables solubility of DGAs in addition to being a hydrogen bond donor. The ability for 1-alcohols to be a hydrogen bond donor is important in DGA systems as H^+ enhance Ln^{3+}

extraction. This suggests that in the presence of 1-alcohols, there should be an increase in distribution ratios. A regression analysis was performed for log D_{Eu} vs log [TODGA] resulting in 2.48 TODGA molecules per Eu and an extracted 1:3 Eu:TODGA complex [81]. Similarly, the regression analysis for log D_{Eu} vs log [HNO_3] resulted in two nitrate molecules per DGA. The mixture of HNO_3 with $NaNO_3$ maintaining a constant nitrate concentration of 3 M, resulted in zero dependence on the concentration of HNO_3. These results suggest that 1-octanol is not sensitive to the nitrate source and has similar D_{Eu} under both conditions. This contrasts with the observation without 1-alcohol, where extraction of Ln in DGA systems is sensitive to the nitrate source, as DGAs are hydrogen bond acceptors. Replacing the HNO_3 with solely $NaNO_3$, resulted in a slight decrease in the number of TODGA per Eu, forming an average of a 1:2 complex. The mechanism for Eu^{3+} extraction by TODGA/1-octanol is hypothesized to be an ion–dipole extraction, strongly dependent on the ionic strength, elevating D_{Eu} at higher concentrations. The ability for Eu^{3+} to be highly extracted by 1-octanol results from the hydrogen bond donors being readily available, preventing the dependence on co-extracted H^+ for large distribution coefficients. Instead, larger distribution coefficients are a function of nitrate concentration in the system.

In addition to understanding the impact of 1-octanol on the Ln-DGA extracted complex, the alkyl chain length of 1-alcohol has been varied with diluents from 1-pentanol to 1-decanol. For TODGA/1-alcohol in contact with 4 M HNO_3 resulted in little to no change across the varying 1-alcohol alkyl chain length, forming an average of 1:2 to 1:3 Eu:TODGA complexes [2]. A 1:2 Ln-DGA complex was observed with Nd^{3+} forming a similar Ln-DGA speciation as Eu^{3+}. [103] Similar results were obtained for TODGA in 2-alcohol and 2-ketone. [2] These results are shown in Fig. 17, where it can be observed that the Ln-DGA complexes in polar diluents have less TODGA molecules involved than in *n*-alkane diluents, forming an average of 1:3 to 1:4 Eu:TODGA complexes. In *n*-alkane diluents there was a dependence on the alkyl chain length, with the largest number of TODGA molecules per Eu occurring for heptane and octane at 3.7. The number of DGAs per Ln are lower in systems with polar diluents than with alkane diluents, stemming from the ability for select polar diluents to interact with the co-extracted polar solutes [2].

In polar diluents extraction was found to be independent of the nitrate source due to either the solvating ability of the diluent or the H^+ present that can engage in hydrogen bonding interactions with TODGA. These interactions decreased the number of DGAs associated with a Ln-DGA complex through reducing outer-sphere DGA interactions with the extracted Ln complex. By solvating the Ln-DGA complex and interacting with the polar solutes in the outer-sphere of the Ln-DGA complex, the polar diluents prevent outer-sphere interactions with additional (DGA)·(HNO_3) adducts. Favorable interactions between polar solutes and polar diluents increase solvation of the complex by decreasing the Ln-DGA aggregate sizes thereby preventing third phase formation.

2.4.2. Chlorinated diluents

Increasing the polarity of the diluent corresponds to a higher dielectric constant, which decreases the number of DGA molecules participating in the extracted Ln-TODGA complex [35,46]. There is no direct dependence of Ln^{3+} distribution coefficient on the dielectric constant of the diluent, but the diluent affects the stoichiometry of the extracted species [46]. Increasing the polarity of the diluent from various 1- and 2-alcohols to dichloroethane exhibited similar results. The average number of TODGA molecules per Eu^{3+} in dichloroethane is 2.20 in 3 M HNO_3, suggesting the formation of primarily 1:2 Eu:TODGA complexes in acidic media [81]. The regression analysis for log D_{Eu} vs log [HNO_3] indicates two nitrate molecules are co-extracted for every Eu^{3+} and varying the concentration of HNO_3 in 3 M (H, Na)NO_3 media resulted in an average of 0.25 HNO_3 molecules per Eu^{3+}. [81] However, as previously discussed these Ln-DGA systems require 3 nitrate anions in order to charge balance the extracted Ln complex. The obtained value of 2 nitrate molecules per Ln complex is likely the result of not accounting for activity of each species during the application of Eqn. (7). The number of TODGA molecules per Eu does not change in neutral media with an average number of 2.11. This suggests that whether in acidic or neutral media, Eu:TODGA form 1:2 complexes in chloroform. These results suggest a similar Eu:TODGA complex is forming in dichloroethane and in 1-octanol. A further understanding of the particular complex that is forming would require spectroscopic techniques on the organic phase from these extraction studies.

Further increasing the polarity of the diluent involves using chloroform to understand changes in coordination of Ln-DGA complexes. In comparison to both 1-octanol and dichloroethane, there are an average of 2.60 TODGA molecules per Eu^{3+} in 3 M HNO_3, but exposure to 3 M $NaNO_3$ decreases the number of TODGA molecules involved slightly to 2.39. [81] This is supportive of the combination of 1:2 and 1:3 Eu:TODGA complexes in chloroform and suggests the overall extracted complex largely remains the same between acidic and neutral media. A regression analysis of log D_{Eu} vs log [HNO_3] resulted in an average of three to four nitric acid molecules co-extracted per Eu^{3+}. In contrast to 1-octanol and dichloroethane, in chloroform there is a dependence on the D_{Eu} on the concentration of HNO_3 in a mixture of HNO_3 and $NaNO_3$ with an overall nitrate concentration of 3 M. This dependence results in an average of two HNO_3 molecules co-extracted per Eu^{3+}. This is similar to the behavior of D_{Eu} on H^+ as observed in *n*-dodecane systems. The distribution coefficients of Eu^{3+} in chloroform can be compared to the *n*-dodecane system by evaluating the stability constants for the β_1 $[Eu(TODGA)_3(HNO_3)]^{3+}$ and β_2 $[Eu(TODGA)_3(HNO_3)_2]^{3+}$ complexes. [81] This resulted in a trend for β_2 corresponding to the trend in Eu^{3+} distribution coefficients, indicating that stabilization of the 1:2 (DGA)·$(HNO_3)_2$ adduct stabilizes the extracted Eu-TODGA species.

Coordination chemistry of Eu^{3+}/TODGA/chloroform was further studied via FT-IR. The concentration of Eu^{3+} in the aqueous phase was varied from 0 to 100 mM, resulting in organic phase Eu^{3+} concentrations of 0 to 30 mM. The final concentration of Eu^{3+} of 30 mM ~ 33 mM, suggests the formation of a 1:3 Eu:TODGA complex [81]. Following Eu^{3+} contact, the C═O vibrational stretch red-shifted from 1656 cm^{-1} to 1614 cm^{-1}, indicative of DGA coordination to Eu^{3+} [81]. In addition, the authors analyzed the O—N—O symmetric stretch to provide information regarding the role of nitrate molecules in this system. The O—N—O symmetric stretch blue-shifted from 1295 cm^{-1} to 1325 cm^{-1} suggesting that nitrates are in the outer-coordination sphere [81]. Further analysis involved collecting TRLFS data for the Eu^{3+} TODGA system to provide insight as to the number of coordinating H_2O molecules. Diluents of either *n*-dodecane, toluene, or 1-octanol with TODGA in contact with 3 M HNO_3, have zero coordinating H_2O molecules to Eu^{3+} [50]. These results are consistent with a $[Eu(TODGA)_3](NO_3)_3$ complex in chloroform media, which follows the hypothesis

Table 4
Stability constants for $[Nd(DGA)_{1-3}]^{3+}$ complexes in MeOH/TMAN. [99].

DGA	Log β_{101}	Log β_{102}	Log β_{103}
TMDGA	3.46	6.66	9.4
TPDGA		9.59	12.92
THDGA		8.17	11.53
TODGA		7.78	10.32
T2EHDGA		7.04	

that in polar diluents the anion will likely participate in outer-sphere effects.

Similar observations for the coordination of TODGA to Eu^{3+} were observed with DMDPhDGA/chloroform in contact with 5 M HNO_3 and either La^{3+} or Lu^{3+}. The C=O vibrational stretch redshifted for both La^{3+} and Lu^{3+}, but a larger redshift was observed in the case of Lu^{3+} suggesting stronger Lu-O bonds with DMDPhDGA [32]. These results are consistent with D_{Ln} as the chemical bond strength is closely related to the magnitude of D_{Ln}, where stronger Ln-O bond strength is generally proportional to high magnitude of D [61]. However, this correlation might not be a direct result of Ln-O bond lengths, as the soft-donor extractants provide a much less obvious relationship between bonding properties and D values [118]. Further investigations into the coordination environment of Ln^{3+} in the DMDPhDGA/chloroform system utilized UV–Visible spectroscopy for Ho^{3+} in 5 M HNO_3 [32]. The coordination environment around Ho^{3+} in 5 M HNO_3 is symmetrical as evident from the symmetrical hypersensitive absorption band. Following extraction of Ho^{3+} by DMDPhDGA/chloroform, a redshift was observed in this absorbance band, indicating a change in the Ho^{3+} inner-coordination sphere [32]. This is likely the result of replacing the coordinating nitrate molecules with coordinating DMDPhDGA molecules.

In dichloroethane, the Ln-DGA complex is independent of the nitrate source as is the case with 1-octanol. However, in chloroform, there is a nitrate dependence similar to that observed in *n*-dodecane. This suggests that the dielectric constant of the diluent plays a large role in the dependence of HNO_3 and organic phase structure, particularly outer-sphere hydrogen bonding. When the Ln-DGA complex and its outer-sphere polar anions are properly solvated, as in the case with diluents having a high dielectric constant (e.g., 1-octanol and dichloroethane), the diluents have a greater propensity to interact with the polar solutes creating minimal dependence on HNO_3. Decreasing the dielectric constant, as with chloroform and dodecane, a HNO_3 dependence is observed because the diluents cannot solvate the Ln-DGA complex as effectively allowing (DGA)·(HNO_3) adducts to interact with the Ln-DGA complex.

2.4.3. Methanol

Supporting this hypothesis of the homoleptic 1:3 Ln:DGA complex with outer-sphere nitrate anions was accomplished via UV–vis spectrophotometric titrations of varying the DGA alkyl chain lengths. A solution of 0.01 M Nd^{3+} with 0.06 M ionic strength of tetramethyl ammonium nitrate (TMAN) was titrated with specific DGAs of interest, (tetramethyl diglycolamide) TMDGA, TPDGA, THDGA, TODGA, TDdDGA, T2EHDGA/MeOH. The stability constants were fit and calculated, as shown in Table 4 [99]. A 1:1 Nd:DGA complex was observed only in the case of TMDGA, with the remaining derivatives forming 1:2 and 1:3 complexes. The exception to this was T2EHDGA which only formed a 1:2 complex.

Under these conditions, increasing the length of the alkyl chain decreases the stability constants with Nd^{3+}. A decrease in stability constants indicates weaker interactions between Nd^{3+} and DGA. Although this experiment used methanol as a diluent instead of *n*-alkanes, the reduced stability constants for Nd:DGA complexes with longer alkyl DGA derivatives is correlated with the extractability of DGAs. As the dielectric constant for methanol is high (32.7), this suggests that the Nd-DGA complex is efficiently solvated preventing the formation of aggregates, supporting typical M:L speciation (1:1, 1:2, and 1:3 complexes) as mentioned in Table 4. The DGAs that form weaker Nd:DGA complexes have lower observed distribution coefficients. This is consistent with the trend in ^1H NMR data obtained for Eu^{3+} in kerosene with 30 vol% 1-octanol, where the shorter DGAs have larger chemical shifts and larger distribution coefficients.

The trend in experimental complexation strength between Nd-DGA complexes, also known as the stability constant, can also be predicted from DFT calculations. There is a more favorable free energy of complexation for Nd-DGA complexes for longer alkyl chains on DGA molecules, consistent with the stability constants shown in Table 4. Additionally, TiBDGA (shorter T2EHDGA derivative) has unfavorable complexation energies in comparison to TBDGA (a shorter TODGA derivative) [99]. The ability for the relationship between the complexation strength of TiBDGA and TBDGA to predict the experimental complexation strength of T2EHDGA and TODGA provides an avenue for future investigations to understand fundamental differences between these two industrially relevant extractants.

3. Supramolecular aggregate structure

In *n*-alkane diluents, the molecular structure has been identified as varying from 1:3 to 1:4 Ln:DGA complexes. The larger number of DGA molecules per Ln, suggests the presence of DGAs participating in the outer-sphere, consistent with the formation of supramolecular aggregates. Further investigation of systems in which these aggregates form requires the combination of dynamic light scattering (DLS), small-angle X-ray (SAXS) and neutron (SANS) scattering. The application of these techniques to characterize organic phases is not yet routine. As it is still in the early days of using these techniques to characterize organic phases, there is a necessity to understand how the data collected from these techniques (especially from large-scale synchrotron and spallation neutron source facilities) has been previously analyzed and what changes need to be considered for improving the state of the literature.

DLS—also referred to as photon correlation spectroscopy—has been applied to solvent extraction systems as early as 1958 to address concerns at that time regarding extraction mechanisms based on aggregation [119]. Thereafter, DLS was used to characterize the influence of aggregation on phase separation in practical hydrometallurgical solvent extraction systems and to determine the size and dispersity of the oil phase aggregates [120,121]. Only within the past decade has DLS been used to investigate aggregate morphologies and the mechanistic nature of phase separation in TODGA chemistry even though the phenomenon of TPF in solvent extraction systems goes back to at least 1936 [122,123]. Even earlier reports of TPF are found in the literature for the purification of large tungsten-oxo clusters from aqueous mineral acids using diethyl ether as the extractant-solvent [124]. With a century of hydrometallurgy and phase separation observations in solvent extraction, remarkably, it's only been recently (by comparison) that TPF of organic phases used for solvent extraction has been cast as a dynamic, critical phenomenon [123,125–128].

Developing a working hypothesis for the structure of extracted Ln^{3+} DGA species involves determining additional physiochemical properties, such as aggregate size and aggregate polydispersity [64]. Supramolecular aggregates composing the nanostructure of the organic phase requires approaching the solution not as simple metal–ligand interactions, but rather as a complex fluid [83,88,129,130]. Measuring aggregate size distribution is achieved through DLS [123,131–134]. Modeling aggregate interactions takes into account composition of aggregates during random aggregate collisions and aggregate growth [64]. These results are strongly dependent on assumptions that are made when modeling the system. The first assumption is that the aggregates are spherical and are under constant Brownian motion from random collisions with solvent molecules [57]. The second assumption—made to simplify modeling—is the application of the Stokes-Einstein equation. However, with the presence of multiple TODGA species, the Stokes-

Einstein equation is an invalid approach, as it is only applicable for systems with monodisperse non-interacting aggregates [54,56].

Calculating accurate information regarding aggregate size hinges upon the measurement of refractive index and viscosity [135]. The refractive index is necessary for calculating the magnitude of the scattering wavevector in terms of reciprocal space [134,135]. If the refractive index is not measured or the Stokes-Einstein equation is used in situations that are not accurately described by non-interacting hard-spheres, the calculated aggregate sizes are to be viewed with caution. Of the array of studies that have collected DLS data, many either made assumptions about or, alternatively, did not measure the refractive index. Therefore, when browsing DLS literature *caveat emptor* is the best approach. Transformation of the scattering intensity from the autocorrelation intensity function to the pair-distance distribution function in real space, provides information regarding aggregate size [89,132,135,136]. Although DLS provides valuable information on the average aggregate size, DLS does not differentiate between different TODGA species, so the results are the combination of monomers, dimers, tetramers and, in general, *n*-mers in the organic phase [57,133]. Developing a better understanding of the size distribution of aggregates could lead to better extraction performance (as measured by D) by controlling the aggregate size through modifying water and extractant concentrations in the organic phase [64].

Until the time that direct, real space (Å) imaging techniques, notably cryo-TEM with atomistic resolution, are applied to organic phases from solvent extraction, multiscale structure observations are indirectly harvested in reciprocal space ($Å^{-1}$) through use of SAXS (small-angle X-ray scattering) and SANS (small-angle neutron scattering). Both find applications to characterize the solute-organized architectures of supramolecular aggregates in the organic phase solvents [88,129,137]. These techniques interrogate the aggregate morphology in bulk fluids through scattering angles much less than 10°, corresponding to small momentum transfer values ($q \leq 1$ $Å^{-1}$) and a resolution that ranges from roughly 5 Å to 100 Å [138–140]. As such, successful data acquisition and modeling require the presence of supra- and micro-molecular (i.e., mesoscale) aggregates, as the absence of aggregates results in weak scattering [54]. Whereas both techniques provide quantitative structural information, they differ in the types of contrast they exploit in a solution sample [138]. SAXS contrast arises from the difference in electron density between the aggregate solutes and the solvent [138]. For these DGA systems, SAXS is more sensitive to the polar core of aggregates than SANS [45] because SANS contrast arises from the large difference in the neutron cross-section between hydrogen and deuterium [138]. The contrast between the deuterated organic solvents and the non-deuterated extractant allows SANS to be sensitive to aggregates as a whole [45]. Specifically for smaller extractants or DGAs, SANS is typically used due to the difficulty in obtaining high contrast between DGA and solvent molecules, commonly *n*-dodecane, with SAXS [85].

Analyzing SAXS/SANS data requires key assumptions to be made for calculating the form factor and the structure factor [138,141]. The form factor is sensitive to aggregate morphology, whereas the structure factor reflects aggregate-aggregate interactions [129]. Inter-aggregate interactions are in dynamic equilibrium, where DGA and phase modifiers participating in aggregates are constantly exchanging with free molecules in the bulk organic phase [94]. Penetration of different diluents or phase modifiers into the aggregate shell limits the swelling and aggregation through changing aggregate binding energy [93]. In the case of synergistic extraction systems, aggregation increases as a result of extracted acid, inducing attractive interactions between extractant and phase modifier [12,89,93]. These observed interactions are dependent on the composition of the organic phase and whether aggregates are polydisperse and/or polymorphous [138]. Assuming these aggregates are spherical, and that Baxter's hard-sphere sticky potential applies, the first approximation for the Percus-Yevick solution is valid if the inter-aggregate distance is equal to 10 % of the aggregate diameter [58,62,94,142,143]. VDW forces act on interactions between protruding alkyl chains to stabilize the aggregates [141]. The assumed complex of sticky spheres in the organic phase refers to reverse micelles with surface adhesion, with short-range interaction potentials arising from microemulsions close to a liquid–liquid phase transition [141,144]. The intensity of these short-range interactions is related to the polarizability of their hydrophilic cores and the inter-aggregate distance [85]. When phase modifiers are incorporated into the system, they dominate the self-assembly, reducing the sticky sphere parameter thus pushing TPF to higher concentrations [94].

SAXS and SANS data for most systems are modeled assuming that the organic phase consists of polar reverse spherical micelles in deuterated and nondeuterated diluents [141]. However, interpretations of both SAXS or SANS data can be misleading vis-a-vis the strength of interaction energies between reverse micelles or, even worse, predict non-attractive interactions, contradicting direct observations of phase splitting as a result of strong attractive associations [144]. Thus, correctly modeling the shape of the aggregate (in terms of the form factor) is relevant for correct modeling of the aggregate solvation (the structure factor) [74]. Throughout the past, the extracted solutes were generally assumed to be incorporated into either spherical or ellipsoidal aggregates prior to understanding their coordination chemistry and aggregate morphologies [144]. More rigorous modeling as well as model-independent approaches, such as GIFT (generalized indirect Fourier transformation), are being applied nowadays. For example, correcting the over simplified fitting of incoherent scattering intensity from hydrogen atoms in SANS provides the correct shape of the aggregate [144]. Applying colloidal models increases the accuracy of SAXS and SANS data fitting by accounting for the *meso*-structuring of reverse micelles in the organic phase [128].

3.1. DGA aggregation following H_2O extraction

In non-polar, alkane diluents, DGAs self-aggregate, and the degree to which self-aggregation occurs is dependent upon the DGA alkyl chain length. Increasing this alkyl chain length, increases the self-aggregation tendency of DGAs according to THDGA < TODGA < TDDGA < TDdDGA. This is the same trend observed for the basicity of DGAs, where DGAs with the highest basicity will have a greater tendency to interact with each other via the polar moieties. For these self-assembled DGA aggregates in *n*-alkanes, the average size was obtained from DLS, and is 2 nm, which exceeds the critical size, as described by the critical aggregate concentration (CAC) for supramolecular aggregates [51].

Extraction of H_2O molecules is critical for the swelling of self-assembled TODGA aggregates, where water networks form inside the polar core of aggregates because of hydrogen bonding [86]. The addition of phase modifiers into the system disrupts the extended water network, especially if they exhibit co-extractant behavior. A decrease in aggregate size was observed for a TODGA/*n*-dodecane system with 0.4 M DHOA, when compared to 5 vol% 1-octanol. Smaller aggregates have increased polarizability and stronger polar-polar interactions within the aggregate core [52]. In the case of 1-octanol, the larger aggregates arise from the hydrogen donating ability of 1-octanol allowing it to interact in different ways with extracted H_2O molecules than the hydrogen bond acceptor DHOA. This is comparable to solvent extraction results where an increase in H_2O extraction by TODGA/*n*-dodecane occurs with use of phase modifiers of large polarities.

Differences in aggregation following H_2O contact with TODGA/*n*-heptane in either 5 vol% 1-octanol or 0.5 M DMDOHEMA was compared by small and wide-angle X-ray scattering (SWAXS). SWAXS data measures the presence of aggregation through scattering intensity increasing at q values less than those for the plateau-like response typical of a dilute, monodisperse entity [44]. As the gas phase speciation is dependent on and closely related to the solution speciation of the organic phase, ESI-MS (electrospray ionization mass spectrometry) has been used to determine the overall number of molecules involved in the complex aggregate [44,129]. Without the presence of phase modifiers, it is likely that one to five TODGA molecules participate in extraction. Introduction of 5 vol% of 1-octanol into the solvent affects extraction (as previously discussed), but 1-octanol molecules are released during ionization [44]. This prevented the number of 1-octanol molecules in each aggregate from being measured. The structure of these aggregates involved molecular dynamics simulations, which are dependent on validation methods [44]. In this work, molecular dynamics simulations were validated from SWAXS data, where 1-octanol participates in the supramolecular aggregate via outer-sphere coordination. In contrast to this, DMDOHEMA forms unique aggregates where some are a mixture of TODGA and DMDOHEMA and others exist with DMDOHEMA as the sole extractant. [44] These results indicate that while 1-octanol appears to be a true phase modifier for H_2O extraction, DMDOHEMA acts as a co-extractant. Therefore, the polar moiety on the phase modifier and their respective interactions with aggregates affects their role in fluid microstructure.

3.2. Aggregation behavior of DGAs in HNO_3

In DGA systems, high extractability of Ln^{3+} is accompanied by the formation of supramolecular aggregates [2,57]. Therefore, understanding the critical point at which DGA systems form supramolecular aggregates is important when designing separation systems. This critical point is often referred to as the CAC, the concentration of acid or metal required to form supramolecular aggregates, such as reverse micelles [48,85,123,132,141], at a known DGA concentration [54,93]. Therefore, the CAC marks the critical point in which the organic phase changes from being comprised of monomers and dimers to predominantly tetramers or supramolecular aggregates. The aggregate size at this critical point is necessary to achieve formation of supramolecular aggregates. Operating below these critical concentrations minimizes both aggregation and TPF [54,93]. The CAC is measured through various interfacial tension techniques [14], where differences between the intermolecular forces at the organic-aqueous interface, with cohesive forces between the molecules creating surface tension can be determined [131]. Effective extractants are determined by their ability to obtain minimum interfacial tension and the rate at which they rearrange to extract ions. Large interfacial tensions for both extractants and phase modifiers are desired to prevent unwanted diffusion into the aqueous phase. Extraction of polar ions reduces the interfacial tension, a behavior associated with formation of reverse micellar-like aggregates [63]. Once the extractant saturates the interface, the CAC can be measured from the inflection points, indicating sufficient extractant activity to form supramolecular aggregates in the bulk organic phase [45].

3.2.1. Aggregation properties of TODGA and T2EHDGA

TODGA is the preferred DGA derivative for industrial solvent extraction, hence several studies have been dedicated to determining the CAC through interfacial tension techniques and understanding its speciation in the organic phase. The CAC of TODGA is observed at 0.1 M TODGA/*n*-dodecane in contact with 2 M HNO_3 and at 0.2 M TODGA/*n*-dodecane in contact with 4 M HNO_3. [46,57,85,87,141] Supramolecular aggregates were confirmed by the slow transition of interfacial tension approaching the CAC [93,141]. Nanostructure of the organic phase results from its phase behavior determined by the physical properties of these critical points [128]. The addition of HNO_3 to the organic phase disrupts the extended water network inside the polar core, changing the water-water and water-TODGA inter-molecular interactions [2,51,53]. These interactions result in the formation of 1:1 and 1:2 (DGA)·(HNO_3) adducts, the morphology of which strongly depends on the polarity of the aggregates, but is independent of TODGA concentration [53,57,141].

Maintaining HNO_3 concentrations initially in the aqueous phase below 1 M, TODGA forms ellipsoidal monomers and dimers in *n*-dodecane, but increasing HNO_3 to 1 M, quickly results in tetramers

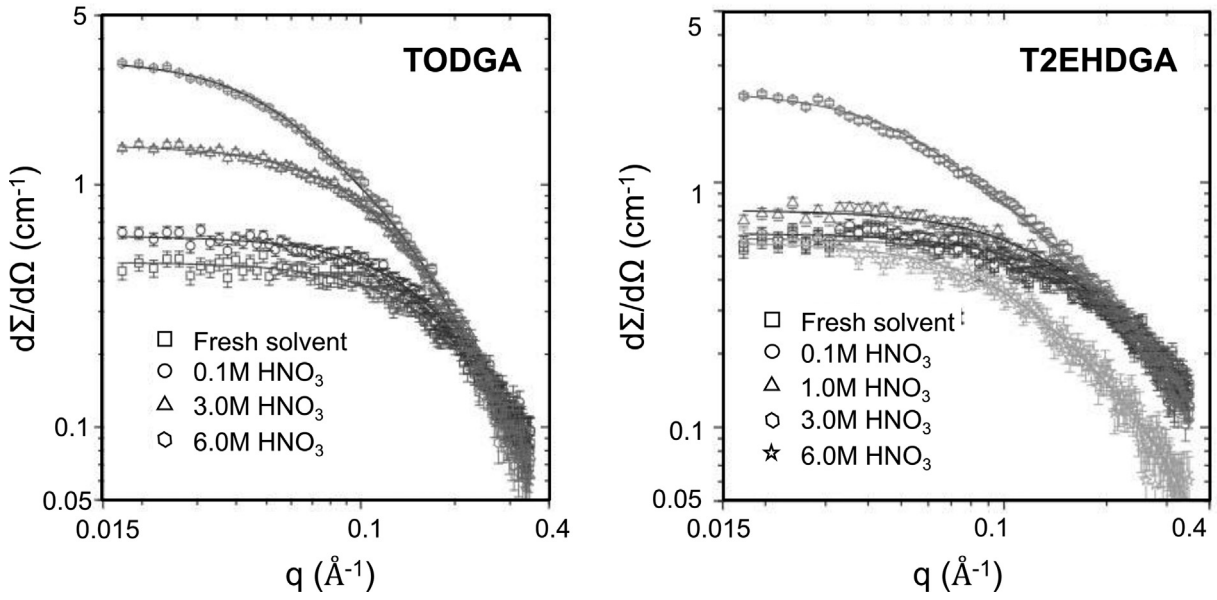

Fig. 18. SANS results for the acidic case with HNO_3 from (left) organic phase: TODGA/*n*-dodecane and (right) organic phase: T2EHDGA/*n*-dodecane. Different concentrations of HNO_3 are denoted by different shapes. Figure obtained from Pathak *et al.* [34].

dominating the organic phase, as evident from SANS. [15,17,85] Increasing HNO_3 beyond 2 M, converts all the dimers to tetramers [57,85]. Understanding the trend in diffusion coefficients in these systems can be related to interactions between aggregates. The initial decrease in diffusion coefficients across varying concentrations of TODGA (0.1–0.3 M) in *n*-dodecane, suggests the presence of an attractive interaction between two tetrameric aggregates [132]. Attractive inter-aggregate interactions observed between tetrameric TODGA aggregates likely arises from intra-aggregate VDW forces via extracted HNO_3 [132]. The presence of attractive interactions leads to an increase in viscosity of the reverse micellar-like solution [132]. Therefore, the extractant number as a function of increasing HNO_3 concentration from 0 to 3 M was investigated using either 0.1 M TODGA/*n*-dodecane or 0.1 M T2EHDGA/*n*-dodecane.

At a HNO_3 concentration of 2 M, the power-law dependence on the small-angle neutron scattering intensity, I(q), was shown to approach −1, as displayed in Fig. 18 [34,49,85,141]. The average diameter of the aggregates maintains similar dimensions, as indicated by the scattering intensities at high q, having similar intensities across varying concentrations of HNO_3. Both features at high q and low q with respect to their intensities, indicate transformation from globular to an elongated or ellipsoidal reverse micellar structure. As shown in Fig. 18, with increasing HNO_3 concentration, the neutron cross section at low scattering angles increases, indicating an increase in both aggregate size and number of extractant molecules per aggregate [34]. In these systems, the number of extractant molecules is consistent between TODGA and T2EHDGA, except for 6 M HNO_3, where a decrease in extractant number is observed for T2EHDGA, due to TPF [34]. Differences in the SANS data are shown in Fig. 18 [34], where it is evident that the power-law dependence is higher with TODGA than T2EHDGA. When 0.1 M TODGA/*n*-alkane is in contact with HNO_3 less than 2.02 M, the organic phase is dominated by spherical monomer and dimer aggregates as indicated by the power-law dependence of zero on I(q). Increasing the concentration of HNO_3 to 2.02 M results in the formation of elongated, potentially rod-like hexameric aggregates [49]. Therefore, the aggregate structure appears dependent on the concentration of HNO_3, as increasing the HNO_3 concentration is correlated with the formation of elongated aggregates.

Under high concentrations of HNO_3 in contact with TODGA/*n*-dodecane solvent, SANS results suggest the ability for TODGA to form spherical aggregates is incorrect; the aggregates are better represented as ellipsoids or cylinders as indicated by a power-law dependence of −1.5 on I(q) [49]. The power-law q-dependence is informative of the aggregate morphology, where power-law of 0 indicates spherical aggregates and power-law of −1 indicates rod-like aggregates [12]. Fourier transformation of the I(q) vs q data into real space yields a pair-distance distribution function with supramolecular aggregate dimensions of approximately 20–40 Å long and 10–14 Å across. Both dimensions increase with increasing extraction of HNO_3 and H_2O, with a more dramatic increase observed with the length at an approximately constant diameter, suggestive of rod-like reverse micelles [49].

Therefore, increasing the concentration of HNO_3 changes the fluid architecture from 1:1 and 1:2 (DGA)· (HNO_3) adducts to 1:4 tetramers. When tetramers dominate the solvent, there is evidence of reverse micelle formation resulting from the merging of TODGA aggregates. Further increasing the concentration of HNO_3 elongates the reverse micelles, likely through the combination of multiple reverse micelles in a worm-like fashion. These results suggest that the concentration of HNO_3 is directly correlated with solution architecture, which is critical to understand for making conclusions regarding Ln studies.

Comparison of the results obtained with small-angle scattering for TODGA systems were made with the T2EHDGA system in an attempt to elucidate structural differences. Similar to the behavior of both TODGA systems, 0.1 M T2EHDGA/*n*-dodecane forms aggregates that are 30 Å long and 6 Å across [114]. Whereas the length for both TODGA and T2EHDGA are similar, they exhibit different aggregate diameters, which could impact their ability to incorporate a Ln. The size of TODGA aggregates is independent of TODGA concentration, whereas the T2EHDGA aggregate size depends on the T2EHDGA concentration [114]. Another explanation for differ-

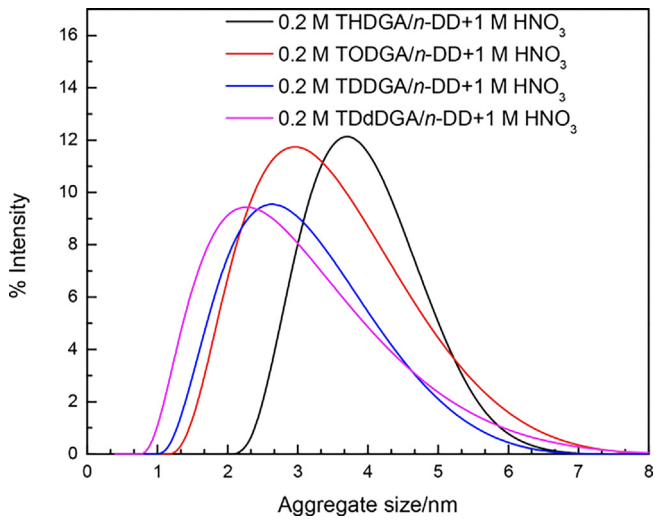

Fig. 19. Average aggregate sizes for a variety of DGAs in *n*-dodecane in contact with 1 M HNO_3, where THDGA (black), TODGA (red), TDDGA (blue), and TDdDGA (pink). Figure obtained from Swami *et al.* [51].

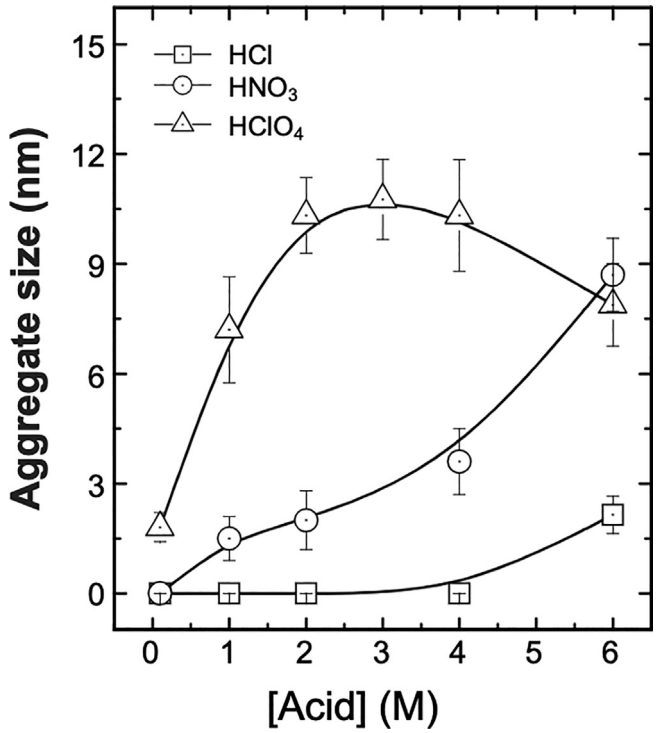

Fig. 20. Aggregate sizes for 0.1 M TODGA/*n*-dodecane in contact with either HCl, HNO_3, or $HClO_4$. Shapes denote the acid, HCl (square), HNO_3 (circle), $HClO_4$ (triangle). Figure obtained from Pathak *et al.* [57].

ences observed between the TODGA and T2EHDGA systems stems from the competing thermal energy – k_BT – that maintains dispersion of reverse micelles in the solvent and the energy of intermicellar attraction that facilitates the adhesion of reverse micelles [34]. Further, in bicontinuous microemulsions, branched surfactants tend to produce micro-emulsions that are more compact resulting in smaller domains [145]. Therefore, the lower distribution coefficients that are observed with T2EHDGA are likely due to the propensity for smaller channels within the bicontinuous microemulsion resulting from the higher inter-surfactant spacing due to the branched 2-ethylhexyl group. However, it is important to note the exact nature of the organic phase under high acid loading, whether it be reverse micelles, bicontinuous microemulsion, or some combination of the two has not yet been determined for these systems.

These studies with small-angle scattering data are important for understanding the fluid architecture because at the molecular level, there was little to no difference observed in the organic phase following acid contact, when in fact there are substantial differences observed following Ln contact. Understanding the different sizes of channels or micelles in the organic phases with TODGA and T2EHDGA could explain the observations in distribution ratios between these two DGAs.

3.2.2. Polydispersity of DGA aggregates

In contrast to the average aggregate dimensions determined for TODGA and T2EHDGA via small-angle scattering techniques, implementation of DLS reveals aggregates with an average diameter of about a 10-fold difference. The average diameter measured by DLS is consistent with the aggregate length measured via small-angle scattering, but the shape of the data shown in Fig. 19 is right-skewed. This suggests that a spherical model is incorrect for these particular DGA systems. After various DGAs were contacted with 1 M HNO_3, the intensity of the pair-distance distribution function remained constant, indicating a significant number of aggregates exist even under low acid conditions [51]. Shorter alkyl chain DGA derivatives extract more H_2O and acid than DGAs with longer alkyl chains, as evident by the larger aggregate sizes (3.9 nm for THDGA vs 2.1 nm for TDdDGA), as seen in Fig. 19 [51].

The trend in aggregate sizes is: THDGA > TODGA > TDDGA > TDdDGA. In the case of these smaller alkyl chain derivatives, polar-polar interactions are dominant, which is observed by the rapid increase in both aggregate size and polydispersity of the THDGA, TODGA, and T2EHDGA systems. Increasing the alkyl chain length, to TDDGA or TDdDGA, results in smaller aggregates from decreasing aggregate swelling and increasing dispersion of aggregates in the diluent [51]. This is observed in the decrease in polydispersity when compared to the shorter alkyl chain DGA derivatives. Increasing the HNO_3 concentration increases the full-width at half-maximum (FWHM) of the pair-distance distribution function, resulting in a greater size distribution of the aggregates. It is difficult to draw conclusions from the DLS data as 1) the refractive indices were not measured and 2) the aggregate shapes were assumed to be spherical. However, if one considers that the "diameter" as modeled by DLS is representative of the length as measured by SANS, it appears that an increase in elongation occurs for DGAs with longer alkyl chains, although this cannot be definitively stated without the SANS data to support it.

In this established trend increasing the concentration of HNO_3 increases the number of different aggregates present in solution with a more drastic change occurring for the shorter DGAs (THDGA, TODGA, T2EHDGA) than the longer DGAs (TDDGA and TDdDGA). The various *n*-mers that are present for the shorter DGAs also form larger aggregates. This correlates to a larger number of DGAs per Ln as previously discussed via solvent extraction, which suggests that the supramolecular aggregate structure in the organic phase is related to molecular structure of the extracted Ln species.

3.2.3. Impacts of H^+ source and Na^+ on aggregation

Inter-aggregate attractive interactions resulting from acid extraction are dependent on the nature of the acid extracted. [54,93] The trend in solvent extraction for different strong acids is mirrored in aggregate sizes, where larger aggregates form in the presence of $HClO_4$ under similar acid concentrations. This study supports previous literature in the case of HNO_3, where a dramatic increase in aggregate size occurs when the concentration of HNO_3 exceeds 0.5 M [85]. In contrast to both $HClO_4$ and HNO_3, extraction of Ln^{3+} using HCl increases based on an exponential curve, with a slight increase in aggregate size with increasing acid concentration [85]. The system involving HCl has the smallest aggregate size and is below the critical size of 2 nm for tetrameric aggregate formation, indicating the presence of only monomers and dimers [85]. Average aggregate sizes for TODGA/*n*-dodecane in contact with either HCl, HNO_3, or $HClO_4$ are shown in Fig. 20 [57].

Aggregate nucleation occurs under lower acid concentrations when solutes have increased polarizability, particularly for mono-acids [54]. The aggregation numbers are also dependent on the pKa of the acid, where stronger acids form larger aggregates [54]. Particularly for $HClO_4$, the aggregates are less diffusive thus appearing larger than aggregates formed in the presence of HNO_3 [54]. The potential for the extracted acid to disrupt the extensive hydrogen bonding network with both H_2O molecules and DGAs occurs in the following order, $HClO_4$ < HNO_3 < HCl. This trend in aggregate sizes is consistent with the trend observed for D values, further supporting the importance of the correlation between supramolecular aggregates and molecular structure. It follows that the surface to charge density of the anion and ability to interact with polar solutes, as evident in the Hoffmeister series and supported by solvent extraction also follows this trend. Therefore, the nature of the counter-ions is relevant to the structure of the aggregates in the organic phase.

The importance of using an acid (HNO_3) instead of a salt ($NaNO_3$) was further supported via SANS, where increasing the concentration of $NaNO_3$ in the presence of 0.01 M HNO_3 did not change the scattering data [34]. The SANS data for $NaNO_3$, increases in intensity, which is the result of adding 0.01 M HNO_3,

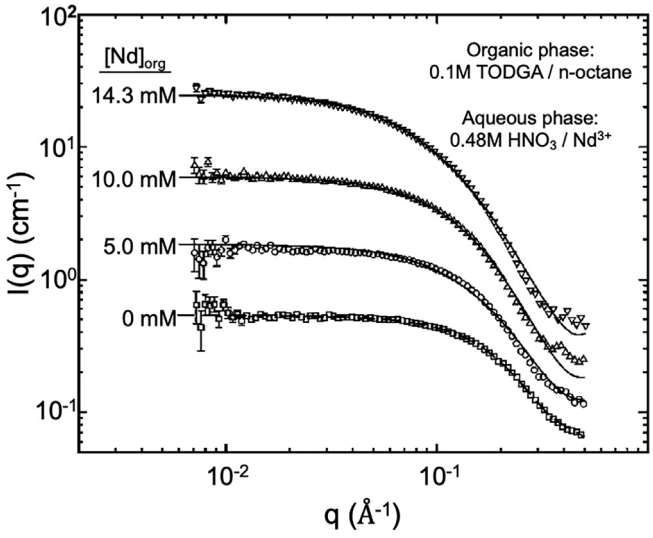

Fig. 21. Varying Nd^{3+} in contact with TODGA/*n*-octane and 0.48 M HNO_3, where the data was offset for clarity. Figure obtained from Jensen *et al.* [85].

and likely not the 1–3 M $NaNO_3$. SANS data for 0.01 M HNO_3/1–3 M $NaNO_3$ are similar to the 0.1 M HNO_3 system. Adding 0.01 M HNO_3 induces the slight changes in aggregation that are observed, with little contribution from $NaNO_3$. Thus, $NaNO_3$ prevents a hydrogen bonding network from forming, thereby restricting the aggregate size making it difficult to extract Ln^{3+}.

3.2.4. Phase modifiers effect on T2EHDGA morphology

The presence of 1-alcohols has previously been shown to impact aggregation resulting from its ability to better solvate the extracted solutes and serve as a hydrogen donor. These systems were further studied with T2EHDGA/*n*-dodecane in either 19 vol % of either 1-octanol, 1-decanol, or 1-isodecanol. Aggregate sizes for their respective systems were evaluated across 1–12 M HNO_3 [53]. The aggregate size decreased from 18.4 nm for *n*-dodecane to 4 nm with addition of 19 vol% 1-alcohol. Increasing the alkyl chain length on the 1-alcohol decreased the aggregate size, resulting in the following trend across increasing the concentration of HNO_3, 1-octanol > 1-isodecanol > 1-decanol. The presence of 19 vol% 1-alcohol inhibits merging of (DGA)(HNO_3) aggregates, restricting the overall aggregate size [53]. Solvent phase properties – namely polarity – are vital for preventing TPF by either restricting aggregate merging or inducing significant structural change that is otherwise not observed in aliphatic diluents.

Evidence for the change in supramolecular aggregate structure upon adding 1-alcohol to the solvent, is provided by the polydispersity of aggregates. Polydispersity provides information as to the complexity regarding the number of extractant species present and is measured by the FWHM of the pair-distance distribution function. T2EHDGA/*n*-dodecane has a FWHM of 13.5 nm, and incorporation of 19 vol% 1-alcohol decreased this to 3 nm [53]. Decreasing the FWHM indicates that 19 vol% 1-alcohol, reduces the variety of aggregate species present. Across these various 1-alcohol phase modifiers, an increase in dispersive VDW forces results in a trend in aggregate distribution according to 1-octanol > 1-isodecanol > 1-decanol [53]. This is the same trend established for the size of the aggregates and remains the same when the HNO_3 is varied [53]. For each 1-alcohol tested, increasing the concentration of HNO_3 increases the FWHM, thus increasing the polydispersity of aggregates in the organic phase [53].

The addition of phase modifiers, specifically 1-alcohols, decreased aggregate size and polydispersity. A smaller aggregate size either restricts supramolecular aggregates from forming or the supramolecular aggregates are very small and do not combine to form larger aggregates. This suggests that 1-alcohol better solvates the extracted polar solutes and/or the (DGA)·(HNO_3) adducts than *n*-dodecane alone.

3.3. Supramolecular structure of extracted Ln^{3+}

It has been hypothesized that Ln^{3+} are extracted by a tetrameric TODGA species, where two TODGA molecules are directly coordinated to Ln^{3+}. The two remaining TODGA are located in the outer-coordination sphere [34]. This is supported by the large molecular volume of TODGA, 1070 $Å^3$, making it difficult to fit four monodentate TODGA molecules around a single $Ln(NO_3)_3$ molecule [49]. If the extracted aggregate is stable prior to Ln^{3+} extraction, any number of uncoordinated TODGA could be present in the extracted complex [49]. Increasing the HNO_3 concentration above 1 M, increases the nitrate dependence to six nitrates per Ln^{3+}, indicating extractant aggregation is mediated by something other than extractant concentration [49]. Distribution coefficients for Ln^{3+} are independent of TODGA concentration, but strongly dependent on HNO_3 concentration [49]. In this regime where hyperstoichiometric Ln:NO_3 complexes form, there is an increase in polydispersity of the organic phase, evident with the formation of large TODGA aggregates. This suggests that these aggregate *n*-mers serve as a better extractant than the monomer–dimer mixture for the Ln^{3+} [49]. Thus, extraction of nitric acid initiates supramolecular ordering of the organic phase to a structure that is selective for the extraction of Ln^{3+} ions [93,94]. The remarkable effects of nitric acid extraction on Ln D values across the period have been reported by Narita *et al.* [32].

Consistent with the aggregate morphology observed following 0.01 M HNO_3 and 3 M $LiNO_3$, contact of Nd^{3+} with TODGA/*n*-dodecane resulted in elongated aggregates [44]. These aggregates are composed of varying numbers of TODGA molecules as predicted by the increase in polydispersity of Nd-DGA systems. Each aggregate is comprised of either 3, 4, or 5 TODGA molecules, further illustrating the importance of outer-sphere DGA interactions. Increasing the concentration of HNO_3 to 2 M resulted in an increase in the length of the aggregates with minimal change to the aggregate diameter [85]. Similarly, this effect on aggregate morphology was observed with increasing Nd^{3+} concentration, as shown in Fig. 21. This observed increase in aggregate length was the result of the number of TODGA molecules present, which varied from 2 to 7, dependent upon the Nd^{3+} concentration.

These studies support the hypothesis that the extractant mechanism is perhaps related to the concentration of acid and Ln^{3+} contacted with the solvent. This suggests a correlation between the D values and aggregate size, where larger aggregates should be the result of a higher extraction of polar solutes. SANS results support the regression analysis from solvent extraction that suggested 3–4 TODGA molecules per Nd. The fact that these two techniques agree, indicates that when the correct assumptions are made, SANS provides valuable information regarding aggregate structure.

3.3.1. Synergistic effect between H^+ and Ln^{3+} on aggregation

Extraction of water and acid serve as nucleating agents for the supramolecular DGA aggregates [94]. Perhaps the importance of

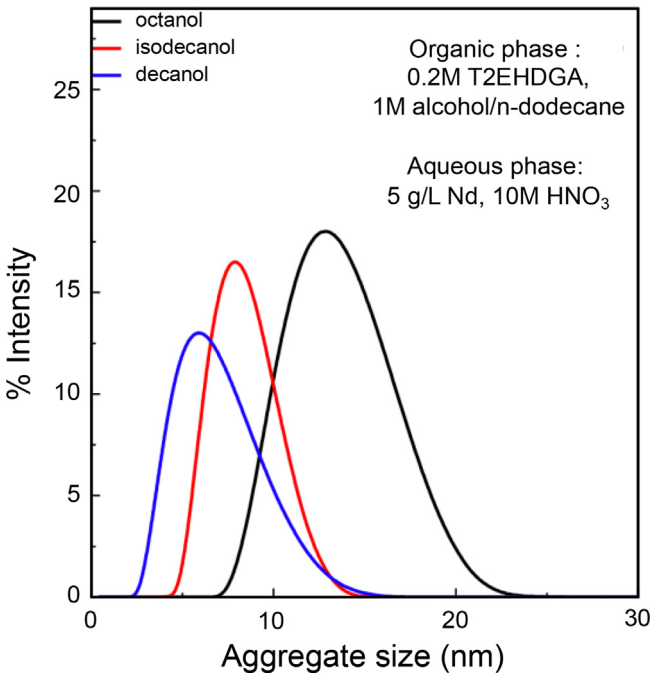

Fig. 22. Pair-distance distribution functions for 0.2 M T2EHDGA/*n*-dodecane with phase modifiers 1-alcohols, following extraction of 5 g/L Nd and 10 M HNO_3. Different colors denote the 1-alcohol used, decanol (blue), isodecanol (red), and octanol (black). Figure obtained from Swami *et al.* [53].

H^+ extraction in facilitating an extensive hydrogen bonding network has not been realized. Previous studies with the malonamide DMDOHEMA resulted in an average of 4.17 hydrogen bonds per Eu^{3+} for 3 M $LiNO_3$, and 18.4 hydrogen bonds per Eu^{3+} for 3 M HNO_3 [146]. Hydrogen bonding within the aggregates is responsible for stabilizing the extracted Ln^{3+} complex as well as bridging the Ln^{3+} to the surrounding extractant molecules, thus creating large supramolecular aggregates [146]. In contrast, the neutral system is starved for hydrogen bonds therefore limiting the size of the aggregates. The significant increase in the number of hydrogen bonds present in the acidic system demonstrates the importance of H^+ for establishing a hydrogen bonding network.

Without the presence of protons to induce hydrogen bonding networks, the aggregates are starved of acidity and the synergistic effect between H^+ and Ln^{3+} for $C{=}O^{\delta-}$ does not occur. This is correlated with the formation of smaller aggregates for neutral systems ($NaNO_3$ or $LiNO_3$), with nitrates mostly coordinating bidentate to Ln^{3+}. Whereas bidentate coordination is typically preferred, under acidic conditions the energy of monodentate coordination approaches that for bidentate coordination, resulting in mixed nitrate denticity to Ln. Monodentate nitrate coordination increases the hydrogen bonding network through the number of available oxygen atoms for hydrogen bonding, as previously shown in Fig. 9.

Due to the importance of supramolecular aggregate formation for extracting Ln^{3+} and, notably the absence of these supramolecular aggregates upon extraction from HCl, it follows that chloride weakens extraction of Ln^{3+} in comparison to nitrate [59,98]. The trend established for inter-aggregate attractive interactions is as follows: $HClO_4$ > HNO_3 > HCl > HCOOH > $LiNO_3$ [54]. This trend is dependent upon the availability of H^+ in facilitating hydrogen bonding networks and the charge-to-surface area ratio of the anion. Extraction of H_2O, which increases the hydrogen bond network, depends on polarizability and dissociation strength of the acid [57].

The impact of H^+ on extraction is consistent with DLS results that determined $NaNO_3$ is less effective for Ln^{3+} extraction when compared with HNO_3 [29]. This observation is mirrored in Ce^{3+}-−malonamide solvent extraction systems with 3 M HNO_3 and 3 M $LiNO_3$ aqueous phases. Nitric acid enhances the extraction of Ce^{3+} in ways that lithium nitrate cannot, namely by the organization of the organic phase—presumably through hydrogen-bonding interactions—into reverse micellar like aggregates [58,147]. Similarly, introducing Eu^{3+} into TODGA and T2EHDGA/*n*-dodecane systems with 0.01 M HNO_3 and 3 M $NaNO_3$ resulted in no change to the small-angle scattering data, when compared to the 0.01 M HNO_3 system [34]. This suggests that $H^+(H_3O^+)$ is critical for initiating aggregation required for extraction of Ln^{3+} ions [34,45].

3.3.2. Phase modifiers impact on Ln^{3+} DGA morphology

The extraction capacity of Ln^{3+} is dependent on aggregate size, and therefore the polarity of the diluent [38,39]. As such, the impact of phase modifiers on aggregate morphology was determined. The aggregate size for T2EHDGA/*n*-dodecane with 19 vol% 1-octanol following Nd^{3+} contact results in the same trend following HNO_3 contact, 1-octanol > 1-isodecanol > 1-decanol. The pair-distance distribution functions corresponding to these systems were obtained with DLS and are shown in Fig. 22. Although 1-octanol and 1-isodecanol formed larger aggregates, they also formed more spherical or ellipsoidal aggregates as represented by the approximate bell-shape pair-distance distribution function. In contrast, the pair-distance distribution function for 1-decanol is right-skewed, forming more elongated aggregates. In each case, the average aggregate size ranged from 5 to 15 nm. In the presence of phase modifiers, the competing dispersion forces in the polar core are effectively quenched [87]. Although both HNO_3 loading and Nd^{3+} prevented TPF, larger aggregate sizes were observed during the Nd^{3+} loading experiments, as HNO_3 is co-extracted along with Nd^{3+}. Increasing extraction of Ln^{3+} with HNO_3, indicates the competition between Ln^{3+} is synergistic rather than antagonistic, as experienced by other neutral extractants [133].

Evidence for a morphology change with increasing Nd^{3+} loading was observed for TODGA/*n*-heptane in contact with 3 M $LiNO_3$ and 0.01 M HNO_3. Upon addition of 5 vol% 1-octanol, the number of TODGA molecules participating in the overall Nd-DGA extracted complex decreased to 2–4. [44] In the presence of 5 vol% 1-octanol, there was a decrease in the power-law X-ray scattering at low q-values, but an I(q) dependence of zero was not observed. This indicates either polydisperse reverse micellar-like aggregates or aggregates independent of Nd^{3+} concentration [44]. Whereas with the phase modifier 0.5 M DMDOHEMA, mixed aggregates formed, increasing the polydispersity of the solutes [44]. The q^0-dependence at low q-values indicates that with DMDOHEMA the aggregates maintain their globular characteristics. Molecular dynamics simulations suggest that polymetallic complexes are bridged by nitrates, where the core is surrounded by TODGA molecules and either 1-octanol or DMDOHEMA, if present, in the system [44]. These results are consistent with those reported for the DMDOHEMA/*n*-heptane system with Eu^{3+} in 3 M $LiNO_3$, which determined that a concentration of 30 mM Eu^{3+} was required to induce changes in the SAXS response, to a power-law dependence of q^{-1} [16]. The SWAXS response for TODGA resembles that of the DMDOHEMA system with a strong q-dependent power-law scattering of −1, indicating a potentially similar microstructure for both malonamides and DGAs.

The result from molecular dynamic simulations deviates from the structure hypothesized from solvent extraction and spectroscopic investigation where 3 TOGDA molecules coordinate to Ln with outer-sphere nitrates that further interact with phase modifiers, which solvate the Ln-DGA complex. As a limited number of studies have been performed with small-angle scattering techniques with Ln in the system, it is imperative that additional studies be performed to draw broader conclusions. However, Berthon *et al.* Describe results from ESI-MS that are consistent with other phase modifier data where a decrease in the average number of DGAs associated with the overall extracted Ln complex is observed [44]. This decrease in number of DGA molecules is attributed to efficient solvation of Ln-DGA complex by the phase modifier pre-

Table 5
Selected issues of contradiction in the published literature for measurements that are inconclusive or where questionable assumptions were made.

Topic	Comment	Ref
Role of nitrates in molecular structure	Nitrates are inner-sphere coordinated to Ln	[17,44]
	Nitrates are located in outer-sphere	[29,66]
EXAFS ambiguities	$[Ln(T2EHDGA)_2(H_2O)_3]^{3+}$ and $[Ln(T2EHDGA)_3]^{3+}$ had the same fit	[24]
Assumptions for aggregate distributions in DLS	The refractive index was assumed and not measured	[17,52,57,87,148]
Effect of Ln^{3+} ion on aggregate size	Addition of Ln does not change aggregate size	[34]
	Addition of Ln results in larger aggregatess	[85]
Charge neutrality of Ln-DGA complex was not achieved	Activity of aqueous phase was neglected in slope analysis	[48,81]

Table 6
A summary of important conclusions for each of the sections in this literature review.

Category	Conclusion	Ref
(DGA)(HNO_3) Adducts	Most common are 1:1 (DGA interacting with hydronium nitrate ion pair) and 1:2 (HNO_3 molecule directly protonates a DGA C=O group)	[77,78]
Extracted Ln-DGA complex	1:3 $[Ln(DGA)_3]^{3+}$ or 1:2 $[Ln(DGA)_2(NO_3)_x(H_2O)_y]^{3-x}$ with outer-sphere anions for charge neutrality	[2,50,58,66,73,80,96]
	Using solvent extraction to predict the number of DGA molecules per extracted Ln-DGA complex, operates at length scales beyond the Ln-O bond	[11]
	Applying dispersion and explicit outer-sphere anions (NO_3^- or Cl^-) in DFT calculations are necessary to predict the experimental trend for D(Ln)	[11,73]
	The trend in D(Ln) has been observed in the ratio of extracted H_2O per free NO_3^- (or outer-sphere effects)	[11]
Phase modifier / solvent effects	Adding phase modifiers does not change the extracted Ln inner-sphere, but changes the hydrogen bonding network in the outer-sphere	[44,65]
	Primary function of phase modifiers appears to be solvation of Ln-DGA complex, reducing outer-sphere interactions of Ln-DGA complex with (DGA)(HNO_3) adducts	[44,65]
	Diluents role in extraction can encourage interactions between Ln-DGA complex and (DGA)(HNO_3) adducts or inhibit them by solvation of the Ln-DGA complex	[2,81,99]
	Diluents with a high dielectric constant can solvate Ln-DGA complexes and have D(Ln) that are independent of H^+ concentration but are dependent on NO_3^-	[81]
Importance of H^+	H^+ enable hydrogen bonding networks to form, allowing Ln-DGA complexes to interact with (DGA)(HNO_3) adducts	[57,78]
	In neutral media, nitrates can coordinate either monodentate or bidentate to Ln	[29,34,81]
Aggregates	Morphologies of DGA aggregates are consistent with elongated sphere, ellipsoids, rod-like, or short cylinders	[85]
	A change in morphology of DGA aggregates requires H^+	[57,85,94]
	β-branching on T2EHDGA results in smaller aggregates than with TODGA	[34,114]
	The lower number of T2EHDGA molecules involved in an extracted Ln-DGA complex might not solely result from the β-branching steric interactions, but from the larger scale organic phase microstructure	[24,34]

venting additional (DGA)·(HNO_3) adduct from hydrogen bonding to the Ln-DGA complex.

4. Outlook

Through use of the multimodal research conducted in the field of chemical separations with DGAs, a variety of multiscale system perspectives have been reported. When surveyed together as done herein, one finds consistent insights into the nature of the organic phases, on the one hand, as well as points of contradiction and disagreement, on the other. Some of the conflicting views can be attributed to the fundamentally different scales of interrogation using, for example, photon probes that cover the infrared to the visible, UV, and X-ray, not to mention the different inherent sensitivities of photons, electrons, and neutrons to soft matter aggregates in complex fluids. Furthermore, one finds results that were either inconclusive or used questionable assumptions in data modeling and analyses. For example, the contents of Table 5 illustrate where some discrepancies are found in the literature of Ln-DGA separation science.

The contradictions within the literature exist largely because of the limited number of physical, spectroscopic and small angle scattering investigations with multiple Ln. Stated simply, there is insufficient evidence to support a structural change across the Ln series. For example, although it would be ideal to collect EXAFS data across the entire series, it has not been done in a systematic manner. In particular, there is a lack of data on the light Ln in these systems. As it has been hypothesized that a structural change is purported to occur around Nd, understanding the structure with the light Ln (i.e., La – Nd) is desired. There are practical problems with the acquisition of L_3-edge EXAFS data for the lightest La; K-edge EXAFS would provide high-resolution structure insights. Errors regarding questionable assumptions in the analysis of small-angle scattering and DLS data can propagate to other results. In particular, molecular dynamics simulations are vitiated when validated with incorrect small-angle scattering data.

To move forward and elucidate the correct organic phase structures, several changes need to be made regarding DGA literature and data collection. Collecting EXAFS on Ln-T2EHDGA complexes will aid in understanding molecular differences between those observed with the Ln-TODGA system. EXAFS would also be beneficial for confirming the role of phase modifiers in the Ln-DGA complex, particularly if they participate in the inner-sphere. Additional spectroscopic investigations, such as FT-IR and UV–vis, would support structural data obtained via EXAFS and determine the role of co-extracted nitrates. Small-angle scattering techniques, specifically SANS in the presence of phase modifiers would show if phase modifiers suppressed aggregation, and to what degree through calculation of the aggregate size and number of extractant molecules per complex. Although the application of these multiple techniques on both TODGA and T2EHDGA systems is vital, it is important to stress that the experimentation needs to be done across the Ln series to elucidate structural changes on both the molecular and supramolecular scale for understanding the unique trend in D values across the Ln period.

5. Concluding remarks

This review focused on understanding the extracted Ln-DGA complexes and how these changed in the presence of phase modifiers, different diluents, and in acidic vs neutral media. Additionally, the results from the molecular structures were used in tandem with small angle scattering and DLS results to provide a more holistic understanding of interactions in DGA systems beyond Ln coordination chemistry. Conclusions from each of these areas are described in Table 6.

Although several pieces of the puzzle regarding the coordination chemistry are in place, the literature still lacks both spectroscopic and scattering data across the Ln series. This is instrumental in evaluating the trends in extracted Ln^{3+} complexes across the series. There are many opportunities for advancement of understanding organic phase properties, especially by use of different techniques, such as (ultra-low-shear) rheometry, viscometry, densitometry, refractometry, electrochemistry, XPCS, calorimetry, vapor pressure osmometry, cryo-TEM with freeze-fracture capabilities. Future efforts would benefit from application of such approaches across the lanthanide series to understand Ln-DGA organic phase complexation in a more systematic fashion.

Funding sources

The authors were supported by the Department of Energy Basic Energy Science program (DE-SC0022217) for this work.

Data availability

No data was used for the research described in the article.

Declaration of Competing Interest

The authors declare that they have no known competing financial interests or personal relationships that could have appeared to influence the work reported in this paper.

Acknowledgment

We thank our Colorado School of Mines colleague Dr. Mark R. Antonio for providing critical comments, perspectives, and insights.

References

[1] M.K. Jha, A. Kumari, R. Panda, J. Rajesh Kumar, K. Yoo, J.Y. Lee, Review on hydrometallurgical recovery of rare earth metals, Hydrometallurgy. 165 (2016) 2–26, https://doi.org/10.1016/j.hydromet.2016.01.035.
[2] I. Kajan, M. Florianova, C. Ekberg, A.V. Matyskin, Effect of diluent on the extraction of europium(III) and americium(III), RSC Adv. 11 (2021) 36707–36718, https://doi.org/10.1039/d1ra07534a, with N, N, N', N'-tetraoctyl diglycolamide (TODGA.
[3] G.A. Picayo, M.P. Jensen, Rare earth separations: Kinetics and mechanistic theories, in: J.-C.G. Bünzli, V.K. Pecharsky (Eds.), Handbook on the Physics and Chemistry of Rare Earths, Elsevier, Amsterdam, 2018: pp. 145–225. 10.1016/bs.hpcre.2018.10.002.
[4] A.S. Kanekar, S.A. Ansari, R.B. Gujar, D.R. Prabhu, P.N. Pathak, P.K. Mohapatra, V.K. Manchanda, Hydrodynamic properties for N, N, N′, N′-tetraalkyl diglycolamides dissolved in n-dodecane system, Can. J. Chem. Eng. 90 (2012) 682–689, https://doi.org/10.1002/cjce.20559.
[5] A.M. Wilson, P.J. Bailey, P.A. Tasker, J.R. Turkington, R.A. Grant, J.B. Love, Solvent extraction: The coordination chemistry behind extractive metallurgy, Chem. Soc. Rev. 43 (2014) 123–134, https://doi.org/10.1039/c3cs60275c.
[6] R.J. Ellis, D.M. Brigham, L. Delmau, A.S. Ivanov, N.J. Williams, M.N. Vo, B. Reinhart, B.A. Moyer, V.S. Bryantsev, "Straining" to separate the rare earths: How the lanthanide contraction impacts chelation by diglycolamide ligands, Inorg. Chem. 56 (2017) 1152–1160, https://doi.org/10.1021/acs.inorgchem.6b02156.
[7] N.N. Hidayah, S.Z. Abidin, The evolution of mineral processing in extraction of rare earth elements using liquid-liquid extraction: A review, Miner. Eng. 121 (2018) 146–157, https://doi.org/10.1016/j.mineng.2018.03.018.
[8] Z. Chen, Z. Li, J. Chen, P. Kallem, F. Banat, H. Qiu, Recent advances in selective separation technologies of rare earth elements : a review, J. Environ. Chem. Eng. 10 (2022), https://doi.org/10.1016/j.jece.2021.107104.
[9] P.F. Lang, B.C. Smith, Ionization energies of lanthanides, J. Chem. Educ. 87 (2010) 875–881, https://doi.org/10.1021/ed100215q.
[10] T. Matsutani, Y. Sasaki, S. Katsuta, Separation of light and middle lanthanides using multistage extraction with diglycolamide extractant, Anal. Sci. 37 (2021) 1603–1609, https://doi.org/10.2116/analsci.21P120.
[11] A.G. Baldwin, A.S. Ivanov, N.J. Williams, R.J. Ellis, B.A. Moyer, V.S. Bryantsev, J. C. Shafer, Outer-sphere water clusters tune the lanthanide selectivity of diglycolamides, ACS Cent. Sci. 4 (2018) 739–747, https://doi.org/10.1021/acscentsci.8b00223.
[12] R.J. Ellis, Acid-switched Eu(III) coordination inside reverse aggregates: Insights into a synergistic liquid-liquid extraction system, Inorg. Chim. Acta. 460 (2017) 159–164, https://doi.org/10.1016/j.ica.2016.08.008.
[13] S.M. Ibrahim, Y. Zhang, Y. Xue, S. Yang, F. Ma, Y. Gao, Y. Zhou, G. Tian, Selective extraction of light lanthanides(III) by N, N-di(2-ethylhexyl)-diglycolamic acid: A comparative study with N, N-dimethyl-diglycolamic acid as a chelator in aqueous solutions, ACS, Omega. 4 (2019) 20797–20806, https://doi.org/10.1021/acsomega.9b03241.
[14] S. Dourdain, I. Hofmeister, O. Pecheur, J.F. Dufrêche, R. Turgis, A. Leydier, J. Jestin, F. Testard, S. Pellet-Rostaing, T. Zemb, Synergism by coassembly at the origin of ion selectivity in liquid-liquid extraction, Langmuir. 28 (2012) 11319–11328, https://doi.org/10.1021/la301733r.
[15] C. Bauer, P. Bauduin, J.F. Dufrêche, T. Zemb, O. Diat, Liquid/liquid metal extraction: Phase diagram topology resulting from molecular interactions between extractant, ion, oil and water, Eur. Phys. J. Spec. Top. 213 (2012) 225–241, https://doi.org/10.1140/epjst/e2012-01673-4.
[16] R.J. Ellis, Y. Meridiano, J. Muller, L. Berthon, P. Guilbaud, N. Zorz, M.R. Antonio, T. Demars, T. Zemb, Complexation-induced supramolecular assembly drives metal-ion extraction, Chem. - Eur. J. 20 (2014) 12796–12807, https://doi.org/10.1002/chem.201403859.
[17] K.R. Swami, A.S. Suneesh, R. Kumaresan, K.A. Venkatesan, M.P. Antony, Dynamic light scattering and FTIR spectroscopic investigations on the reverse micelles produced during the extraction of Nd(III) and nitric acid in tetra ethylhexyl diglycolamide, ChemistrySelect. 2 (2017) 11177–11186, https://doi.org/10.1002/slct.201701465.
[18] D.F. Peppard, G.W. Mason, J.L. Maier, W.J. Driscoll, Fractional extraction of the lanthanides as their di-alkyl orthophosphates, J. Inorg. Nucl. Chem. 4 (1957) 334–343, https://doi.org/10.1016/0022-1902(57)80016-5.
[19] Z. Kolarik, Review: Dissociation, self-association, and partition of monoacidic organophosphorus extractants, Solvent Extr. Ion Exch. 28 (2010) 707–763, https://doi.org/10.1080/07366299.2010.515172.
[20] D. Li, Development course of separating rare earths with acid phosphorus extractants: A critical review, J. Rare Earths. 37 (2019) 468–486, https://doi.org/10.1016/j.jre.2018.07.016.
[21] K. Ishida, S. Takeda, T. Takahashi, T. Sato, Extraction behaviors of rare earth elements in solvent extraction with single and mixed extractant systems: Extraction of rare earths by phosphoric acid esters containing bulky alkyl groups II, Shigen Sozai. 111 (1995) 114–118, https://doi.org/10.2473/shigentosozai.111.114.
[22] M.P. Jensen, R. Chiarizia, J.S. Ulicki, B.D. Spindler, D.J. Murphy, M.M. Hossain, A. Roca-Sabio, A. de Blas, T. Rodríguez-Blas, Solvent extraction separation of trivalent americium from curium and the lanthanides, Solvent Extr. Ion Exch. 33 (2015) 329–345, https://doi.org/10.1080/07366299.2015.1046292.
[23] Y. Liu, C. Zhao, Z. Liu, Y. Zhou, C. Jiao, M. Zhang, H. Hou, Y. Gao, H. He, G. Tian, Extraction and stripping behaviors of 14 lanthanides from nitric acid medium by N, N'-dimethyl-N, N'-dioctyl diglycolamide, J. Radioanal. Nucl. Chem. 325 (2020) 409–416, https://doi.org/10.1007/s10967-020-07242-1.
[24] D. Stamberga, M.R. Healy, V.S. Bryantsev, C. Albisser, Y. Karslyan, B. Reinhart, A. Paulenova, M. Foster, I. Popovs, K. Lyon, B.A. Moyer, S. Jansone-Popova, Structure activity relationship approach toward the improved separation of rare-earth elements using diglycolamides, Inorg. Chem. 59 (2020) 17620–17630, https://doi.org/10.1021/acs.inorgchem.0c02861.
[25] S.A. Ansari, P. Pathak, P.K. Mohapatra, V.K. Manchanda, Chemistry of diglycolamides: Promising extractants for actinide partitioning, Chem. Rev. 112 (2012) 1751–1772, https://doi.org/10.1021/cr200002f.
[26] H. Du, X. Peng, Y. Cui, G. Sun, Effect of diglycolamide ligands structure on extraction performance of heavy rare earth ions, Solvent Extr. Res. Dev., Jpn. 27 (2020) 81–89, https://doi.org/10.15261/serdj.27.81.
[27] Y. Sasaki, M. Matsumiya, M. Nakase, K. Takeshita, Extraction and separation between light and heavy lanthanides by N, N, N', N'-tetraoctyl-diglycolamide from organic acid, Chem. Lett. 49 (2020) 1216–1219, https://doi.org/10.1246/CL.200431.
[28] E.A. Mowafy, D. Mohamed, Extraction behavior of trivalent lanthanides from nitric acid medium by selected structurally related diglycolamides as novel extractants, Sep. Purif. Technol. 128 (2014) 18–24, https://doi.org/10.1016/j.seppur.2014.03.005.
[29] E. Campbell, V.E. Holfeltz, G.B. Hall, K.L. Nash, G.J. Lumetta, T.G. Levitskaia, Extraction behavior of Ln(III) ions by T2EHDGA/n-dodecane from nitric acid and sodium nitrate solutions, Solvent Extr. Ion Exch. 36 (2018) 331–346, https://doi.org/10.1080/07366299.2018.1447261.
[30] Y. Sasaki, Y. Sugo, K. Morita, K.L. Nash, The effect of alkyl substituents on actinide and lanthanide extraction by diglycolamide compounds, Solvent Extr. Ion Exch. 33 (2015) 625–641, https://doi.org/10.1080/07366299.2015.1087209.
[31] Z.X. Zhu, Y. Sasaki, H. Suzuki, S. Suzuki, T. Kimura, Cumulative study on solvent extraction of elements by N, N, N′, N′-tetraoctyl-3-oxapentanediamide (TODGA) from nitric acid into n-dodecane, Anal. Chim. Acta. 527 (2004) 163–168, https://doi.org/10.1016/j.aca.2004.09.023.
[32] H. Narita, T. Yaita, K. Tamura, S. Tachimori, Study on the extraction of trivalent lanthanide ions with N, N'-dimethyl-N, N'-diphenyl-malonamide and-diglycolamide, J. Radioanal. Nucl. Chem. 239 (1999) 381–384, https://doi.org/10.1007/BF02349516.
[33] R. Flores, M.A. Momen, M.R. Healy, S. Jansone-Popova, K.L. Lyon, B. Reinhart, M.C. Cheshire, B.A. Moyer, V.S. Bryantsev, The coordination chemistry and stoichiometry of extracted diglycolamide complexes of lanthanides in extraction chromatography materials, Solvent Extr. Ion Exch. 40 (2022) 6–27, https://doi.org/10.1080/07366299.2021.1956121.
[34] P.N. Pathak, S.A. Ansari, P.K. Mohapatra, V.K. Manchanda, A.K. Patra, V.K. Aswal, Role of alkyl chain branching on aggregation behavior of two symmetrical diglycolamides: Small angle neutron scattering studies, J. Colloid Interface Sci. 393 (2013) 347–351, https://doi.org/10.1016/j.jcis.2012.10.023.
[35] S. Murakami, M. Matsumiya, Y. Sasaki, S. Suzuki, S. Hisamatsu, K. Takao, Investigation into coordination states of diglycolamide and dioxaoctanediamide complexes with lanthanide elements using spectroscopic methods, Solvent Extr. Ion Exch. 35 (2017) 233–250, https://doi.org/10.1080/07366299.2017.1336049.
[36] H. Suzuki, Y. Tsubata, T. Kurosawa, M. Shibata, T. Kawasaki, S. Urabe, T. Matsumura, Highly practical and simple ligand for separation of Am(III) and Eu(III) from highly acidic media, Anal. Sci. 32 (2016) 477–479, https://doi.org/10.2116/analsci.32.477.

[37] Y. Sasaki, Y. Tsubata, Y. Kitatsuji, Y. Sugo, N. Shirasu, Y. Morita, T. Kimura, Extraction behavior of metal Ions by TODGA, DOODA, MIDOA, and NTAamide extractants from HNO3 to n-dodecane, Solvent Extr. and Ion Exch. 31 (2013) 401–415, https://doi.org/10.1080/07366299.2013.800431.
[38] E.A. Mowafy, D. Mohamed, Extraction and separation of Nd(III), Sm(III), Dy (III), Fe(III), Ni(II), and Cs(I) from concentrated chloride solutions with N, N, N′, N′-tetra(2-ethylhexyl) diglycolamide as new extractant, J. Rare Earths. 33 (2015) 432–438, https://doi.org/10.1016/S1002-0721(14)60437-3.
[39] E.A. Mowafy, A. Alshammari, D. Mohamed, Extraction behaviors of critical rare earth elements with novel structurally tailored unsymmetrical diglycolamides from acidic media, Solvent Extr. Ion Exch. 40 (2021) 387–411, https://doi.org/10.1080/07366299.2021.1925002.
[40] S. Kannan, M.A. Moody, C.L. Barnes, P.B. Duval, Lanthanum(III) and uranyl(VI) diglycolamide complexes: Synthetic precursors and structural studies involving nitrate complexation, Inorg. Chem. 47 (2008) 4691–4695, https://doi.org/10.1021/ic7025076.
[41] E. Metwally, A.S. Saleh, S.M. Abdel-Wahaab, H.A. El-Naggar, Extraction behavior of cerium by tetraoctyldiglycolamide from nitric acid solutions, J. Radioanal. Nucl. Chem. 286 (2010) 217–221, https://doi.org/10.1007/s10967-010-0641-2.
[42] Y. Sasaki, T. Kimura, K. Oguma, Solvent extraction of various metals including actinides by bidentate and tridentate diamides, J. Ion Exch. 18 (2007) 354–359, https://doi.org/10.5182/jaie.18.354.
[43] Y. Sasaki, Y. Sugo, S. Suzuki, S. Tachimori, The novel extractants, diglycolamides, for the extraction of lanthanides and actinides in HNO3-n-dodecane system, Solvent Extr. Ion Exch. 19 (2001) 91–103, https://doi.org/10.1081/SEI-100001376.
[44] L. Berthon, A. Paquet, G. Saint-Louis, P. Guilbaud, How phase modifiers disrupt third-phase formation in solvent extraction solutions, Solvent Extr. Ion Exch. 39 (2021) 204–232, https://doi.org/10.1080/07366299.2020.1831782.
[45] J. Rey, M. Bley, J.F. Dufrêche, S. Gourdin, S. Pellet-Rostaing, T. Zemb, S. Dourdain, Thermodynamic description of synergy in solvent extraction: II, Thermodynamic balance of driving forces implied in synergistic extraction, Langmuir. 33 (2017) 13168–13179, https://doi.org/10.1021/acs.langmuir.7b02068.
[46] M. Alyapyshev, V. Babain, I. Eliseev, E. Kenf, L. Tkachenko, New polar fluorinated diluents for diamide extractants, J. Radioanal. Nucl. Chem. 310 (2016) 785–792, https://doi.org/10.1007/s10967-016-4907-1.
[47] Y. Liu, C. Zhao, Z. Liu, S. Liu, Y. Zhou, C. Jiao, M. Zhang, Y. Gao, H. He, S. Zhang, Study on the extraction of lanthanides by isomeric diglycolamide extractants: An experimental and theoretical study, RSC Adv. 12 (2021) 790–797, https://doi.org/10.1039/d1ra07020g.
[48] M.B. Singh, S.R. Patil, A.A. Lohi, V.G. Gaikar, Insight into nitric acid extraction and aggregation of N, N, N', N'-tetraoctyl diglycolamide (TODGA) in organic solutions by molecular dynamics simulation, Sep. Sci. Technol. 53 (2018) 1361–1371, https://doi.org/10.1080/01496395.2018.1445107.
[49] T. Yaita, A.W. Herlinger, P. Thiyagarajan, M.P. Jensen, Influence of extractant aggregation on the extraction of trivalent f-element cations by a tetraalkyldiglycolamide, Solvent Extr. Ion Exch. 22 (2004) 553–571, https://doi.org/10.1081/SEI-120039640.
[50] P.N. Pathak, S.A. Ansari, S. v. Godbole, A.R. Dhobale, V.K. Manchanda, Interaction of Eu3+ with N,N,N′,N′-tetraoctyl diglycolamide: A time resolved luminescence spectroscopy study, Spectrochim. Acta, Part A . 73 (2009) 348–352. 10.1016/j.saa.2009.02.040.
[51] K. Rama Swami, K.A. Venkatesan, M.P. Antony, Aggregation behavior of alkyldiglycolamides in n-dodecane medium during the extraction of Nd(III) and nitric acid, Ind. Eng. Chem. Res. 57 (2018) 13490–13497, https://doi.org/10.1021/acs.iecr.8b02396.
[52] K.R. Swami, T. Prathibha, K.A. Venkatesan, Aggregation and organic phase splitting behavior of a synergic extractant system probed by dynamic light scattering spectroscopy, J. Mol. Liq. 291 (2019), https://doi.org/10.1016/j.molliq.2019.111320.
[53] K.R. Swami, K.A. Venkatesan, Unraveling the role of phase modifiers in the extraction of Nd(III) from nitric acid medium in tetra-bis(2-ethylhexyl) diglycolamide in n-dodecane containing long chain aliphatic alcohols, J. Mol. Liq. 296 (2019), https://doi.org/10.1016/j.molliq.2019.111741.
[54] C. Déjugnat, S. Dourdain, V. Dubois, L. Berthon, S. Pellet-Rostaing, J.F. Dufrêche, T. Zemb, Reverse aggregate nucleation induced by acids in liquid-liquid extraction processes, Phys. Chem. Chem. Phys. 16 (2014) 7339–7349, https://doi.org/10.1039/c4cp00073k.
[55] M. Spadina, J.-F. Dufreche, S. Pellet-Rostaing, S. Marcelja, T. Zemb, Molecular forces in liquid–liquid extraction, Langmuir. 37 (2021) 10637–10656, https://doi.org/10.1021/acs.langmuir.1c00673.
[56] K.R. Swami, K.A. Venkatesan, P. Sahu, S.M. Ali, The effect of alkyl chain length attached to the diglycolamide and n-paraffin on the aggregation behaviour of diglycolamide and MD simulation of aggregates, J. Mol. Struct. 1221 (2020), https://doi.org/10.1016/j.molstruc.2020.128795.
[57] P.N. Pathak, S.A. Ansari, S. Kumar, B.S. Tomar, V.K. Manchanda, Dynamic light scattering study on the aggregation behaviour of N, N, N′, N′-tetraoctyl diglycolamide (TODGA) and its correlation with the extraction behaviour of metal ions, J. Colloid Interface Sci. 342 (2010) 114–118, https://doi.org/10.1016/j.jcis.2009.10.015.
[58] R.J. Ellis, M.R. Antonio, Coordination structures and supramolecular architectures in a cerium(III)–malonamide solvent extraction system, Langmuir. 28 (2012) 5987–5998, https://doi.org/10.1021/la3002916.
[59] D.M. Brigham, A.S. Ivanov, B.A. Moyer, L.H. Delmau, V.S. Bryantsev, R.J. Ellis, Trefoil-shaped outer-sphere ion clusters mediate lanthanide(III) ion transport with diglycolamide ligands, J. Am. Chem. Soc. 139 (2017) 17350–17358, https://doi.org/10.1021/jacs.7b07318.
[60] R.J. Ellis, M.K. Bera, B. Reinhart, M.R. Antonio, Trapped in the coordination sphere: nitrate ion transfer driven by the cerium(iii/iv) redox couple, Phys. Chem. Chem. Phys. 18 (2016) 31254–31259, https://doi.org/10.1039/C6CP06528G.
[61] G. Ferru, B. Reinhart, M.K. Bera, M. Olvera De La Cruz, B. Qiao, R.J. Ellis, The lanthanide contraction beyond coordination chemistry, Chem. - Eur. J. 22 (2016) 6899–6904, https://doi.org/10.1002/chem.201601032.
[62] T. Zemb, M. Duvail, J.F. Dufrêche, Reverse aggregates as adaptive self-assembled systems for selective liquid-liquid cation extraction, Isr. J. Chem. 53 (2013) 108–112, https://doi.org/10.1002/ijch.201200091.
[63] C. Erlinger, D. Gazeau, T. Zemb, C. Madic, L. Lefrançois, M. Hebrant, C. Tondre, Effect of nitric acid extraction on phase behavior, microstructure and interactions between primary aggregates in the system dimethyldibutyltetradecylmalonamide (DMDBTDMA) / n-dodecane / water: A phase analysis and small angle X-ray scattering (SAXS) characterisation study, Solvent Extr. and Ion Exch. 16 (1998) 707–738, https://doi.org/10.1080/07366299808934549.
[64] J.L. Lemyre, S. Lamarre, A. Beaupré, A.M. Ritcey, A new approach for the characterization of reverse micellar systems by dynamic light scattering, Langmuir. 26 (2010) 10524–10531, https://doi.org/10.1021/la100541m.
[65] D. Whittaker, A. Geist, G. Modolo, R. Taylor, M. Sarsfield, A. Wilden, Applications of diglycolamide based solvent extraction processes in spent nuclear fuel reprocessing, part 1: TODGA, Solvent Extr. Ion Exch. 36 (2018) 223–256, https://doi.org/10.1080/07366299.2018.1464269.
[66] M.R. Antonio, D.R. McAlister, E.P. Horwitz, An europium(III) diglycolamide complex: Insights into the coordination chemistry of lanthanides in solvent extraction, Dalton Trans. 44 (2015) 515–521, https://doi.org/10.1039/c4dt01775g.
[67] B.G. Tokheim, S.S. Kelly, R.C. Ronald, K.L. Nash, Synthesis and characterization of new unsymmetrical diglycolamide extractants for lanthanide ion partitioning: part one—straight-chain alkyl derivatives, J. Radioanal. Nucl. Chem. 326 (2020) 789–800, https://doi.org/10.1007/s10967-020-07368-2.
[68] A. Leoncini, J. Huskens, W. Verboom, Ligands for f-element extraction used in the nuclear fuel cycle, Chem. Soc. Rev. 46 (2017) 7229–7273, https://doi.org/10.1039/c7cs00574a.
[69] E.J. Werner, S.M. Biros, Supramolecular ligands for the extraction of lanthanide and actinide ions, Org. Chem. Front. 6 (2019) 2067, https://doi.org/10.1039/C9QO00242A.
[70] Z. Liu, H. Li, Y. Liu, C. Zhao, C. Jiao, Y. Zhou, M. Zhang, Y. Gao, Recent progress on the structure-performance relationship between diglycolamide extractants and f-elements, Solvent Extr. Ion Exch. 40 (2022) 540–570, https://doi.org/10.1080/07366299.2021.2006884.
[71] N.K. Gupta, Ionic liquids for transuranic extraction (TRUEX)—Recent developments in nuclear waste management: A review, J. Mol. Liq. 269 (2018) 72–91, https://doi.org/10.1016/j.molliq.2018.08.036.
[72] P.K. Mohapatra, Diglycolamide-based solvent systems in room temperature ionic liquids for actinide ion extraction: A review, Chem. Prod. Process. Model. 10 (2015) 135–145, https://doi.org/10.1515/cppm-2014-0030.
[73] S.M. Ali, S. Pahan, A. Bhattacharyya, P.K. Mohapatra, Complexation thermodynamics of diglycolamide with f-elements: Solvent extraction and density functional theory analysis, Phys. Chem. Chem. Phys. 18 (2016) 9816–9828, https://doi.org/10.1039/c6cp00825a.
[74] G. Ferru, D. Gomes Rodrigues, L. Berthon, O. Diat, P. Bauduin, P. Guilbaud, Elucidation of the structure of organic solutions in solvent extraction by combining molecular dynamics and X-ray scattering, Angew. Chem. Int. Ed. 53 (2014) 5346–5350, https://doi.org/10.1002/anie.201402677.
[75] J.R. Perumareddi, G.V.S. Rayudu, V. Ramachandra Rao, V.S. Sastri, J.C.G. Bunzli, V.R. Sastri, Spectroscopy of lanthanide complexes, in: Modern Aspects of Rare Earths and Their Complexes, Elsevier, Amsterdam, 2003: pp. 569–731.
[76] M. Matsumiya, Y. Tsuchida, Y. Sasaki, R. Ono, M. Nakase, K. Takeshita, Trichotomic separation of light and heavy lanthanides and Am by batchwise multi-stage extractions using TODGA, J. Radioanal. Nucl. Chem. 327 (2021) 597–607, https://doi.org/10.1007/s10967-020-07464-3.
[77] L. Lefrançois, J.J. Delpuech, M. Hébrant, J. Chrisment, C. Tondre, Aggregation and protonation phenomena in third phase formation: An NMR study of the quaternary malonamide/dodecane/nitric acid/water system, J. Phys. Chem. B. 105 (2001) 2551–2564, https://doi.org/10.1021/jp002465h.
[78] E.L. Campbell, V.E. Holfeltz, G.B. Hall, K.L. Nash, G.J. Lumetta, T.G. Levitskaia, Nitric acid and water extraction by T2EHDGA in n-dodecane, Solvent Extr. Ion Exch. 35 (2017) 586–603, https://doi.org/10.1080/07366299.2017.1400161.
[79] K. Bell, A. Geist, F. McLachlan, G. Modolo, R. Taylor, A. Wilden, Nitric acid extraction into TODGA, Procedia Chem. 7 (2012) 152–159, https://doi.org/10.1016/j.proche.2012.10.026.
[80] Z. Chen, X. Yang, L. Song, X. Wang, Q. Xiao, H. Xu, Q. Feng, S. Ding, Extraction and complexation of trivalent rare earth elements with tetraalkyl diglycolamides, Inorg. Chim. Acta. 513 (2020) 1–11, https://doi.org/10.1016/j.ica.2020.119928.
[81] Y. Sasaki, P. Rapold, M. Arisaka, M. Hirata, T. Kimura, C. Hill, G. Cote, An additional insight into the correlation between the distribution ratios and the aqueous acidity of the TODGA system, Solvent Extr. Ion Exch. 25 (2007) 187–204, https://doi.org/10.1080/07366290601169345.

[82] P.S. Sit, Studying molecular-scale protein-surface interactions in biomaterials, Characterization of Biomaterials, Elsevier Ltd., in, 2012, pp. 182–223.
[83] R.J. Ellis, L. D'Amico, R. Chiarizia, M.R. Antonio, Solvent extraction of cerium (III) using an aliphatic malonamide: The role of acid in organic phase behaviors, Sep. Sci. Technol. 47 (2012) 2007–2014, https://doi.org/10.1080/01496395.2012.697506.
[84] S.A. Ansari, P.N. Pathak, V.K. Manchanda, M. Husain, A.K. Prasad, V.S. Parmar, N, N, N', N'-Tetraoctyl diglycolamide (TODGA): A promising extractant for actinide-partitioning from high-level waste (HLW), Solvent Extr. Ion Exch. 23 (2005) 463–479, https://doi.org/10.1081/SEI-200066296.
[85] M.P. Jensen, T. Yaita, R. Chiarizia, Reverse-micelle formation in the partitioning of trivalent f-element cations by biphasic systems containing a tetraalkyldiglycolamide, Langmuir. 23 (2007) 4765–4774, https://doi.org/10.1021/la0631926.
[86] B. Sadhu, A.E. Clark, Molecular dynamics and network analysis reveal the contrasting roles of polar solutes within organic phase amphiphile aggregation, J. Mol. Liq. 359 (2022), https://doi.org/10.1016/j.molliq.2022.119226.
[87] T. Prathibha, K.A. Venkatesan, M.P. Antony, Comparison in the aggregation behaviour of amide extractant systems by dynamic light scattering and ATR-FTIR spectroscopy, Colloids Surf A. 538 (2018) 651–660, https://doi.org/10.1016/j.colsurfa.2017.11.035.
[88] R. Motokawa, S. Suzuki, H. Ogawa, M.R. Antonio, T. Yaita, Microscopic structures of tri-n-butyl phosphate/n-octane mixtures by x-ray and neutron scattering in a wide q range, J. Phys. Chem. B. 116 (2012) 1319–1327, https://doi.org/10.1021/jp210808r.
[89] R.J. Ellis, T.L. Anderson, M.R. Antonio, A. Braatz, M. Nilsson, A SAXS study of aggregation in the synergistic TBP-HDBP solvent extraction system, J. Phys. Chem. B. 117 (2013) 5916–5924, https://doi.org/10.1021/jp401025e.
[90] A.N. Turanov, V.K. Karandashev, M. Boltoeva, Solvent extraction of intra-lanthanides using a mixture of TBP and TODGA in ionic liquid | Elsevier Enhanced Reader, Hydrometallurgy. 195 (2020), https://doi.org/10.1016/j.hydromet.2020.105367.
[91] V. Chavan, S. Patra, A.K. Pandey, V. Thekkethil, M. Iqbal, J. Huskens, D. Sen, S. Mazumder, A. Goswami, W. Verboom, Understanding nitric acid-induced changes in the arrangement of monomeric and polymeric methacryloyl diglycolamides on their affinity toward f-element ions, J. Phys. Chem. B. 119 (2015) 212–218, https://doi.org/10.1021/jp510170v.
[92] E.R. Bertelsen, N.C. Kovach, B.J. Reinhart, B.G. Trewyn, M.R. Antonio, J.C. Shafer, Multiscale investigations of europium(III) complexation with tetra-n-octyl diglycolamide confined in porous solid supports, CrystEngComm. 22 (2020) 6886–6899, https://doi.org/10.1039/d0ce00956c.
[93] D. Bourgeois, A. el Maangar, S. Dourdain, Importance of weak interactions in the formulation of organic phases for efficient liquid/liquid extraction of metals, Curr. Opin. Colloid Interface Sci. 46 (2020) 36–51, https://doi.org/10.1016/j.cocis.2020.03.004.
[94] T. Zemb, C. Bauer, P. Bauduin, L. Belloni, C. Déjugnat, O. Diat, V. Dubois, J.F. Dufrêche, S. Dourdain, M. Duvail, C. Larpent, F. Testard, S. Pellet-Rostaing, Recycling metals by controlled transfer of ionic species between complex fluids: en route to ''ienaics", Colloid Polym. Sci. 293 (2015) 1–22, https://doi.org/10.1007/s00396-014-3447-x.
[95] T. Kawasaki, S. Okumura, Y. Sasaki, Y. Ikeda, Crystal structures of Ln(III) (Ln = La, Pr, Nd, Sm, Eu, and Gd) complexes with N, N, N', N'-tetraethyldiglycolamide associated with homoleptic [Ln(NO3)(6))](3-), Bull. Chem. Soc. Jpn. 87 (2014) 294–300, https://doi.org/10.1246/bcsj.20130259.
[96] S. Okumura, T. Kawasaki, Y. Sasaki, Y. Ikeda, Crystal structures of lanthanoid (III) (Ln(III), Ln = Tb, Dy, Ho, Er, Tm, Yb, and Lu) nitrate complexes with N, N, N', N'-tetraethyldiglycolamide, Bull. Chem. Soc. Jpn. 87 (2014) 1133–1139, https://doi.org/10.1246/bcsj.20140139.
[97] D. Xu, Z. Shah, Y. Cui, L. Jin, X. Peng, H. Zhang, G. Sun, Recovery of rare earths from nitric acid leach solutions of phosphate ores using solvent extraction with a new amide extractant (TODGA), Hydrometallurgy. 180 (2018) 132–138, https://doi.org/10.1016/j.hydromet.2018.07.005.
[98] L. Qiu, J. Li, W. Zhang, A. Gong, X. Yuan, Y. Liu, Extraction and back-extraction behaviors of La(III), Ce(III), Pr(III), and Nd(III) single rare earth and mixed rare earth by TODGA, Sensors. 21 (2021) 8316, https://doi.org/10.3390/s21248316.
[99] A. Sengupta, A. Bhattacharyya, W. Verboom, S.M. Ali, P.K. Mohapatra, Insight into the complexation of actinides and lanthanides with diglycolamide derivatives: Experimental and density functional theoretical studies, J. Phys. Chem. B. 121 (2017) 2640–2649, https://doi.org/10.1021/acs.jpcb.6b11222.
[100] P. Wessling, U. Muellich, E. Guerinoni, A. Geist, P.J. Panak, Solvent extraction of An(III) and Ln(III) using TODGA in aromatic diluents to suppress third phase formation, Hydrometallurgy. 192 (2020), https://doi.org/10.1016/j.hydromet.2020.105248.
[101] J. Yang, Y. Cui, G. Sun, Y. Nie, G. Xia, G. Zheng, Extraction of Sm(III) and Nd(III) with N, N, N′, N′-tetrabutyl-3- oxy-diglycolamide from hydrochloric acid, J. Serb. Chem. Soc. 78 (2013) 93–100, https://doi.org/10.2298/JSC110922077Y.
[102] R.B. Gujar, S.A. Ansari, M.S. Murali, P.K. Mohapatra, V.K. Manchanda, Comparative evaluation of two substituted diglycolamide extractants for ''actinide partitioning", J. Radioanal. Nucl. Chem. 284 (2010) 377–385, https://doi.org/10.1007/s10967-010-0467-y.
[103] S. Tachimori, Y. Sasaki, S.-I. Suzuki, Modification of TODGA-n-dodecane solvent with a monoamide for high loading of lanthanides(III) and actinides (III), Solvent Extr. Ion Exch. 20 (2002) 687–699. 10.1081=SEI-120016073.
[104] E.P. Horwitz, D.R. McAlister, A.H. Thakkar, Synergistic enhancement of the extraction of trivalent lanthanides and actinides by tetra-(n-octyl) diglycolamide from chloride media, Solvent Extr. Ion Exch. 26 (2007) 12–24, https://doi.org/10.1080/07366290701779423.
[105] B. Kang, H. Tang, Z. Zhao, S. Song, Hofmeister series: Insights of ion specificity from amphiphilic assembly and interface property, ACS Omega. 5 (2020) 6229–6239, https://doi.org/10.1021/acsomega.0c00237.
[106] A. Wilden, P.M. Kowalski, L. Klaß, B. Kraus, F. Kreft, G. Modolo, Y. Li, J. Rothe, K. Dardenne, A. Geist, A. Leoncini, J. Huskens, W. Verboom, Unprecedented inversion of selectivity and extraordinary difference in the complexation of trivalent f elements by diastereomers of a methylated diglycolamide, Chem. - Eur. J. 25 (2019) 5507–5513, https://doi.org/10.1002/chem.201806161.
[107] T. Hosseinnejad, S. Dehghanpour, S. Basiri-Nasab, A DFT study on the complexation of La3+ ion with malonamide and diglycolamide ligands, Russ. J. Phys. Chem. A. 88 (2014) 2004–2011, https://doi.org/10.1134/S0036024414110156.
[108] T. Hosseinnejad, S. Nikoo, Computational study on the complexation behavior of tetrapropyl diglycolamide with Ln3+ (Ln = Nd, Pm, Sm, and Eu) cation series, Russ. J. Phys. Chem. A. 89 (2015) 1599–1604, https://doi.org/10.1134/S0036024415090332.
[109] J. Narbutt, A. Wodyński, M. Pecul, The selectivity of diglycolamide (TODGA) and bis-triazine-bipyridine (BTBP) ligands in actinide/lanthanide complexation and solvent extraction separation-a theoretical approach, Dalton Trans. 44 (2015) 2657–2666, https://doi.org/10.1039/c4dt02657h.
[110] V. Radchenko, T. Mastren, C.A.L. Meyer, A.S. Ivanov, V.S. Bryantsev, R. Copping, D. Denton, J.W. Engle, J.R. Griswold, K. Murphy, J.J. Wilson, A. Owens, L. Wyant, E.R. Birnbaum, J. Fitzsimmons, D. Medvedev, C.S. Cutler, L.F. Mausner, M.F. Nortier, K.D. John, S. Mirzadeh, M.E. Fassbender, Radiometric evaluation of diglycolamide resins for the chromatographic separation of actinium from fission product lanthanides, Talanta. 175 (2017) 318–324, https://doi.org/10.1016/j.talanta.2017.07.057.
[111] X. Peng, J. Su, H. Li, Y. Cui, J.Y. Lee, G. Sun, Theoretical elucidation of rare earth extraction and separation by diglycolamides from crystal structures and DFT simulations, J. Rare Earths. 39 (2021) 858–865, https://doi.org/10.1016/j.jre.2020.09.013.
[112] A. Dhawa, A. Rout, N.R. Jawahar, K.A. Venkatesan, A systematic approach for achieving the maximum loading of Eu(III) in TODGA/n-dodecane phase with the aid of TBP phase modifier, J. Mol. Liq. 341 (2021), https://doi.org/10.1016/j.molliq.2021.117397.
[113] J. Rey, S. Dourdain, J.F. Dufrêche, L. Berthon, J.M. Muller, S. Pellet-Rostaing, T. Zemb, Thermodynamic description of synergy in solvent extraction: I, Enthalpy of mixing at the origin of synergistic aggregation, Langmuir. 32 (2016) 13095–13105, https://doi.org/10.1021/acs.langmuir.6b02343.
[114] M. Basu, P. Sinharoy, J. Ramkumar, S.L. Gawali, B. Dutta, J.N. Sharma, Thermodynamics of mixing of TEHDGA with isodecanol in dodecane: Effect of equilibration with aqueous nitric acid, J. Solution Chem. 48 (2019) 1318–1335, https://doi.org/10.1007/s10953-019-00914-x.
[115] F. Feixas, E. Matito, J. Poater, M. Solà, Understanding conjugation and hyperconjugation from electronic delocalization measures, J. Phys. Chem. A. 115 (2011) 13104–13113, https://doi.org/10.1021/jp205152n.
[116] A.R. Katrifzky, R.D. Topsom, The sigma- and pi-inductive effects, J. Chem. Educ. 48 (1971) 427–431, https://doi.org/10.1021/ed048p427.
[117] T. Yaita, M. Hirata, H. Narita, S. Tachimori, H. Yamamoto, N.M. Edelstein, J.J. Bucher, D.K. Shuh, L. Rao, Coordination properties of diglycolamide to trivalent curium And lanthanides studied by XAS XRD and XPS methods, Evaluation of Speciation Technology, in, 1999, pp. 273–280.
[118] M.P. Jensen, A.H. Bond, Comparison of covalency in the complexes of trivalent actinide and lanthanide cations, J. Am. Chem. Soc. 124 (2002) 9870–9877, https://doi.org/10.1021/ja0178620.
[119] K.A. Allen, Aggregation of some of the amine extractant species in benzene, J. Phys. Chem. 62 (1958) 1119–1123, https://doi.org/10.1021/j150567a024.
[120] J.F. Blain, T. Kikindai, D. Gourisse, A study of third phase formation in trilaurylamine solutions, in: A.A. Kertes, Y. Marcus (Eds.), Solvent Extraction Research: Proceedings on the 5th International Conference on Solvent Extraction Chemistry (5th ICSEC), Wiley-Interscience, New York, 1969, pp. 201–209.
[121] R.D. Neuman, M.A. Jones, N.-F. Zhou, Photon correlation spectroscopy applied to hydrometallurgical solvent extraction systems, Colloids Surf. 46 (1990) 45–61, https://doi.org/10.1016/0166-6622(90)80047-8.
[122] R.W. Dodson, G.J. Forney, E.H. Swift, The extraction of ferric chloride from hydrochloric acid solutions by isopropyl ether, J. Am. Chem. Soc. 58 (1936) 2573–2577, https://doi.org/10.1021/ja01303a058.
[123] R. Ganguly, J.N. Sharma, N. Choudhury, Phase separation in the TODGA reverse micellar solutions in dodecane: Identifying an upper consolute temperature and an associated critical behavior, Soft Matter. 8 (2012) 1795–1800, https://doi.org/10.1039/c2sm06030b.
[124] H. Wu, Contribution to the chemistry of phosphomolybdic acids, phosphotungstic acids, and allied substances, J. Biol. Chem. 43 (1920) 189–220, https://doi.org/10.1016/S0021-9258(18)86325-6.
[125] R.J. Ellis, Critical exponents for solvent extraction resolved using SAXS, J. Phys. Chem. B. 118 (2014) 315–322, https://doi.org/10.1021/jp408078v.
[126] D. Sheyfer, Q. Zhang, J. Lal, T. Loeffler, E.M. Dufresne, A.R. Sandy, S. Narayanan, S.K.R.S. Sankaranarayanan, R. Szczygiel, P. Maj, L. Soderholm, M.R. Antonio, G. B. Stephenson, Nanoscale critical phenomena in a complex fluid studied by X-ray photon correlation spectroscopy, Phys. Rev. Lett. 125 (2020), https://doi.org/10.1103/PhysRevLett.125.125504.

[127] D. Sheyfer, M.J. Servis, Q. Zhang, J. Lal, T. Loeffler, E.M. Dufresne, A.R. Sandy, S. Narayanan, S.K.R.S. Sankaranarayanan, R. Szczygiel, P. Maj, L. Soderholm, M.R. Antonio, G.B. Stephenson, Advancing chemical separations: Unraveling the structure and dynamics of phase splitting in liquid–liquid extraction, J. Phys. Chem. B. 126 (2022) 2420–2429, https://doi.org/10.1021/acs.jpcb.1c09996.
[128] M.J. Servis, S. Nayak, S. Seifert, The pervasive impact of critical fluctuations in liquid–liquid extraction organic phases, J. Chem. Phys. 155 (2021), https://doi.org/10.1063/5.0074995.
[129] M.R. Antonio, R. Chiarizia, B. Gannaz, L. Berthon, N. Zorz, C. Hill, G. Cote, Aggregation in solvent extraction systems containing a malonamide, a dialkylphosphoric acid and their mixtures, Sep. Sci. Technol. 43 (2008) 2572–2605, https://doi.org/10.1080/01496390802121537.
[130] R. Poirot, X. le Goff, O. Diat, D. Bourgeois, D. Meyer, Metal recognition driven by weak interactions: A case study in solvent extraction, ChemPhysChem. (2016) 2112–2117, https://doi.org/10.1002/cphc.201600305.
[131] H.B. Bohidar, M. Behboudnia, Characterization of reverse micelles by dynamic light scattering, Colloids Surf, A. 178 (2001) 313–323, https://doi.org/10.1016/S0927-7757(00)00736-6.
[132] R. Ganguly, J.N. Sharma, N. Choudhury, TODGA based w/o microemulsion in dodecane: An insight into the micellar aggregation characteristics by dynamic light scattering and viscometry, J. Colloid Interface Sci. 355 (2011) 458–463, https://doi.org/10.1016/j.jcis.2010.12.039.
[133] N. Kumari, P.N. Pathak, Dynamic light scattering studies on the aggregation behavior of tributyl phosphate and straight chain dialkyl amides during thorium extraction, J. Ind. Eng. Chem. 20 (2014) 1382–1387, https://doi.org/10.1016/j.jiec.2013.07.022.
[134] P.A. Hassan, S. Rana, G. Verma, Making sense of Brownian motion: Colloid characterization by dynamic light scattering, Langmuir. 31 (2015) 3–12, https://doi.org/10.1021/la501789z.
[135] C.h. Venkateswara Rao, A. Rout, K.A. Venkatesan, Probing the absence of third phase formation during the extraction of trivalent metal ions in an ionic liquid medium, New J. Chem. 43 (2019) 5099–5108, https://doi.org/10.1039/C8NJ06267F.
[136] O. Glatter, G. Fritz, H. Lindner, J. Brunner-Popela, R. Mittelbach, R. Strey, S.U. Egelhaaf, Nonionic micelles near the critical point: Micellar growth and attractive interaction, Langmuir. 16 (2000) 8692–8701, https://doi.org/10.1021/la000315s.
[137] T.S. Grimes, M.P. Jensen, L. Debeer-Schmidt, K. Littrell, K.L. Nash, Small-angle neutron scattering study of organic-phase aggregation in the TALSPEAK process, J. Phys. Chem. B. 116 (2012) 13722–13730, https://doi.org/10.1021/jp306451d.
[138] H. Schnablegger, Y. Singh, The SAXS Guide, 3rd ed.,., Anton Paar GmbH, 2013.
[139] C.D. Putnam, M. Hammel, G.L. Hura, J.A. Tainer, X-ray solution scattering (SAXS) combined with crystallography and computation: Defining accurate macromolecular structures, conformations and assemblies in solution, Q. Rev. Biophys. 40 (2007) 191–285, https://doi.org/10.1017/S0033583507004635.
[140] S.H. Chen, Small-angle neutron-scattering studies of the structure and interaction in micellar and microemulsion systems, Annu. Rev. Phys. Chem. 37 (1986) 351–399, https://doi.org/10.1146/annurev.pc.37.100186.002031.
[141] S. Nave, G. Modolo, C. Madic, F. Testard, Aggregation properties of N, N, N1, N1 - Tetraoctyl-3-oxapentanediamide (TODGA) in n-dodecane, Solvent Extr. Ion Exch. 22 (2004) 527–551, https://doi.org/10.1081/SEI-120039721.
[142] A. Guinier, G. Fournet, C.B. Walker, Scattering of X-rays, Wiley, New York, 1955.
[143] R.J. Baxter, Percus – Yevick equation for hard spheres with surface adhesion, J. Chem. Phys. 40 (2003) 2770–2774, https://doi.org/10.1063/1.1670482.
[144] R. Motokawa, T. Kobayashi, H. Endo, J. Mu, C.D. Williams, A.J. Masters, M.R. Antonio, W.T. Heller, M. Nagao, A telescoping view of solute architectures in a complex fluid system, ACS Cent. Sci. 5 (2019) 85–96, https://doi.org/10.1021/acscentsci.8b00669.
[145] J. Klier, C.J. Tucker, T.H. Kalantar, D.P. Green, Properties and applications of microemulsions, Adv. Mater. 12 (2000) 1751–1756, https://doi.org/10.1002/1521-4095(200012)12:23<1751::AID-ADMA1751>3.0.CO;2-I.
[146] B. Qiao, T. Demars, M. Olvera De La Cruz, R.J. Ellis, How hydrogen bonds affect the growth of reverse micelles around coordinating metal ions, J. Phys. Chem. Lett. 5 (2014) 1440–1444, https://doi.org/10.1021/jz500495p.
[147] R.J. Ellis, Y. Meridiano, R. Chiarizia, L. Berthon, J. Muller, L. Couston, M.R. Antonio, Periodic behavior of lanthanide coordination within reverse micelles, Chem. - Eur. J. 19 (2013) 2663–2675, https://doi.org/10.1002/chem.201202880.
[148] P. Narayanan, K.R. Swami, T. Prathibha, K.A. Venkatesan, Insights into the third phase formation behaviour of N, N-didodecyl-N', N'-dioctyl diglycolamide in n-dodecane investigated by dynamic light scattering and FTIR spectroscopy, ChemistrySelect. 7 (2022), https://doi.org/10.1002/slct.202202610.